THE UNIVERSITY OF ALBERTA

HIGH TEMPERATURE THERMODYNAMIC STUDY OF CHROMIUM CARBIDE AND CARBON DIOXIDE UTILIZING SOLID ELECTOLYTES

BY

CRAIG DENNIS EASTMAN

A THESIS

SUBMITTED TO THE FACULTY OF GRADUATE STUDIES AND RESEARCH IN PARTIAL FULFILLMENT OF THE REQUIREMENTS FOR THE DEGREE OF MASTER OF SCIENCE

IN

METALLURGICAL ENGINEERING

DEPARTMENT OF MINING, METALLURGICAL AND PETROLEUM ENGINEERING

EDMONTON, ALBERTA

SPRING 1990

ISBN 0-315-60292-9

THE UNIVERSITY OF ALBERTA

RELEASE FORM

NAME OF AUTHOR : CRAIG DENNIS EASTMAN

TITLE OF THESIS : HIGH TEMPERATURE THERMODYNAMIC STUDY OF CHROMIUM CARBIDE AND CARBON DIOXIDE UTILIZING SOLID ELECTROLYTES

DEGREE : MASTER OF SCIENCE

YEAR THIS DEGREE GRANTED : SPRING 1990

(Student's signature)
826, Burley Close
Edmonton, Alberta
Canada, T6R 1W9
(Student's permanent address)

Date : April 19/90

THE UNIVERSITY OF ALBERTA

FACULTY OF GRADUATE STUDIES AND RESEARCH

THE UNDERSIGNED CERTIFY THEY HAVE READ, AND RECOMMEND TO THE FACULTY OF GRADUATE STUDIES AND RESEARCH FOR ACCEPTANCE, A THESIS ENTITLED, 'HIGH TEMPERATURE THERMODYNAMIC STUDY OF CHROMIUM CARBIDE AND CARBON DIOXIDE UTILIZING SOLID ELECTROLYTES'

SUBMITTED BY CRAIG DENNIS EASTMAN

IN PARTIAL FUFILLMENT OF THE REQUIREMENTS FOR THE

DEGREE OF MASTER OF SCIENCE

IN METALLURGICAL ENGINEERING.

Thomas H. Etsell

(Supervisor)

J. E. Mathon

Committee Chairman

Samuel A. Bradford

Committee Member

Jerzy Szpunar

Committee Member

Date :

Abstract

Both calcia-stabilized zirconia (CSZ) and yttria-doped thoria (YDT) were utilized in measuring the electromotive forces (e.m.f.) produced in chromium carbide thermodynamic cells. Available experimental data for the free energy of formation of chromium carbide (Cr_3C_2) indicate that the present cell configuration produces oxygen pressures that are unsuitable for use with CSZ. Running the identical cell with YDT was required due to the low oxygen pressures, but the presence of a three-phase mixture at the cathode prevented equilibrium from being obtained rapidly. The best values obtained for the free energy of formation using YDT consist of :

$$\Delta G^o_{Cr_3C_2} (\pm 208 \text{ cal/mole}) = -6248 - 11.39\,T \quad R^2 = 0.76 \quad (1088 \text{ to } 1208 \text{ K})$$

$$\Delta G^o_{Cr_3C_2} (\pm 208 \text{ cal/mole}) = -5427 - 10.77\,T \quad R^2 = 0.83 \quad (1124 \text{ to } 1353 \text{ K})$$

An alternate cell configuration is recommended which replaces the solid three-phase cathode with gaseous oxygen to eliminate any difficulty in reaching equilibrium. The anode would consist of a solid-gas phase mixture.

In the second part of the experiment yttria-stabilized zirconia (YSZ) was used in measuring the electromotive force created by the oxidation of carbon monoxide to carbon dioxide. This thermodynamic cell utilized a gas mixture of CO and CO_2 for the establishment of an oxygen partial pressure at the anode, with pure oxygen for the cathode. It was found that mixtures dilute in either component produced results which were sensitive to polarization at the anode. The mixtures which consisted of significant amounts of both CO and CO_2 provided the best results which agreed fairly closely with accepted values.

For the reaction $CO + \frac{1}{2}O_2 = CO_2$ the best value obtained was :

$$\Delta G^o\ (\pm 95\ \text{cal / mol}) = -65807\ -19.64\ T \quad R^2 = 0.99\ \ (781 \text{ to } 1423\ \text{K})$$

Further improvements to cell design and operation are recommended, which could provide an extremely accurate means for measuring oxygen partial pressures in CO-CO_2 mixtures.

Acknowledgements

I am deeply grateful to my supervisor, Dr. Tom Etsell, for providing continuous guidance and motivation throughout my studies.

I would also like to thank the Alberta Microelectronic Center for providing the computer system for publication of this thesis.

This work is dedicated to Marilyn, for persevering during the writing of the thesis.

TABLE OF CONTENTS

LIST OF TABLES

LIST OF FIGURES

LIST OF SYMBOLS

Chapter 2

Symbol	Description	Units
C_p	Specific heat at constant pressure	calories / mol Kelvin
E	Electromotive force (e.m.f.)	volts
F	Faraday constant	calories / V equiv
ΔG	Change in free energy	calories / mol
ΔG^o	Free energy change at standard conditions	calories / mol
ΔG^o_f	Free energy of formation from elements	calories / mol
ΔG_T	Change in free energy at temperature T	calories / mol
ΔG_{T_2}	Free energy at temperature T_2	calories / mol
ΔH	Change in enthalpy	calories / mol
$\Delta H_{reaction}$	Enthalpy of a reaction	calories / mol
$\Delta H_{products}$	Enthalpy of products of a reaction	calories / mol
$\Delta H_{reactants}$	Enthalpy of reactants of a reaction	calories / mol
ΔH_{298}	Enthalpy at 298 Kelvin	calories / mol
ΔH^o_{298}	Enthalpy at 298 K - standard state	calories / mol
ΔH_{T_2}	Enthalpy at temperature T_2	calories / mol
i_o	Exchange current density	A / cm^2
i	Current density	A / cm^2
P	Pressure	Pascal(Newton / m^2)
S	Entropy	calories / mol Kelvin
S_o	Entropy at absolute zero	calories / mol Kelvin
S^o_{298}	Entropy at 298K - standard state	calories / mol Kelvin

Symbol	Description	Units
$S_{products}$	Entropy of products of a reaction	calories / mol Kelvin
$S_{reactants}$	Entropy of reactants of a reaction	calories / mol Kelvin
ΔS	Change in entropy	calories / mol Kelvin
ΔS_{298}	Entropy at 298 Kelvin	calories / mol Kelvin
$\Delta S_{reaction}$	Entropy of a reaction	calories / mol Kelvin
ΔS_{T_2}	Entropy at temperature T_2	calories / mol Kelvin
T	Temperature	Kelvin (K)
V	Volume	cubic metre (m^3)
z	Number of moles of electrons transferred	equiv / mol
β	Tafel constant	volts
η_a	Activation polarization	volts

Chapter 3

Symbol	Description	Units
A	Area	square metres (m^2)
A	Molar ratio of intrinsic defects	dimensionless
$[A]_B$	An alloy of the metals A and B	dimensionless
AX	Compound of A and X	dimensionless
A^{z+}	Cation A, which dissolves into electrolyte	
B	Ratio of mobilities of x_1 and x_2	dimensionless
B^{z+}	Cation B, which dissolves into electrolyte	
CX	Compound of C and X	dimensionless
$[CX]_{DX}$	Solution of the compounds CX and DX	dimensionless
C^{z+}	Cation C, which dissolves into electrolyte	
Ca''_{Zr}	Ca^{+2} ion occupying a Zr^{+4} ion site	
D	Diffusion coefficient of an ion	cm^2 / s
D_i	Interstitial diffusion coefficient	cm^2 / s
D_o	Constant of ionic diffusion	cm^2 / s
D_t	Tracer diffusion coefficient	cm^2 / s
DX	Compound of D and X	dimensionless
D^{z+}	Cation D, which dissolves into electrolyte	
e	Electronic charge	coulombs
f	Correlation factor	dimensionless
$h^{\cdot}$	Electron holes	
I	Current	amperes
k	Boltzmann's constant	calories / Kelvin
K_1	Equilibrium constant (low oxygen pressure)	dimensionless

Symbol	Description	Units
K'_1	Reaction constant (low oxygen pressure)	dimensionless
K''_1	Reaction constant (low oxygen pressure)	dimensionless
K''_2	Reaction constant (high oxygen pressure)	dimensionless
L	Length	metre
L	Component of electrolyte	dimensionless
M	Component of electrolyte	dimensionless
n	Number of charge carriers	carriers / m^3
N	Total number of diffusing ions per unit volume	carriers / m^3
N_i	Number of interstitials per unit volume	carriers / m^3
O_i''	Interstitial oxygen ions	
O_o	Oxygen ion on an oxygen site	
O^{2-}	Oxygen anion	
$P_\ominus$	Oxygen pressure where ionic conductivity equals conductivity due to excess electrons	atmospheres
$P_\oplus$	Oxygen pressure where ionic conductivity equals conductivity due to electron holes	atmospheres
P_{O_2}	Partial pressure of oxygen	atmospheres
P''_{O_2}	Oxygen pressure at cathode	atmospheres
P'_{O_2}	Oxygen pressure at anode	atmospheres
Pt'	Platinum lead - anode	dimensionless
Pt"	Platinum lead - cathode	dimensionless
q	Charge of diffusing ion	coulomb / ion
q	Charge per carrier	coulomb / carrier
Q	Activation energy for diffusion	calories / mole
R	Gas constant	calories/Kelvin mol
R	Resistance to the flow of electrons	ohms (Ω)

Symbol	Description	Units
t_e	Transference number due to electronic conduction	dimensionless
$\bar{t}_e$	Average electronic transference number	dimensionless
t_{ion}	Ionic transference number	dimensionless
$\bar{t}_{ion}$	Average ionic transference number	dimensionless
$t_{O^{-2}}$	Oxygen anion transference number	dimensionless
$t_{X^{2+}}$	Ionic transference number for electrode cation component X, where X equals A, B, C, D, L, or M.	dimensionless
$t_{X^{-2}}$	Transference number of the ionic species X^{-2}	dimensionless
V	Potential difference between two electrodes	volts
V_{Me}''	Cation vacancies	
$V_{\ddot{O}}$	Oxygen vacancy	
$x_{1 \text{ or } 2}$	Mole fraction of an intrinsic defect either interstitials and vacancies or cation and anion vacancies	dimensionless
x_o	Square root of the product of the molar fractions of two complementary defects, either of Frenkel or Schottky type.	dimensionless
X_2	Gaseous Component	dimensionless
X^{2-}	Charge of ionic species	
X^{z-}	Ionic species	
Y'_{Th}	Y^{+3} ion occupying a Th^{+4} ion site	
Y'_{Zr}	Y^{+3} ion occupying a Zr^{+4} ion site	
$Z_{X^{-2}}$	Integer value for the no. of moles of electrons	dimensionless

Symbol	Description	Units
α'	Phase associated with Pt lead at anode	dimensionless
α''	Phase associated with Pt lead at cathode	dimensionless
β'	Interfacial region at anode / electrolyte side	dimensionless
β''	Interfacial region at cathode / electrolyte side	dimensionless
ε	Electric field	volt / metre
μ	Mobility of carriers	m^2 / volt s
μ_e'	Mobility of excess electrons	m^2 / volt s
$\bar{\mu}_e^{\alpha}$	Electrochemical potential at electrode	calories / mol
$\bar{\mu}_e Pt''$	Electrochemical potential at Pt'' (cathode)	calories / mol
$\bar{\mu}_e Pt'$	Electrochemical potential at Pt' (anode)	calories / mol
$\mu_{h^\bullet}$	Mobility of electron holes	m^2 / volt s
$\bar{\mu}_i^{\alpha''}$	Electrochemical potential at cathode	calories / mol
$\bar{\mu}_i^{\alpha'}$	Electrochemical potential at anode	calories / mol
μ_{O_2}	Chemical potential for oxygen in an ideal mixture	calories / mole
$\mu^o_{O_2}$	Standard chemical potential of oxygen	calories / mole
$\Delta\mu_{O_2}$	Variance of the chemical potential of O_2	calories / mole
$\mu' X_2$	Chemical potential at anode due to X_2	calories / mol
$\mu'' X_2$	Chemical potential at cathode due to X_2	calories / mol
$\mu^{\alpha}_{X_2}$	Chemical potential of the gas phase	calories / mol
$\bar{\mu}^{\alpha}_{X^{2-}}$	Electrochemical potential of the ionic species	calories / mol
$\bar{\mu}^{\beta}_{X^{2-}}$	Electrochemical potential in the β'' or β' region	calories / mol
$\Delta\mu_{X_2}$	Variance of the chemical potential of X_2	calories / mole

Symbol	Description	Units
ρ	Resistivity of a material	ohm m
σ	Electrical conductivity	1 / ohm m
σ	Ionic conductivity of an impure crystal	1 / ohm m
σ_e'	Partial conductivity due to excess electrons	1 / ohm m
σ_h.	Partial conductivity due to electron holes	1 / ohm m
σ_{ion}	Ionic conductivity	1 / ohm m
σ_o	Ionic conductivity of pure crystals	1 / ohm m
σ_t	Total conductivity	1 / ohm m
$\overline{v}$	Net drift velocity of carriers	m / s
$\phi^{\alpha''}$	Local electrical potential at cathode	volts
$\phi^{\alpha'}$	Local electrical potential at anode	volts

Chapter 4

Symbol	Description	Units
$\Delta G^{o}_{Cr_3C_2}$	Free energy of formation for Cr_3C_2	calories / mol
K_p	Equilibrium constant	dimensionless
$\bar{P}_{O_2}$	Average oxygen partial pressure	atmospheres
P_{CO}	Partial pressure of carbon monoxide	atmospheres
R^2	Coefficient of correlation	dimensionless
$\bar{t}_{ion}$	Average ionic transference	dimensionless
α	Constant for the partial entropy of transfer	millivolts/Kelvin

Chapter 5

Symbol	Description	Units
P_{CO_2}	Partial pressure of carbon dioxide	atmospheres
P_{O_2}	Partial pressure of oxygen	atmospheres

1.0 Introduction

The use of solid electrolytes provides a precise method for the solution of many important metallurgical problems. Early work by Kiukkola and Wagner[1] on calcia stabilized zirconia and doped thoria compounds was the catalyst for the recent explosion of work in the field of solid electrolytes. At the same time Ure[2] published work on calcium fluoride solid electrolytes which are used as fluorine ion conductors. The solid electrolyte β alumina has been known for over 70 years (first discussed by Rankin and Merwin [3]) to be a cationic conductor of alkali metal ions (i.e. Li^+, Na^+, Ag^+) from room temperature to ≈ 1000 °C. They exhibit extremely high ionic conductivity which is due to loosely packed alkali metal ions. The inorganic silver ion conductors were the first known examples of high ionic conductivity in the solid state (Tuband and Lorenz [4]). They possess extremely high conductivities in excess of 1 ohm^{-1} m^{-1}.

The combination of these varied electrolytes and others provides :

1. A diverse selection of solid electrolytes for ionic conduction of various ions.
2. Solid electrolytes that can function at room temperature with conductivities comparable to liquid electrolytes.
3. Ionic conductivity that is obtainable over a wide range of operating conditions.

Examples of applications are :

1. High energy storage systems for use as a storage medium for load levelling in electric utilities, and as a power source for electric vehicles and buses.
2. Oxygen pumps to transfer oxygen across a solid electrolyte where the current corresponds to the amount of oxygen transferred to or from gaseous or liquid media. In this manner the partial pressure of oxygen can be controlled in flowing gas

streams[5] , measurements of the amount of absorption of oxygen by powders[6] can be performed, and the electrolytic dissociation of water vapor to pure hydrogen can be realized[7].

3. Cells using solid oxide electrolytes can measure the dissolved oxygen content in liquid metals accurately and quickly. Most other techniques measure the total oxygen content, but the dissolved oxygen content primarily influences properties of refined metals.
4. The direct / indirect conversion of various forms of energy into electrical energy. Solid oxides have been used in electrochemical, thermoelectric, and magnetohydrodynamic generators [8].
5. The acquisition of electromotive force (e.m.f.) measurements from galvanic cells to determine thermodynamic values in chemical reactions. The two types of chemical reactions typically examined are the free energy of formation of binary and ternary compounds and the study of activities of individual species in solutions. Numerous reviews on this technique have been presented as evidence to the power of this method [8, 9-17].

The application of oxygen-anionic permeable electrolytes to high temperatures and ultra-low oxygen pressures is only possible with a relatively small selection of solid electrolytes. The two groups consist of those electrolytes of either the fluorite structure (CeO_2 and ThO_2) or the distorted fluorite structure (ZrO_2 and HfO_2). Since CeO_2 tends to be easily reduced at high temperatures and the commercial availability of HfO_2 is limited, ZrO_2 and ThO_2 are the most commonly used oxide electrolyte materials. With these two electrolyte materials, solutions are possible to situations that were previously not attainable or if attainable at all, by far less accurate means. In the preceding section a small sampling of the

possible applications was listed. This is by no means complete, as every year further applications for these advanced ceramics are invented.

It is in the area of e.m.f. measurements that the accuracy of a large number of chemical reactions at both high temperature and ultra low oxygen pressure can be improved upon. Through the use of ZrO_2 and ThO_2, the presently available thermodynamic data can be measured over an extremely wide range of operational parameters.
The zirconia and thoria electrolytes are part of the next generation of advanced functional ceramics, which promise to provide more efficient solutions to material problems, resulting in a higher standard and improved quality of life.

The first part in the experimental section of this thesis is concerned with the free energy of formation of chromium carbide (Cr_3C_2). This reaction is important in that the reaction of carbon with chromium to form the three carbides Cr_3C_2, Cr_7C_3, and $Cr_{23}C_6$ is critical in steel alloys due to their precipitation behavior in high chromium steels and superalloys. The majority of early studies are unreliable whereas the solid state ionic technique promises improved experimental accuracy. A accurate understanding of their thermodynamic properties is essential for predicting their chemical behavior in various environments.

In the second part the thermodynamics of the oxidation of carbon monoxide to carbon dioxide was measured with a solid state ionic cell. Improved thermodynamic data for this reaction along with an accurate cell are required in many chemical and metallurgical processes, e.g, the manufacture of steel, the reduction of metal oxides, welding processes, etc.

2.0 Thermodynamics

2.1 Introduction to Thermodynamics

Thermodynamics is the study of energy and its transformation. The properties consisting of specific volume, pressure, density, and temperature are considered to be macroscopic properties. They represent the average effects of a large number of molecules as opposed to a microscopic approach, where the motions of the individual molecules are studied. Thermodynamics is only concerned with changes of energy and not with the mechanism by which that change occurs. It also has nothing to say about the rate at which a predicted change will occur; this question is of concern to chemical kinetics. Thermodynamics is based on three fundamental laws.

2.2 First Law of Thermodynamics

The first law of thermodynamics is the law of conservation of energy which states that energy can be converted from one form into another but cannot be created or destroyed.

For any process which occurs at constant pressure the heat absorbed or evolved is equal to the change in enthalpy (ΔH). The value of ΔH is defined to be positive if the reaction is endothermic and heat is going into the system, and negative if the reaction is exothermic and heat is leaving the system.

In the simplest case where the specific heat at constant pressure (C_p) remains constant $\Delta H = C_p \Delta T$, where ΔH has units of cal/mol. However, in most cases, the specific heat changes continuously with temperature so the integrated form has to be utilized, given by :

$$\Delta H = \int_{T_1}^{T_2} C_p \, dT = \int_{T_1}^{T_2} \left(a + bT + cT^{-2} \right) dT \qquad (2.1)$$

where T_1 and T_2 are the initial and final temperatures in K, C_p has units of cal/mol K, and ΔH has units of cal/mole. Since C_p can vary with temperature (T) a term consisting of $a + bT + cT^{-2}$ is required.

For a given reaction the enthalpy is given by :

$$\Delta H_{reaction} = \Delta H_{products} - \Delta H_{reactants} \qquad (2.2)$$

Note : for elements, $\Delta H^{\circ}_{298} = 0$

The superscript ^{o} indicates that a substance is in its standard state which is defined as :

1. If in solution the concentration is 1 molal (1 mole of substance per 1000 grams of solvent).
2. For a solid it is required to be in the most stable crystalline form.
3. The standard state does not refer to any particular temperature - it can in fact be any chosen; in this case 298 K was chosen.

2.3 Second Law of Thermodynamics

The second law defines the direction in which any chemical or physical process involving energy takes place. It states that heat cannot pass from a colder to a warmer body without work being provided by an external agency.

The first law of thermodynamics stipulates for chemical or physical changes to occur that only energy need be conserved. It provides no basis for determining if a proposed change is spontaneous. However the second law of thermodynamics provides criteria for making predictions of spontaneity.

For a thermodynamic process, the entropy of the universe will either increase or for the case of a reversible process remain at the same level. Entropy increases in the universe from irreversibility during a given process. It is impossible for any thermodynamic process to occur which involves a reduction in the entropy of the universe.

It can been stated that as the temperature of a substance goes up its entropy increases. The entropy change (ΔS) due to heating can be calculated as follows :

$$\Delta S = \int_{T_1}^{T_2} \frac{C_p}{T} dT = \int_{T_1}^{T_2} \frac{\left(a + bT + cT^{-2}\right)}{T} dT \qquad (2.3)$$

Tables of entropy at standard temperature and a pressure of 1 atm have calculated the value for S^o_{298} through the use of the equation :

$$S^o_{298} = S_o + \Delta S = S_o + \int_0^{298} \frac{C_p}{T} dT = S_o + \int_0^{298} \frac{\left(a + bT + cT^{-2}\right)}{T} dT \qquad (2.4)$$

where S_o is the entropy of the substance at absolute zero and ΔS is the change in entropy due to heating, C_p is the specific heat which is not a constant through the temperature range, and entropy has units of cal/mole K.

As is the case with enthalpy, for a chemical reaction the entropy of a reaction is equal to :

$$\Delta S_{reaction} = S_{products} - S_{reactants} \tag{2.5}$$

2.4 Third Law of Thermodynamics

The Gibbs free energy function G is defined by the equation :

$$G = H - T S \tag{2.6}$$

For a change at constant temperature and pressure :

$$\Delta G = \Delta H - T\Delta S \tag{2.7}$$

For a spontaneous reaction conducted at constant pressure and temperature where ΔG is negative, the decrease in the Gibbs free energy is a measure of the maximum useful work that the system can do. Useful work is used to indicate that ΔG does not include pressure-volume work. Since only a spontaneous reaction has the capacity to do work, ΔG is a measure of spontaneity. This particular equation is important in that it provides the important link between entropy (ΔS) and enthalpy (ΔH). Enthalpy alone cannot determine whether a reaction will proceed i.e. knowing whether a reaction is exothermic (releases heat, $-\Delta H$) or endothermic (absorbs heat, $+\Delta H$) is insufficient. There are endothermic reactions which will proceed due to the nature of their entropy change i.e. a significantly large positive value of ΔS. The enthalpy change will generally determine whether a reaction will occur, with large negative values usually indicating a spontaneous reaction whereas positive values usually indicating a non-spontaneous reaction; however, there are endothermic reactions where the entropy is large enough so that the reaction will proceed. Most reactions are known accurately at 298 K or within a small temperature range, whereas in most metallurgical systems the temperatures are considerably higher.

As a first approximation for reactions at temperatures other than 298 K the following is used assuming that ΔH and ΔS vary only slightly with temperature :

$$\Delta G_T = \Delta H_{298} - T\Delta S_{298} \tag{2.8}$$

This equation can be used for temperatures other than 298K if the values for C_p are small or the two terms involving C_p tend to cancel out, any latent heats present are not significant, and the entropy changes involved in any transformations are also small. However if the reaction does not meet the above requirements corrections for the individual terms will be required :

$$\Delta G_{T_2} = \Delta H_{T_2} - T_2\, \Delta S_{T_2} \tag{2.9}$$

The individual terms in the equation (i.e. ΔH_{T_2} and ΔS_{T_2}) are calculated for the temperature T_2.

Through the use of solid electrolyte cells, it is possible to measure accurately and precisely free energies and other thermodynamic functions over wide ranges of temperature and pressure. All that is required is the measurement of a voltage produced by a simply constructed galvanic cell.

2.5 Electromotive Force Cells

To obtain the useful work from a chemical reaction is to make it produce electrical work by having it serve as the cell reaction of a voltaic cell. In the normal operation of a discharging cell, less than the maximum amount of useful work is obtained due to the internal resistance of the cell, concentration changes which occur within the cell as it delivers current, and activation polarization. The deviation from equilibrium voltage is known as the overvoltage or activation polarization (η_a) in volts, which is related to the exchange current density i_o by the equation:

$$\eta_a = \pm\beta \log\frac{i}{i_o} \tag{2.10}$$

where i is the current in A / cm^2, β is the Tafel constant, and i_o is the exchange current density in A / cm^2 which is the rate of oxidation and reduction for an electrode reaction at equilibrium.

It is obvious from equation (2.10) depending on the value of β, that any large flows of current in comparison to the exchange current density at either electrode would result in a significant perturbation from the equilibrium voltage. In the case of thermodynamic measurements, a large exchange current density would minimize the activation polarization. Unfortunately, there is no way of theoretically predicting exchange current densities; they have to be measured and there is very little information for solid electrolytes. Therefore, it is important to check that the cell is operating reversibly by passing a current in either direction through the cell or temporarily disconnecting the external circuit and then checking to see that the cell returns to the original voltage.

By eliminating or reducing the current flow to negligible levels the reversible electromotive force of the reaction can be determined. This current flow can be due to either electrical leakage from the external circuit (which is essentially eliminated by using a potentiometer

with high impedance) and/or from electronic conductivity within the solid electrolyte (which is minimized by operating the cell at the appropriate pressure and temperature).

If a cell is operating reversibly, the maximum electromotive force is measured which can be used to calculate the Gibbs free energy of a reaction by using the equation :

$$\Delta G = - zFE^{o} \qquad (2.11)$$

where z is the number of moles of electrons transferred which is a positive number equal to the number of electrons transferred in the cell reaction, E^{o} is the reversible e.m.f. of the cell in volts, and F is the value of the Faraday (F = 23060.36 +/- 0.065 cal/V equiv).

Under conditions of reversible operation the cell is exactly balanced against an external electromotive force so that no charging or discharging of the cell takes place, and therefore the cell effectively would allow only an infinitesimal quantity of electricity to pass. When the chemical reaction occurs the quantity of electric charge that flows is equal to zF and when this quantity of electrical charge is transported across a potential difference given by E^{o}, the amount of work expended is equal to zFE^{o}.

Utilizing equation (2.11) and electromotive force measurements from a cell operating reversibly, it is possible to determine ΔG^{o}, ΔH^{o}, and ΔS^{o} for the cell reaction. Due to the improved accuracy of electrical measurements, the determination of thermodynamic properties by this method is more exact than through the use of equilibrium constants or the calorimetric determination of the enthalpies of reaction. In addition, by using solid electrolytes under the appropriate conditions of temperature and pressure, it is possible to measure thermodynamic values in regions not normally reached.

The standard free energy change ΔG^{o} is the free energy change for a reaction at a chosen temperature (usually 25°C) and usually 1 atm in which the reactants are in their standard states and are converted to products in their standard states. For the formation of

compounds, ΔG^{o}_{f} is defined as the change in standard free energy when one mole of the compound is prepared from its constituent elements, where the standard free energy of formation of any element is zero. The value of ΔG^{o} for a reaction is equal to the sum of the standard free energies of formation of the products minus the sum of the standard free energies of formation of the reactants.

3.0 SOLID STATE IONIC MATERIALS

3.1 Fundamental Electrical Characteristics

Materials are divided into three categories, conductors, insulators, and semiconductors. Metals are conductors since they contain delocalized electrons which can move in three dimensions throughout the metal; in this case bonding electrons are associated with all atoms in a metallic structure. Insulators consist of ceramics and polymeric materials with strongly held electrons and non-diffusing ions. A semiconductor is a material having a resistivity between that of a conductor and an insulator and having a negative temperature coefficient of resistance (i.e. as temperature rises conductivity increases).

The ionic electrolytes used for the experimental apparatus are ceramics which exhibit ionic conductivity over a useful range of temperature and chemical potential (i.e. oxygen pressure in the case of oxide ionic electrolytes). As in electronic semiconductors these ionic semiconductors have increased conductivity with increased temperature.

Resistance is defined as the ratio of the potential difference between the ends of a conductor to the electrical current flowing in the conductor. Ohm's law describes this phenomena as follows :

$$R = V / I \tag{3.1}$$

where V is the potential difference between two electrodes in volts, I is the current flowing in amperes, and R is the resistance in volts/ampere or ohms (Ω).

The extent to which a conductor resists the flow of a given current depends upon its physical dimensions, the nature of the material of which it is made, its temperature, and in some cases the extent to which it is illuminated. Conductivity σ ($ohm^{-1}m^{-1}$) depends on

the number of charge carriers n (carriers /m^3), the charge q (C / carrier), and the mobility μ (m^2/volt s) of the charge carriers.

The equation has the form :

$$\sigma = n\ q\ \mu \tag{3.2}$$

In metals and semiconductors in which electrons are the charge carriers, the charge per carrier is :

0.16×10^{-18} C. For ionic materials where the charge is carried by diffusing ions the charge is an integer number of electron charges being either + or - depending on whether if the carriers are cations or anions. In the case of calcia stabilized zirconia the O^{-2} anions would carry a charge of -0.32×10^{-18}

C / carrier.

Mobility μ (m^2/ volt second) results from a net or drift velocity $\bar{v}$ (m/s) of a carrier in an electric field ε (volt/m) given by the equation :

$$\mu = \bar{v} / \varepsilon \tag{3.3}$$

The resistivity ρ (Ω-m) of a material is related to its conductivity by :

$$\sigma = 1/\rho \tag{3.4}$$

Resistivity of a material can be related to resistance R (Ω) by :

$$R = \rho L / A \tag{3.5}$$

where L (m) is the length and A (m^2) is the cross sectional area.

3.2 Ionic Conductivity and Temperature

Ionic conductivity arises from the diffusion of ions under the influence of an electric potential gradient. Equation (3.6) relates the interstitial diffusion coefficient D_i to the conductivity σ :

$$\frac{\sigma}{D_i} = \frac{N_i q^2}{k T} \tag{3.6}$$

where N_i is the number of interstitial ions per unit volume, q is the charge of the diffusing ion, k is Boltzmann's constant, and T the temperature in K.

The tracer coefficient D_t is usually measured for a diffusing ion which uses a vacancy mechanism, where each jump of the tracer is correlated and equation (3.6) becomes :

$$\frac{\sigma}{D_t} = \frac{N q^2}{f k T} \tag{3.7}$$

In this case N is the total number of diffusing ions per unit volume and the correlation factor f is a crystallographic quantity that takes into account that the conductivity follows the motion of the defect whereas tracer diffusion would follow the ion under examination directly.

The value for the correlation factor f varies with the mechanism and is discussed thoroughly by Barr and LeClaire[18]. For approximate values of D, f can be estimated at 1, since it usually lies between 0.5 and 1.5. There are some fundamental problems with this equation since it applies only where one ion and one diffusional mechanism is operating. This is not always the case, as neutral species may contribute to D but not to σ, resulting in unjustified high values for D.

For the diffusion of an ion in a solid, equation (3.8) relates the diffusion coefficient D to the temperature T :

$$D = D_0 \exp^{-Q/RT} \tag{3.8}$$

where D_0 (cm^2/s) is a constant, Q (cal/mole) the activation energy for the process, R is the gas constant (cal/mol K), and T (K) the absolute temperature

For CaO stabilized ZrO_2 a typical value for D_0 equals 0.018 cm^2/s and 31.2 ± 4.3 cal/mole for Q in the temperature range 800-1097 °C [19]. The activation energies of yttria stabilized zirconia and yttria doped thoria are discussed in section 3.9 and 3.10.

As temperature is varied D is found to possess discrete values resulting in a curve that appears as the plot in Fig. 3-1 of Log D versus 1/Temperature.

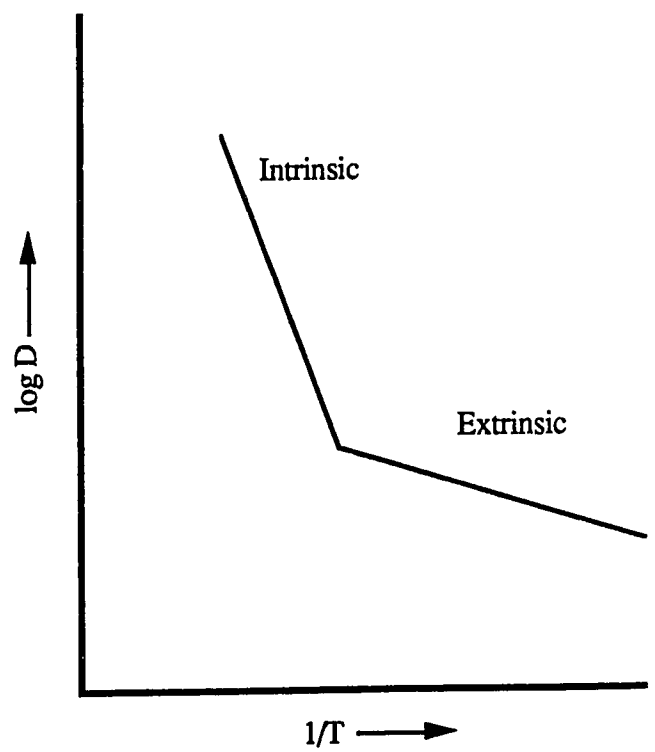

Fig. 3-1. Log D versus 1/Temperature (K).

In the high temperature region (T > 1/2 of melting point), the diffusion is found to be intrinsic where the diffusing species are formed and ionic motion is due to the available thermal energy. In this region Q will be high at approximately 150 +/- 50 kcal/mole for

oxides above 1000 °C. Intrinsic diffusion is found to vary sharply with oxygen pressure for the oxides. For lower temperatures extrinsic factors such as impurities and inhomogeneities will assist or retard self-diffusion in a solid, changing the value of D_O and Q which results in the change of the curve in Fig. 3-1. Due to these reasons the value for D can vary dramatically between samples in the lower temperature regions. For oxides in the extrinsic region Q will run at about 60 +/- 40 kcal/mole. The main conclusion from this with respect to the value of D, is that the diffusion coefficients at the higher temperatures are fairly consistent from study to study assuming that crystal orientations and oxygen pressures are the same. However at lower temperatures in the extrinsic region, the values can vary greatly with a group of experimenters, due to impurity concentrations and crystallinity. As shown in Fig. 3-2 as temperature increases ionic conductivity rises.

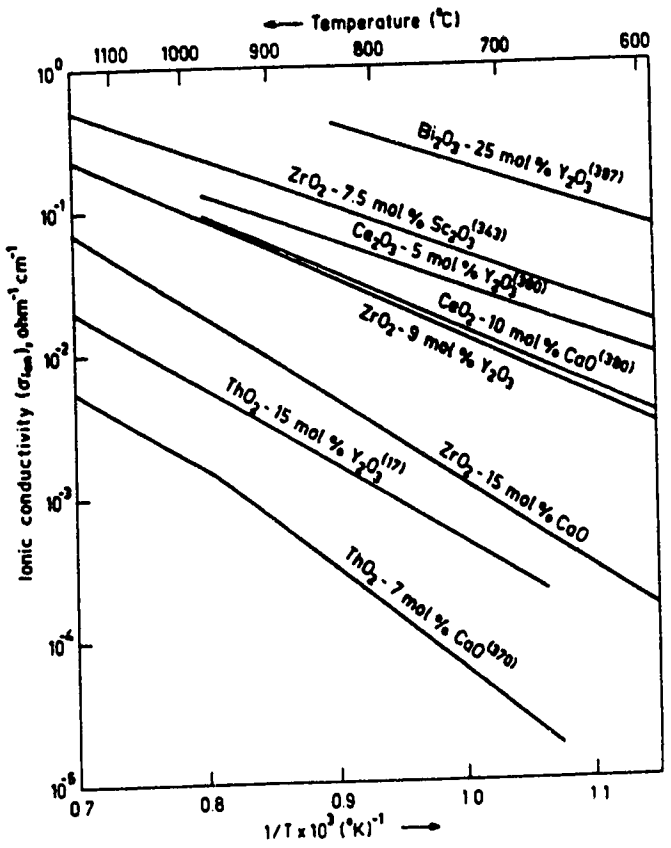

Fig. 3-2. Log Ionic Conductivity (1/ohm cm) versus 1/Temperature (K) [20].

3.3 Ionic Conductivity and Dopant Concentration

The conductivity ratio between the pure and impure crystals has been shown to follow [21] :

$$\frac{\sigma}{\sigma_o} = \left(A + \frac{B}{A}\right) / \ (1 + B) \qquad (3.9)$$

where σ_o & σ represent the ionic conductivity of the pure and impure crystal , $A = x_1/x_o = x_o/x_2$, with x_1 and x_2 being the mole fractions of the two intrinsic defects in the dissociated state, such that $x_1 \ x_2 = x_o^2$ and B = ratio of the mobilities of defects x_2 and x_1.

At a specific temperature the conductivity varies linearly with the addition of the impurity up to about 1% defect concentration at which the rate of increase of the conductivity slows and eventually the conductivity begins to drop. As shown in Fig. 3-3 the behavior of ThO_2 doped with CaO and Y_2O_3 displays this phenomenon up to about 3-4% when the relationship breaks down and the ionic conductivity decreases. An explanation for this phenomenon is that clustering or ordering of defects takes place[22] as the defect concentration increases.

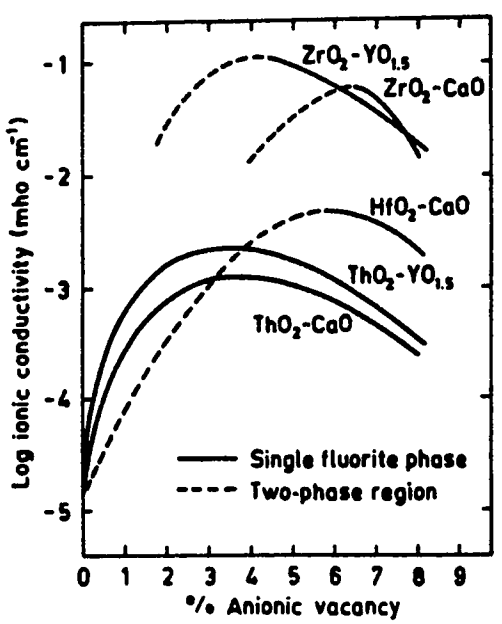

Fig. 3-3. Log of Ionic Conductivity versus % Anionic Vacancy[21].

3.4 Ionic Transference Number

In ionic solids the presence of ionic defects result in ionic conductivity, with electronic defects resulting in electronic conductivity which is undesirable in solid electrolytes. For a solid electrolyte to be practical the ratio of ionic to electronic conductivity should exceed at least 100. The total conductivity is given as :

$$\sigma_t = \sum_i n_i z_i e \mu_i \tag{3.10}$$

where n_i, z_i, and μ_i are the concentration, valency, and mobility of the ith charge carrying species and e is the electronic charge.

The total conductivity σ_t of a mixed conductor is the sum of the partial conductivities of ions σ_{ion} , excess electrons $\sigma_{e'}$, and electron holes σ_h. given by :

$$\sigma_t = \sigma_{ion} + \sigma_{e'} + \sigma_h. \tag{3.11}$$

The ionic transference number t_{ion} is given by the equation :

$$t_{ion} = \frac{\sigma_{ion}}{\sigma_t} = \frac{\sigma_{ion}}{\sigma_{ion} + \sigma_{e'} + \sigma_h.} \tag{3.12}$$

For a solid electrolyte to be useful the ratio of ionic to electronic defects should exceed 100-1000, due to electronic defects being considerably more mobile.

3.5 Derivation of Electromotive Force Equations for Solid Electrolytes

For a galvanic cell consisting of two chemically identical electrodes with a solid state electrolytic solution of $(L,M)X_2$ and two electrodes reversible to the same ionic species X^z, the cell can be represented by :

$$Pt', X_2(\mu'_{X_2}) \mid \overset{\text{Solid Electrolyte}}{(L,M)X_2} \mid X_2(\mu''_{X_2}), Pt'' \qquad (3.13)$$

where the quantities μ'_{X_2} and μ''_{X_2} represent the chemical potentials established at the electrodes by the partial pressures of the gaseous component X_2 or by the condensed phase equilibria represented by the typical reactions :

$$[A]_B + \tfrac{1}{2}X_2 = AX \qquad (3.14)$$

where $[A]_B$ represents an alloy of the metals A and B or by the equation :

$$C + \tfrac{1}{2}X_2 = [CX]_{DX} \qquad (3.15)$$

where $[CX]_{DX}$ represents a solution of the compounds CX and DX.

When the above constituents are available at the electrodes the associated cations A^{z+}, B^{z+}, C^{z+}, D^{z+} may dissolve into the solid electrolyte with the cell written as :

$$\begin{array}{ccccccc} & AX & & & CX & & \\ & BX & & \text{Solid Electrolyte} & DX & & \\ Pt',X_2(\mu'_{X_2}) \mid & (L,M)X_2 & \mid & (L,M)X_2 & \mid (L,M)X_2 \mid & X_2(\mu''_{X_2}),Pt'' & (3.16) \\ \alpha' & \beta' & & & \beta'' & \alpha'' & \end{array}$$

where α' or α'' is the phase associated with the Pt leads at the anode or cathodes, and β' or β'' refers to the interfacial regions at the anode/solid electrolyte and the cathode/electrolyte junctions.

If local thermodynamic equilibrium is maintained at the interfaces between the various phases the following treatment is applicable whereby the product of the electromotive force given by E and the Faraday constant (F) is given by :

$$FE = F(\phi^{\alpha''} - \phi^{\alpha'}) = \frac{1}{z_i}(\overline{\mu}_i^{\alpha''} - \overline{\mu}_i^{\alpha'}) = -(\overline{\mu}_e^{Pt''} - \overline{\mu}_e^{Pt'}) \qquad (3.17)$$

where $\phi^{\alpha''}$ and $\phi^{\alpha'}$ are the local electrical potentials in volts between the left and right side of the cell, z_i is the charge associated with the species i, $\overline{\mu}_i^{\alpha''}$ and $\overline{\mu}_i^{\alpha'}$ are the electrochemical potentials established at the right and left electrodes, and $\overline{\mu}_e^{Pt''}$ and $\overline{\mu}_e^{Pt'}$ are the electrochemical potentials established at the two electrode-electrolyte interfaces.

At each electrode-electrolyte interface, the following chemical equilibrium is established if the cell is reversible :

$$\frac{1}{2}X_2 - z_{X^{-2}}e^- = X^{2-} \qquad (3.18)$$

where $z_{X^{-2}}$ is equivalent to the charge on the anionic species X^{2-} (in the case of oxide electrolytes equal to -2) and e- is an electron.

Therefore for the case of oxide electrolytes :

$$\frac{1}{2}O_2 + 2e^- = O^{2-} \qquad (3.19)$$

where O^{2-} is an oxygen anion in the electrolyte.

By multiplying equation (3.18) by two and setting the chemical potential of the gas phase X_2 equal to $\mu^{\alpha}_{X_2}$ with the electrochemical potentials given by $\bar{\mu}^{\alpha}_{e}$ and $\bar{\mu}^{\alpha}_{X_2}$:

$$\mu^{\alpha}_{X_2} - 2z_{X^{-2}}\bar{\mu}^{\alpha}_{e} = 2\bar{\mu}^{\alpha}_{X^{2-}} \tag{3.20}$$

By rearranging equation (3.20) and since :

$$\bar{\mu}_e^{\alpha} = \bar{\mu}_e^{Pt}; \qquad \bar{\mu}^{\alpha}_{X^{2-}} = \bar{\mu}^{\beta}_{X^{2-}} \tag{3.21}$$

it follows that :

$$\bar{\mu}_e^{Pt} = \frac{1}{2\,z_{X^{2-}}}(\mu^{\alpha}_{X_2} - 2\bar{\mu}^{\beta}_{X^{2-}}) \tag{3.22}$$

Using $FE = -(\bar{\mu}_e^{Pt''} - \bar{\mu}_e^{Pt'})$ from equation (3.17) and equation (3.22) above results in :

$$FE = -\frac{1}{2\,z_{X^{2-}}}(\mu^{\alpha''}_{X_2} - \mu^{\alpha'}_{X_2}) + \frac{1}{z_{X^{2-}}}(\bar{\mu}^{\beta''}_{X^{2-}} - \bar{\mu}^{\beta'}_{X^{2-}}) \tag{3.23}$$

The second term in equation (3.23) given by $\frac{1}{z_{X^{2-}}}(\bar{\mu}^{\beta''}_{X^{2-}} - \bar{\mu}^{\beta'}_{X^{2-}})$ represents the electrochemical potential of the ionic species X^{2-}, which is established in the solid electrolyte phases β'' and β' in contact with the right and left electrode. If the second term in the equation is not negligible and the dissolution of the electrode components is minimal, the second term according to irreversible thermodynamics [23,24] for finite electronic conduction consists of :

Case 2. If there is dissolution of the electrode components but $t_{X^{-2}} = 1$, all the transference numbers in the integral in equation (3.24) would essentially be equivalent to zero and again equation (3.23) would reduce to equation (3.25).

Case 3 . For the case where there is finite electronic conduction but negligible dissolution of A,B,C, and / or D in the electrolyte, and if there are only small deviations from stoichiometry in the electrolyte, the transference numbers $t_{L^{+4}} + t_{M^{+4}} + t_e + t_{X^{-2}} = 1$ and $d\mu_{LX_2} \cong d\mu_{MX} \cong 0$ then $t_e + t_{X^{-2}} = 1$.

The irreversible diffusion potential in equation (3.24) would reduce to :

$$\frac{1}{z_{X^{2-}}}(\bar{\mu}^{\beta''}_{X^{2-}} - \bar{\mu}^{\beta'}_{X^{2-}}) = -\int_{\beta'}^{\beta''} \frac{t_e}{4}\, d\mu_{X_2} \qquad (3.26)$$

Case 4. If A,B,C, and D dissolve in the electrolyte but the transference numbers of $t_{A^{+2}}$, $t_{B^{+2}}$, $t_{C^{+2}}$, $t_{D^{+2}}$, $t_{L^{+4}}$, and $t_{M^{+4}}$ of the ionic constituents are negligible. This would result in $t_e + t_{X^{-2}} = 1$. The irreversible diffusion potential in equation (3.24)would again reduce to equation (3.26).

From these manipulations two solutions to equation 3.22 are possible consisting of :

1. In case 1 and 2 if the diffusion potential in equation (3.23) is found to be negligible and since the charge on the species X^{2-} is equal to -2 equation (3.25) reduces to :

$$E = \frac{1}{4F}\Delta\mu_{X_2} \qquad (3.27)$$

Case 2. If there is dissolution of the electrode components but $t_{X^{-2}} = 1$, all the transference numbers in the integral in equation (3.24) would essentially be equivalent to zero and again equation (3.23) would reduce to equation (3.25).

Case 3 . For the case where there is finite electronic conduction but negligible dissolution of A,B,C, and / or D in the electrolyte, and if there are only small deviations from stoichiometry in the electrolyte, the transference numbers $t_{L^{+4}} + t_{M^{+4}} + t_e + t_{X^{-2}} = 1$ and $d\mu_{LX_2} \cong d\mu_{MX} \cong 0$ then $t_e + t_{X^{-2}} = 1$.

The irreversible diffusion potential in equation (3.24) would reduce to :

$$\frac{1}{z_{X^{2-}}}(\bar{\mu}^{\beta''}_{X^{2-}} - \bar{\mu}^{\beta'}_{X^{2-}}) = -\int_{\beta'}^{\beta''} \frac{t_e}{4}\, d\mu_{X_2} \qquad (3.26)$$

Case 4. If A,B,C, and D dissolve in the electrolyte but the transference numbers of $t_{A^{+2}}$, $t_{B^{+2}}$, $t_{C^{+2}}$, $t_{D^{+2}}$, $t_{L^{+4}}$, and $t_{M^{+4}}$ of the ionic constituents are negligible. This would result in $t_e + t_{X^{-2}} = 1$. The irreversible diffusion potential in equation (3.24)would again reduce to equation (3.26).

From these manipulations two solutions to equation 3.22 are possible consisting of :

1. In case 1 and 2 if the diffusion potential in equation (3.23) is found to be negligible and since the charge on the species X^{2-} is equal to -2 equation (3.25) reduces to :

$$E = \frac{1}{4F}\Delta\mu_{X_2} \qquad (3.27)$$

If oxygen is the active species equation (3.27) becomes :

$$E = \frac{1}{4F} \Delta\mu_{O_2} \tag{3.28}$$

Since $\mu_{O_2} = \mu^{\circ}_{O_2} + RT \ln P_{O_2}$ where μ_{O_2} is the chemical potential for oxygen in an ideal mixture, $\mu^{\circ}_{O_2}$ is the standard chemical potential of oxygen, R is the gas constant, T the temperature in K, and P_{O_2} the oxygen partial pressure, it follows from equation (3.28) that:

$$E = \frac{RT}{4F} \ln \frac{P''_{O_2}}{P'_{O_2}} \tag{3.29}$$

In this case the cell measures the electromotive force due to different oxygen pressures on opposite sides of the electrolyte.

2. In case 3 and 4 the diffusion potential is significant so that it must be evaluated. The diffusion potential is given by :

$$\frac{1}{z_{X^{2-}}}(\bar{\mu}^{\beta''}_{X^{2-}} - \bar{\mu}^{\beta'}_{X^{2-}}) = -\int_{\beta'}^{\beta''} \frac{t_e}{4} d\mu_{X_2} \tag{3.30}$$

Since $\bar{\mu}^{\alpha}_{x^{2-}} = \bar{\mu}^{\beta}_{x^{2-}}$, combining equation (3.23) with equation (3.30) results in :

$$E = \frac{1}{4F}(\mu^{\alpha''}_{X_2} - \mu^{\alpha'}_{X_2}) - \frac{1}{4F}\int_{\mu^{\alpha'}_{x_2}}^{\mu^{\alpha''}_{x_2}} t_e \, d\mu_{X_2} \tag{3.31}$$

Since the first part of equation (3.31) consists of :

$$\mu_{x_2}^{\alpha''} - \mu_{x_2}^{\alpha'} \text{ which equals } \int_{\mu_{x_2}^{\alpha'}}^{\mu_{x_2}^{\alpha''}} d\mu_{X_2} \tag{3.32}$$

equation (3.31) becomes :

$$E = \frac{1}{4F}\int_{\mu_{x_2}^{\alpha'}}^{\mu_{x_2}^{\alpha''}} d\mu_{X_2} - \frac{1}{4F}\int_{\mu_{x_2}^{\alpha'}}^{\mu_{x_2}^{\alpha''}} t_e\, d\mu_{X_2} \tag{3.33}$$

Given that $t_{X^{-2}} + t_e = 1$ and therefore $t_{ion} = t_{X^{-2}} = 1 - t_e$ it follows that :

$$E = \frac{1}{4F}\int_{\mu_{x_2}^{\alpha'}}^{\mu_{x_2}^{\alpha''}} t_{ion} d\mu_{X_2} \tag{3.34}$$

The formula for the e.m.f. of an oxygen cell with electronic and ionic conduction is given by :

$$E = \frac{1}{4F}\int_{\mu_{O_2}'}^{\mu_{O_2}''} t_{ion}\, d\,\mu_{O_2} \tag{3.35}$$

Considering the case where there is mixed conduction, integration of equation (3.35) is possible if P_{O_2}'' and P_{O_2}' are similar in magnitude, resulting in :

$$E = \bar{t}_{ion}\frac{RT}{4F}\ln\frac{P_{O_2}''}{P_{O_2}'} \tag{3.36}$$

where $\bar{t}_{ion}$ is the average transference number for the oxygen anion carrier species in the oxide electrolyte.

It should be noted that equation (3.36) applies to an ideal cell where local equilibrium at the phase boundaries is established. In the case where $\bar{t}_{ion}$ is smaller than unity an internal short circuit will result in cathodic and anodic reactions with finite rates.

The final equation to be discussed is derived from equation (3.12) consisting of :

$$t_{ion} = \left(1 + \frac{\sigma_{e'}}{\sigma_{ion}} + \frac{\sigma_{h\cdot}}{\sigma_{ion}}\right)^{-1} \tag{3.37}$$

3.6 Conductivity and Oxygen Pressure

The formation of defect structures in the solid electrolytes used will now be described. For ZrO_2 stabilized with CaO the major defect is oxygen vacancies ($V_{\ddot{O}}$ with an effective +2 charge), which form extrinsically when CaO and ZrO_2 form a solid solution according to :

$$CaO \Rightarrow Ca''_{Zr} + O_o + V_{\ddot{O}} \qquad (3.38)$$

where Ca''_{Zr} is a Ca^{+2} ion occupying a Zr^{+4} ion site (therefore Ca''_{Zr} carries a net effective charge of -2), and O_o is an oxygen ion on an oxygen site.

With ZrO_2 stabilized with Y_2O_3 the major defect is oxygen vacancies ($V_{\ddot{O}}$) which form according to:

$$Y_2O_3 \Rightarrow 2Y'_{Zr} + 3O_o + V_{\ddot{O}} \qquad (3.39)$$

where Y'_{Zr} is a Y^{+3} ion occupying a Zr^{+4} ion site (therefore Y'_{Zr} carries a net effective charge of -1).

Finally for ThO_2 doped with Y_2O_3 the major defect is again oxygen vacancies ($V_{\ddot{O}}$) which form similar to ZrO_2 - Y_2O_3 according to :

$$Y_2O_3 \Rightarrow 2Y'_{Th} + 3O_o + V_{\ddot{O}} \qquad (3.40)$$

where Y'_{Th} is a Y^{+3} ion occupying a Th^{+4} ion site resulting in Y'_{Th} carrying a net effective charge of -1.

Next the relationship between partial conductivities ($\sigma_{e'}$ and $\sigma_{h\cdot}$) with oxygen partial pressure is discussed. The two conditions to be considered are low and high oxygen pressure.

Case 1. Low Oxygen Pressure

With decreased oxygen pressure in the atmosphere surrounding the electrolyte, oxygen will be lost from the lattice according to the reaction :

$$O_O = \frac{1}{2}O_2(P_{O_2}) + V_{\ddot{O}} + 2e' \tag{3.41}$$

where $V_{\ddot{O}}$ is an oxygen vacancy and e' is an excess electron.

For the case where an equilibrium is established between the the gas phase and the oxide, the mass action law can be applied to equation (3.41) resulting in :

$$e' = K_1 P_{O_2}^{-1/4} \left(V_{\ddot{O}}\right)^{-1/2} \tag{3.42}$$

According to equation (3.41) the concentration of oxygen vacancies is one half of the concentration of electrons and when the concentration of all other defects is small it follows that :

$$e' = K_1' P_{O_2}^{-1/6} \tag{3.43}$$

For stabilized zirconia and thoria based solutions the concentration of oxygen vacancies is fixed by chemical doping resulting in equation (3.42) reducing to :

$$e' = K_1'' P_{O_2}^{-1/4} \tag{3.44}$$

The partial conductivity $\sigma_{e'}$ is proportional to the mobility and concentration of excess electrons. If the mobility of the excess electrons $\mu_{e'}$ is not a function of the oxygen pressure :

$$\sigma_{e'} = K_1'' F \mu_{e'} P_{O_2}^{-1/4} \tag{3.45}$$

Case 2. High Oxygen Pressure

The second case is where the oxygen pressure is high enough so that excess oxygen will be accommodated within the oxide lattice. In this case interstitial oxygen ions O_i'' and electron holes $h^{\cdot}$ are formed according to :

$$\frac{1}{2}O_2(P_{O_2}) = O_i'' + 2h^{\cdot} \tag{3.46}$$

or cation vacancies are formed by the equation :

$$\frac{1}{2}O_2(P_{O_2}) = V_{Me}'' + 2h^{\cdot} + MeO \tag{3.47}$$

where V_{Me}'' are cation vacancies, $h^{\cdot}$ are electron holes and MeO is a metal oxide.

In both cases electron holes $h^{\cdot}$ are formed so as to maintain electrical neutrality.

For the case in equation (3.46) when either :

$$O_i'' = \frac{1}{2}h^{\cdot} \tag{3.48}$$

or in equation (3.47) where :

$$V_{Me}'' = \frac{1}{2}h^{\cdot} \tag{3.49}$$

is applicable it can be shown that the concentration of electron holes is proportional to $P_{O_2}^{1/6}$ for both equations (3.46) and (3.47). This relationship with oxygen pressure is valid if the concentration of all other defects is small in comparison. For this situation the electrolyte behaves as p-type semiconductor which is not suitable for use in an ionic oxygen cell.

In the situation where the concentration of oxygen vacancies in the electrolyte is large due to chemical doping, the free lattice sites are filled as follows :

$$\tfrac{1}{2}O_2(P_{O_2}) + V_{\ddot{O}} = O_o + 2h^{\cdot} \tag{3.50}$$

Since $V_{\ddot{O}}$ is nearly constant the following equation is appropriate :

$$h^{\cdot} = K_2'' \, P_{O_2}^{1/4} \tag{3.51}$$

It follows from this that the partial conductivity of the holes is given by :

$$\sigma_{h^{\cdot}} = K_2'' \, F \, \mu_{h^{\cdot}} \, P_{O_2}^{1/4} \tag{3.52}$$

There are two special values of P_{O_2} at which the ionic conductivity equals either the conductivity of the excess electrons designated by $P_{\ominus}$ and given by the equation :

$$\sigma_{ion} = \sigma_{e'} = K_1'' \, F \, \mu_{e'} \, P_{\ominus}^{-1/4} \tag{3.53}$$

or where the ionic conductivity equals the conductivity of excess holes designated by $P_{\oplus}$ and given by the equation :

$$\sigma_{ion} = \sigma_{h^{\cdot}} = K_2'' \, F \, \mu_{h^{\cdot}} \, P_{\oplus}^{1/4} \tag{3.54}$$

Substituting (3.45), (3.52), (3.53), and (3.54), into (3.37) results in :

$$t_{ion} = \left[1 + \frac{K_1'' \, F \, \mu_{e'} \, P_{O_2}^{-1/4}}{K_1'' \, F \, \mu_{e'} \, P_{\ominus}^{-1/4}} + \frac{K_2'' \, F \, \mu_{h^{\cdot}} \, P_{O_2}^{1/4}}{K_2'' \, F \, \mu_{h^{\cdot}} \, P_{\oplus}^{1/4}} \right]^{-1} \tag{3.55}$$

which is equivalent to :

$$t_{ion} = \left[1 + \left(\frac{P_{O_2}}{P_{\ominus}}\right)^{-1/4} + \left(\frac{P_{O_2}}{P_{\oplus}}\right)^{1/4} \right]^{-1} \tag{3.56}$$

According to equation (3.56) as the oxygen pressure is varied there are three regions of operation, consisting of :

1. A region where the conductivity due to either electron holes or excess electrons is negligible compared to the ionic conductivity
2. The second area is where the conductivity due to excess electrons becomes significant and eventually exceeds the contribution due to ionic species.
3. The third and final region is where the conductivity is primarily due to electron holes. These phenomena are displayed in Fig. 3-4 where the oxygen pressure is varied logarithmically and the ionic transference number varies from 0 to 1.0. From this figure it can be observed that there are two values of oxygen pressure $P_{\ominus}$ and $P_{\oplus}$ at which $t_{ion} = 0.5$ and $t_e = 0.5$.

The insertion of (3.56) into (3.35) results in :

$$E = \frac{1}{4F}\int_{\mu_{O_2}'}^{\mu_{O_2}''} \left[1 + \left(\frac{P_{O_2}}{P_{\ominus}}\right)^{-1/4} + \left(\frac{P_{O_2}}{P_{\oplus}}\right)^{1/4} \right]^{-1} d\,\mu_{O_2} \tag{3.57}$$

Integration of (3.57) results in the equation :

$$E = \frac{RT}{F}\left[\ln\frac{P_{\oplus}^{1/4} + P_{O_2}'^{\,1/4}}{P_{\oplus}^{1/4} + P_{O_2}''^{\,1/4}} + \ln\frac{P_{\ominus}^{1/4} + P_{O_2}''^{\,1/4}}{P_{\ominus}^{1/4} + P_{O_2}'^{\,1/4}} \right] \tag{3.58}$$

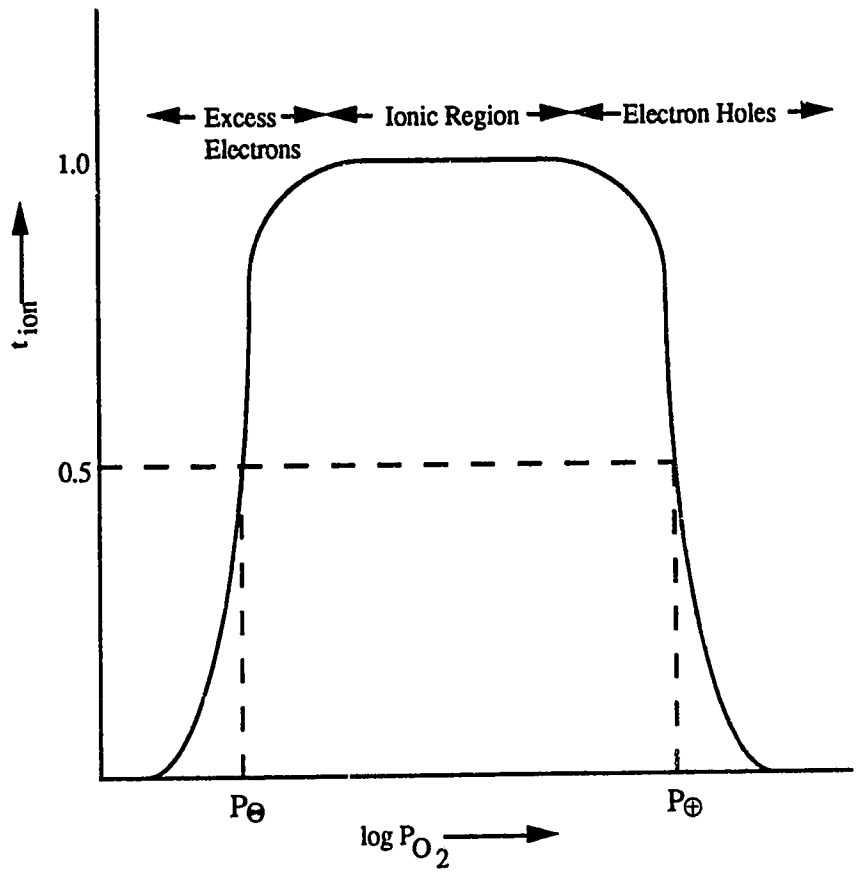

Fig. 3-4. Log of Oxygen Pressure versus t_{ion}.

From equation (3.58) a class of operating conditions can be determined.

1. When $P_\oplus \gg P''_{O_2} > P'_{O_2} \gg P_\Theta$ equation (3.58) reduces to :

$$E = \frac{RT}{4F} \ln \frac{P''_{O_2}}{P'_{O_2}} \qquad \text{as in equation (3.29)}$$

which is the optimum operating condition for a thermodynamic cell.

2. In the case when $P_{\oplus} \gg P_{\ominus} \gg P''_{O_2} > P'_{O_2}$ the e.m.f. is zero and the electrolyte behaves like an excess electron-semiconductor. When $P''_{O_2} > P'_{O_2} \gg P_{\oplus} \gg P_{\ominus}$ again the e.m.f. force is zero but in this case the electrolyte behaves like an electron hole semiconductor.

3. For the case when $P_{\oplus} \gg P''_{O_2} \gg P_{\ominus} \gg P'_{O_2}$:

$$E = \frac{RT}{4F} \ln \frac{P''_{O_2}}{P_{\ominus}} \tag{3.59}$$

In this case the e.m.f. has a value that only depends on the oxygen pressure P''_{O_2}.

4. For the case when $P''_{O_2} \gg P_{\oplus} \gg P'_{O_2} \gg P_{\ominus}$:

$$E = \frac{RT}{4F} \ln \frac{P_{\oplus}}{P'_{O_2}} \tag{3.60}$$

In this case the e.m.f. has a value that only depends on the oxygen pressure P'_{O_2}.

5. For the case where $P''_{O_2} \gg P_{\oplus} \gg P_{\ominus} \gg P'_{O_2}$:

$$E = \frac{RT}{4F} \ln \frac{P_{\oplus}}{P_{\ominus}} \tag{3.61}$$

For this case the e.m.f. is given by a constant value.

3.7 Ionic Conduction Domains

In Table 3-1 some values are given for the onset of electronic conduction. The value of log P_Θ corresponds to the oxygen pressure in atmospheres at which the electrolyte has t_{ion} = 0.5. For accurate thermodynamic measurements (i.e. $t_{ion} > 0.99$) P_{O_2} would have to be approx. 8 orders of magnitude higher than P_Θ as given in Table 3-1 (according to equation 3.56).

Table 3-1. Values of P_Θ for CSZ, YSZ, and YDT .

Electrolyte	Log P_Θ	P_Θ (atm.) 1000°C	Temp Range °C	Reference
ThO_2-8m/oY_2O_3	$-\frac{56250}{T} + 13.36$	1.5×10^{-31}	730-1130	25
ThO_2-10 to 20 m/oY_2O_3	$-\frac{57900}{T} + 12.4$	8.3×10^{-34}	700-1600	26
ThO_2-8 m/o-Y_2O_3	$-\frac{82970}{T} + 26.38$	1.6×10^{-39}	1200-1650	27
ZrO_2-7 m/o Y_2O_3	$-\frac{57500}{T} + 14.5$	2.1×10^{-31}	1200 -1650	28
ZrO_2-7.5 m/o Y_2O_3	$-\frac{58600}{T} + 15.9$	7.4×10^{-31}	1550 - 1650	29
ZrO_2-14 m/o CaO	$-\frac{68400}{T} + 21.59$	7.2×10^{-33}	1200 - 1650	27
ZrO_2-10 m/o CaO	$-\frac{57700}{T} + 15.8$	3.0×10^{-30}	1550 - 1650	29
ZrO_2-10 m/o CaO	$-\frac{54500}{T} + 14.0$	1.5×10^{-29}	600 - 1400	30
ZrO_2-12 m/o CaO	$-\frac{46750}{T} + 9.10$	2.4×10^{-28}	1000 - 1400	31

Fig. 3-5 shows the ionic domains where $t_{ion} > 0.99$ of various electrolytes; the figure shows that calcia stabilized zirconia is more useful for higher pressures when compared to yttria stabilized thoria. Yttria doped thoria is suitable for lower oxygen pressures when compared to both types of zirconia electrolyte.

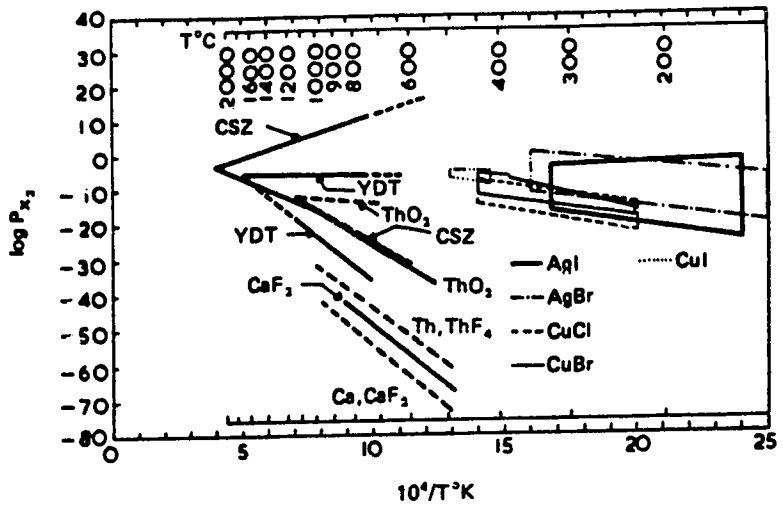

Fig. 3-5. Ionic Domains for Halide and Oxide Electrolytes [32]

In this section the relationship between t_{ion}, temperature and oxygen pressure is calculated for the electrolytes used in this thesis by utilizing the equation :

$$t_{ion} = \left[1 + \left(\frac{P_{O_2}}{P_{\oplus}}\right)^{\frac{1}{4}} + \left(\frac{P_{O_2}}{P_{\ominus}}\right)^{-\frac{1}{4}} \right]^{-1} \tag{3.56}$$

For zirconia-calcia the following data were used from Friedman et al. [33] for a commercial grade ZrO_2 / 3-4 wt. percent CaO electrolyte :

$$\log P_{\oplus} = -29.4\,(\pm 13.4) + \frac{5.1\,(\pm 1.9) \times 10^4}{T} \quad (1040 - 1250\,°C) \tag{3.62}$$

$$\log P_{\ominus} = 31.5\ (\pm 12.4) - \frac{7.4\ (\pm 1.8) \times 10^4}{T} \quad (1040 - 1250\ ^\circ C) \tag{3.63}$$

The plot of t_{ion}, temperature, and $\log P_{O_2}$ is shown in Fig. 3-6 for zirconia-calcia.

For zirconia-yttria the following data were used from Strickler and Carson [34]

$$P_{\oplus} = 4.55 \times 10^3 \exp \frac{3.04}{kT} (eV) \quad (500 - 1600\ ^\circ C) \tag{3.64}$$

$$P_{\ominus} = 5.23 \times 10^{14} \exp - \frac{11.8}{kT} (eV) \quad (500 - 1600\ ^\circ C) \tag{3.65}$$

The plot of t_{ion}, temperature, and $\log P_{O_2}$ is shown in Fig. 3-7 for zirconia-yttria .

For thoria-yttria the following data were used from Etsell [26] :

$$\log P_{\oplus} = 1.8 \quad (500 - 1600\ ^\circ C) \tag{3.66}$$

$$\log P_{\ominus} = \frac{-57900}{T} + 12.4 \quad (500 - 1600\ ^\circ C) \tag{3.67}$$

The plot of t_{ion}, temperature, and $\log P_{O_2}$ for thoria-yttria is shown in Fig. 3-8.

From Fig. 3-6, 3-7, and 3-8 some general conclusions can be made :

1. In general there are no large differences in the ionic domain between zirconia-calcia and zirconia-yttria.
2. The ionic domain of thoria-yttria extends into significantly lower oxygen pressure when compared to doped zirconia electrolytes.
3. The ionic domains of doped zirconia electrolytes extend into atmospheric oxygen pressures whereas thoria-yttria is good up to approx. 10^{-6} atm of oxygen.

As temperature increases the electrolytic domain width decreases, which would indicate that the activation energy for electronic conduction via excess electrons is much larger than for ionic conduction. For n-type electronic conduction the activation energy is equivalent to the

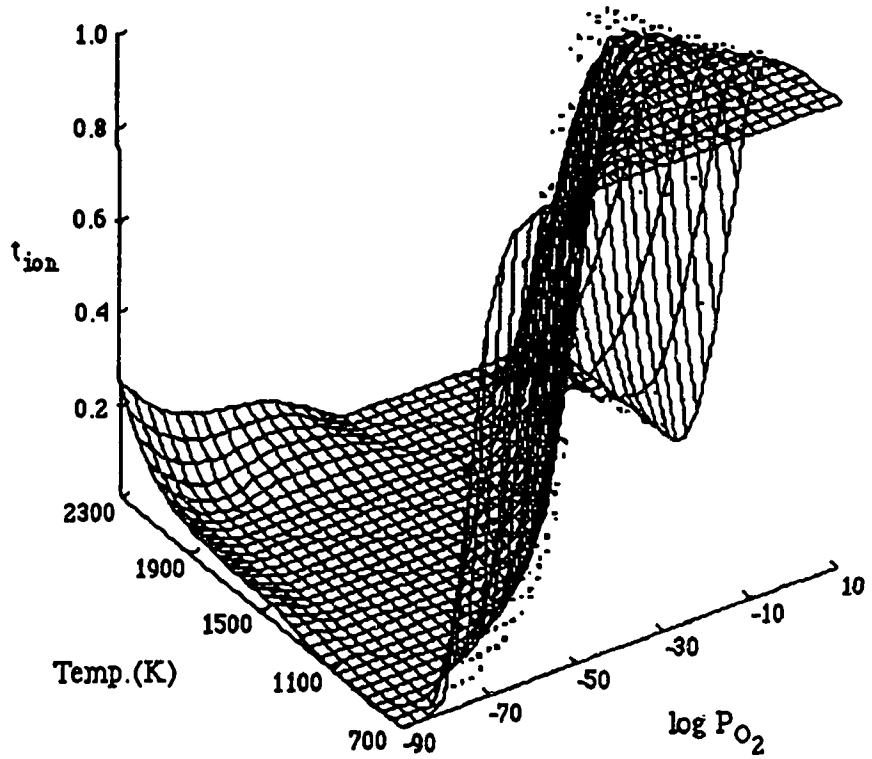

Fig. 3-6. Zirconia - Calcia t_{ion} versus Temperature versus log P_{O_2}.

bandgap energy, which must be large since the number of intrinsic electronic defects in solid electrolytes is very small. The bandgap energy of ZrO_2 is approx. 5.6 eV [35]. This can be compared to the activation energy for ionic conduction which is equal to the oxygen-ion migration enthalpy for ZrO_2(CaO) at 1.2 eV[36]. Above approx. 2200 °C a direct p to n transition occurs; at these high temperatures the concentration of intrinsic electrons and electron holes is high enough to overcome the extrinsic oxygen ion conductivity. The precise location of the electrolytic domain is affected by the impurity content of the solid

electrolyte. Specifically, the content of impurities like iron and manganese is extremely harmful since they can donate or accept electrons by changing their valence state. It has been shown experimentally that the mobilities for electronic defects in ionic solids are from 100 to 1000 times greater than ionic defects[11,37]. Due to this various investigators disagree as to the precise location of the domain boundaries[32]. Accordingly it is good practice to operate a solid electrolyte near the center of its electrolytic domain.

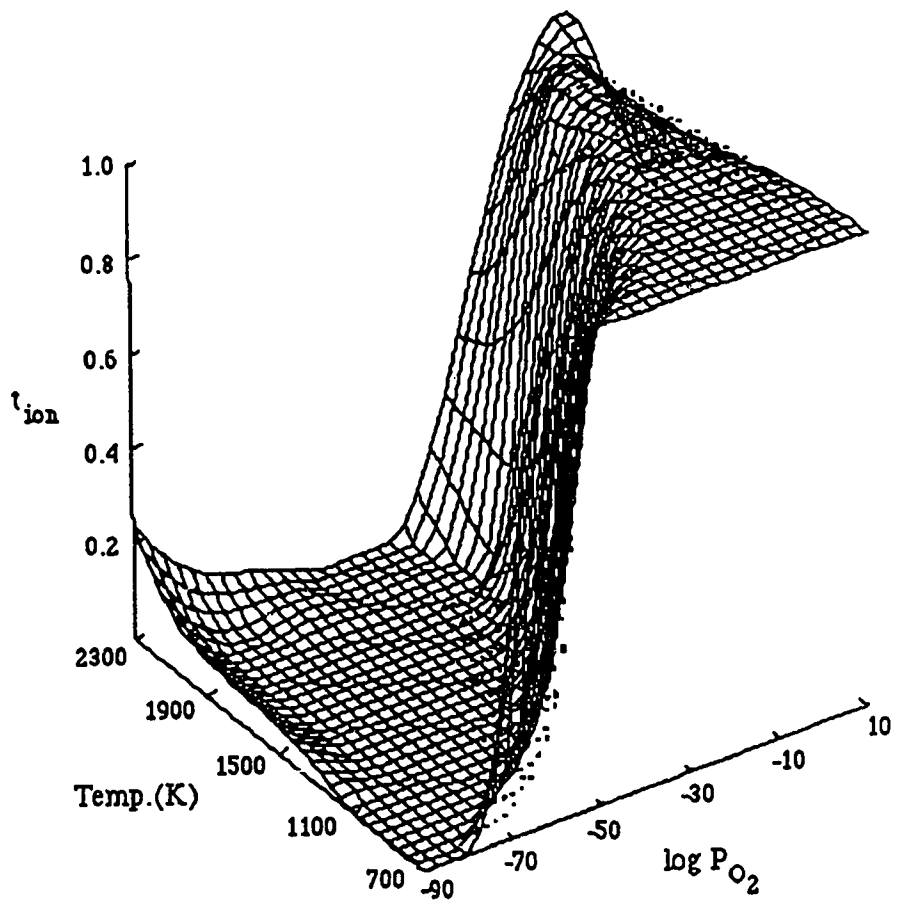

Fig. 3-7. Zirconia - Yttria t_{ion} versus Temperature versus log P_{O_2}.

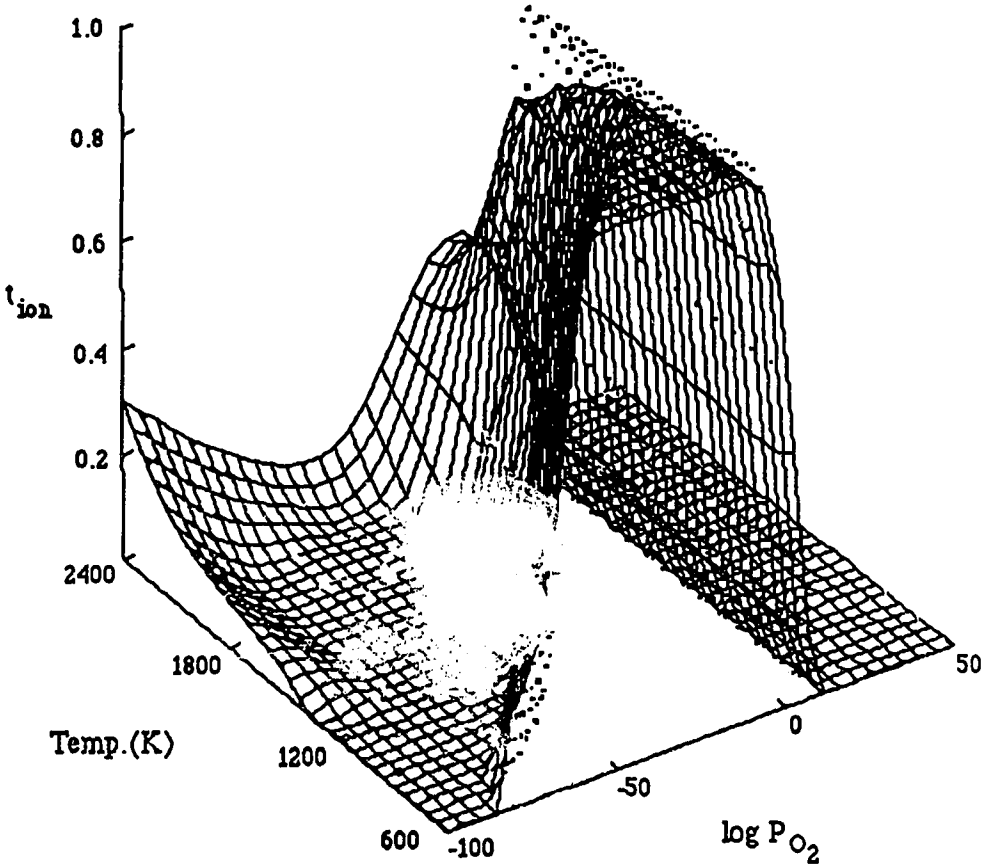

Fig. 3-8. Thoria-Yttria t_{ion} versus Temperature and log P_{O_2}.

3.8 Practical Operating Considerations

There are two problems which can occur in operating a solid state cell outside the electrolytic domain. The first problem is that the open-circuit cell potential is lowered according to the equation :

$$E = \frac{1}{4F}\int_{\mu_{O_2}'}^{\mu_{O_2}''} t_{ion}\, d\,\mu_{O_2} \tag{3.35}$$

If the electronic transference number is known and is essentially constant, given that t_{ion} = 1 - t_e (t_e is the electronic transference number) and since $\mu_{O_2} = \mu^{o}_{O_2} + RT \ln P_{O_2}$, equation (3.35) simply reduces to :

$$E = (1 - t_e)\frac{RT}{4F}\ln\frac{P''_{O_2}}{P'_{O_2}} \tag{3.68}$$

The most accurate method would be to establish a calibration curve, which is determined by measuring the relationship between the sensor potential and known concentrations.

A more serious problem can occur if certain conditions of operation are present resulting in widely fluctuating readings. With an electronic current, electrons can migrate from the negative to the positive electrode, and at the same time oxygen ions will move in the opposite direction so as to maintain local electro-neutrality throughout the electrolyte. If diffusional processes in the electrodes do not supply or remove oxygen fast enough at the electrode-electrolyte interfaces, an oxide layer forms at the negative electrode and a metal layer will form at the positive electrode. This effect is shown in Fig. 3-9 for two phase

metal-metal oxide electrodes. As stated previously this layer formation results in unstable cell potentials due to polarization, since the metal-metal oxide mixtures no longer establish a fixed oxygen potential at the electrode-electrolyte interfaces.

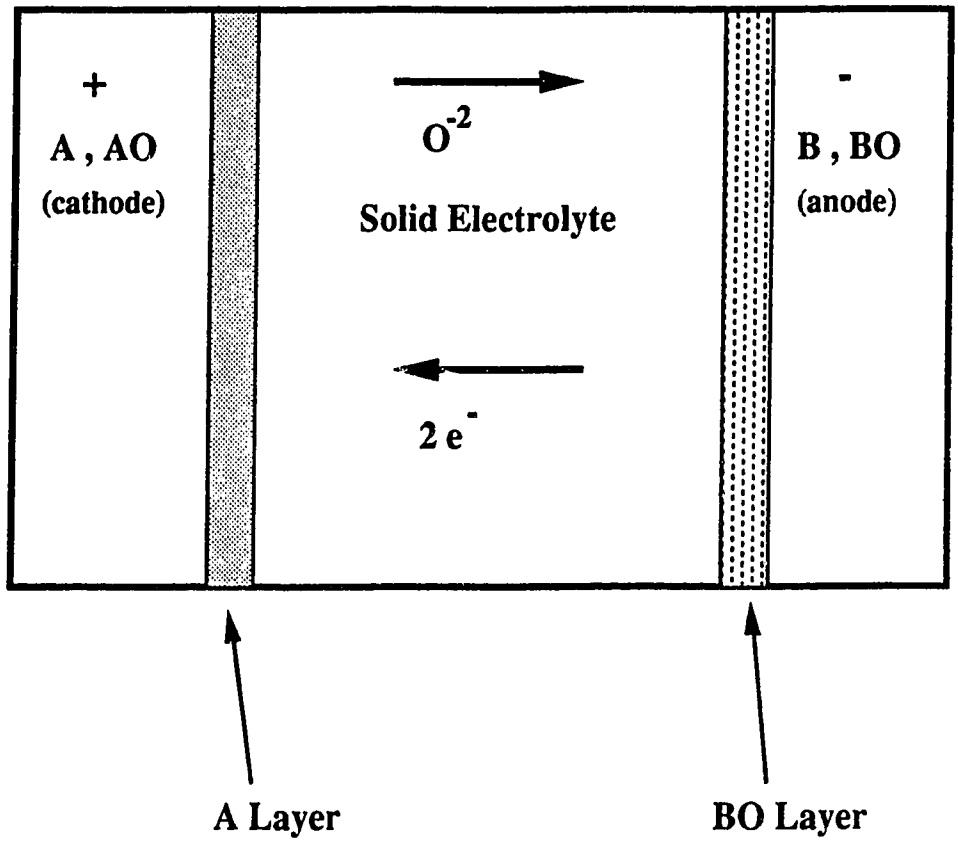

Fig. 3-9 Polarization of Electrodes due to Layer Formation.

In the case of ionic operation the electrode reactions would consist of :

1. At the cathode gaseous oxygen is ionized and incorporated as O^{2-} in the electrolyte :

$$O_2(P''_{O_2}) + 4e' \rightarrow 2O^{2-} \qquad (3.69)$$

2. At the anode ionized oxygen is released as gaseous oxygen :

$$2O^{2-} \rightarrow O_2(P'_{O_2}) + 4e' \tag{3.70}$$

Combining the cathode and anode reactions results in the overall reaction of :

$$O_2(P''_{O_2}) \rightarrow O_2(P'_{O_2}) \tag{3.71}$$

In this situation oxygen is transferred from the cathode to the anode by oxygen anions.

The reference electrode is another important component of an electrochemical cell. In theory, any mixture be it gas, liquid or solid which can establish a constant chemical potential is suitable as a reference electrode. It has been shown that solid reference electrodes have advantages with respect to chemical and mechanical stability[36,38]. Solid reference electrode systems must have diffusional processes which are rapid enough so as to maintain a constant chemical potential at the electrode-electrolyte interface. This eliminates the formation of layers of metal or metal oxide at the electrode-electrolyte interface and also chemical potential variations due to chemical reactions[36,39]. Chemical reactions can occur within the electrode or between an electrode and either the electrolyte, container materials, or gas phase, etc. resulting in a variation of the chemical potential at the electrode-electrolyte interface.

With respect to speed, gas phase reference electrodes are quicker kinetically than solid phase reference electrodes. Subsequently equilibrium is more readily obtained with a gas phase electrode. This will prove to be a critical factor in the recommended changes to the cell configurations utilized in this thesis.

3.9 Zirconia Solid Electrolytes

The majority of electrolytes that display oxygen ion conduction consist of crystal structures of the fluorite type consisting of either ThO_2, CeO_2, ZrO_2 or HfO_2. Zirconia has an advantage of higher conductivity and can be used at oxygen partial pressures near atmospheric pressure, whereas ThO_2 electrolytes have superior thermodynamic stability at lower oxygen partial pressures.

Pure ZrO_2 at room temperature is in a monoclinic crystal structure which will change to a tetragonal form above 1200 °C [40] and then to a cubic structure at 2300 °C. By adding some aliovalent oxides the high temperature cubic fluorite phase is stabilized in the zirconia. Probably the most common solid solution is that of ZrO_2-CaO; this electrolyte was first demonstrated by Kiukkola and Wagner [1]. The predominant defect in this solution is anion vacancies which has been confirmed by x-ray intensity[41,42] and by density[43] measurements. The CaO stabilized material used in this experiment was of the partially stabilized zirconia type (PSZ) with between 7 and 8 mol % CaO. These electrolytes are found to possess greater resistance to thermal fluctuations and higher mechanical strength along with a loss in electrical conductivity. They have been found to be suitable for experimental work with respect to ionic transference numbers and oxygen permeability[44,45].

In addition to calcia stabilized zirconia, zirconia stabilized with yttria (Y_2O_3) has also been used. This electrolyte displays unusually high ionic conductivity as shown in figures 3-2 and 3-3. The high ionic conductivity, observed by Nernst[46] as early as 1899, led to it being the first to be used in the construction of solid oxide electrolyte fuel cells[47]. In comparison to ZrO_2-CaO, ZrO_2-Y_2O_3 displays a lower activation energy of 18-25 kcal/mol. One concern of ZrO_2-Y_2O_3 and ZrO_2-CaO is that they show a tendency to decrease in conductivity when used at 1000 °C as shown by Markin et al.[48]. This phenomena is believed to be due to defect ordering and the possible formation of a pyrochlore phase[49].

3.10 Thoria Solid Electrolytes

Pure ThO_2 exists in the cubic CaF_2 state from room temperature up to the melting point ; therefore it does not need any stabilization. The addition of impurities dramatically increases the defect concentration of pure ThO_2. Measurement of the electrical conductivity has determined that oxygen vacancies are the mobile defects[50,51] and the conductivity is purely anionic over a range of oxygen activity and temperature[52,53] . The conductivity values of ThO_2 based materials are significantly lower than ZrO_2 based materials as shown in Fig. 3-3. The activation energy for ionic conduction is approximately 23-28 kcal/mol and ThO_2 based electrolytes do not display electronic conductivity at oxygen activities as low as those obtained with the Cr-Cr_2O_3 reference electrode. In Fig. 3-10 the relationship between ionic conductance and the log of oxygen partial pressure[53] is displayed for ThO_2-Y_2O_3. At pressures of 10^{-6} atm and higher, pure and doped ThO_2 begin to display significant electronic conductivity (i.e. the ionic transference number is less than 1.0).

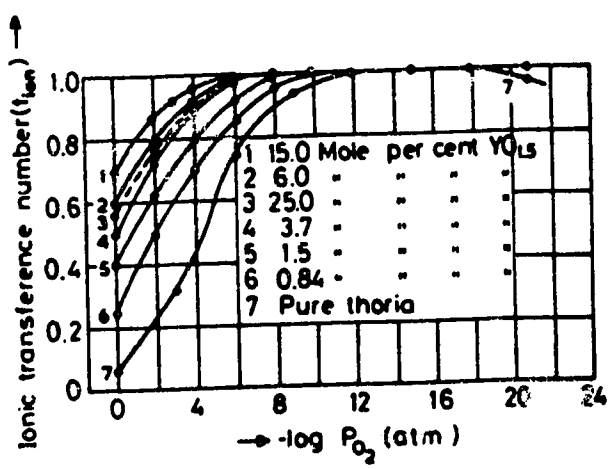

Fig. 3-10. Ionic Transference Number of ThO_2-Y_2O_3 as a Function of Oxygen Pressure at 1000°C [53].

On the other hand, at extremely low oxygen pressures (i.e. 10^{-20} atm at 1000 °C) only, does pure ThO_2 display significant electronic conduction; the doped ThO_2 can be used at even lower oxygen pressures. It can be concluded that increasing the concentration of yttria enlarges the range of ionic conductivity, especially at lower oxygen pressures and to some degree also at higher oxygen pressures.

4.0 Chromium Carbide Cell

4.1 Literature Values for the Free Energy of Formation of Chromium Carbide

Values for the free energy of formation of chromium carbide (Cr_3C_2) display wide variations which, in part at least, is due to the wide range of experimental techniques. Utilizing the Knudsen method the dissociation pressure of Cr_3C_2 was determined between 1900-2100 K by Fujishiro and Gocken[54]. By using data for the vapor pressure of pure chromium[55,56] the free energy of formation for Cr_3C_2 calculated as :

$$\Delta G^\circ_{Cr_3C_2}(\text{cal/mole}) = -9900 - 1.29\,T \qquad (4.1)$$

Utilizing gas equilibration between 1070-1300 K Alekseyev and Shvartsman[57] determined the free energy of formation for Cr_3C_2 to be :

$$\Delta G^\circ_{Cr_3C_2}(\text{cal/mole}) = -1900 - 0.3\,T \qquad (4.2)$$

Measuring the dissociation pressure of Cr_3C_2 Vintaykin[58] determined the free energy of formation of Cr_3C_2 between 1373-1573 K :

$$\Delta G^\circ_{Cr_3C_2}(\text{cal/mole}) = -8200 - 7.0\,T \qquad (4.3)$$

Kelley et al.[59] measured CO pressure over a mixture of Cr_3C_2, Cr_2O_3, and graphite and calculated the free energy of formation of Cr_3C_2 from 1200-1400 K to be :

$$\Delta G^\circ_{Cr_3C_2}(\text{cal/mole}) = -20780 - 4.5\,T \qquad (4.4)$$

Gleiser[60] utilized the same technique as Kelley to calculate the free energy of formation of Cr_3C_2 from 1300-1400 K to be :

$$\Delta G^\circ_{Cr_3C_2}(\text{cal/mole}) = -25900 - 3.9\,T \qquad (4.5)$$

In both Kelley's and Gleiser's data, the results were non-reproducible and were uncertain to +/-10 kcal. There is considerable discrepancy between the two experimenters considering that they used the same techniques. It has been postulated that they did not allow equilibria in the systems to take place and that there were CO concentration gradients between the specimens and gases[61] . Utilizing the electromotive force method with a CaF_2 electrolyte, Kleykamp[62] determined the free energy of formation of Cr_3C_2 from 880-1100 K to be :

$$\Delta G^\circ_{Cr_3C_2}\text{cal/mole} = -7200 - 8.0\,T \qquad (4.6)$$

Similarly, Tanaka et al.[63] also used a CaF_2 electrolyte for determining the free energy of formation of Cr_3C_2 ; however, Tanaka used a single crystal of CaF_2 whereas Kleykamp had used sintered CaF_2. Tanaka produced the following value for the range from 885-1095 K :

$$\Delta G^\circ_{Cr_3C_2}(\text{cal/mole}) = -13300 - 4.15\,T \qquad (4.7)$$

There are large differences between the results of Kleykamp and Tanaka probably due to electronic conduction in the electrolyte used by Kleykamp. It should be mentioned that Tanaka calculated his results with data obtained from Storms [61] and Wicks and Block[64].

Storms[61] estimated values for the free energy of formation in the range from 800-1500 K to be :

$$\Delta G^{\circ}_{Cr_3C_2}(\text{cal/mole}) = -14800 \ -3.42\ T \qquad (4.8)$$

Wicks and Block[64] in a similar manner also estimated the free energy of formation in the range from 800 - 1500 K at :

$$\Delta G^{\circ}_{Cr_3C_2}(\text{cal/mole}) = -18700 \ -3.95\ T \qquad (4.9)$$

Using a thoria-yttria stabilized electrolyte, Mabuchi, Sano, and Matsushita[65] determined the free energy of formation in the range from 1073-1303 K at :

$$\Delta G^{\circ}_{Cr_3C_2}(\pm 330\ \text{cal/mole}) = -10400 \ -7.35\ T \qquad (4.10)$$

Kulkarni and Worrell[66] combined original work on the free energy of formation of $Cr_{23}C_6$ with work from Kelley et al.[59] to determine an equation for the free energy of formation for Cr_3C_2 from 1300-1500 K :

$$\Delta G^{\circ}_{Cr_3C_2}(\pm 400\ \text{cal/mole}) = -16400 \ - 4.4\ T \qquad (4.11)$$

Using an electromotive cell consisting of a BaF_2-BaC_2 electrolyte, Coltters and Belton[67] determined the free energy of formation for Cr_3C_2 from 1466-1796 K :

$$\Delta G^{\circ}_{Cr_3C_2}(\pm 287\ \text{cal/mole}) = -22194 \ - 4.64\ T \qquad (4.12)$$

In Fig. 4-1 the values from the various authors are displayed; it can be observed that the data derived from the e.m.f. techniques fall approximately in the same area. The other data derived from CO pressure techniques are found to be significantly different.

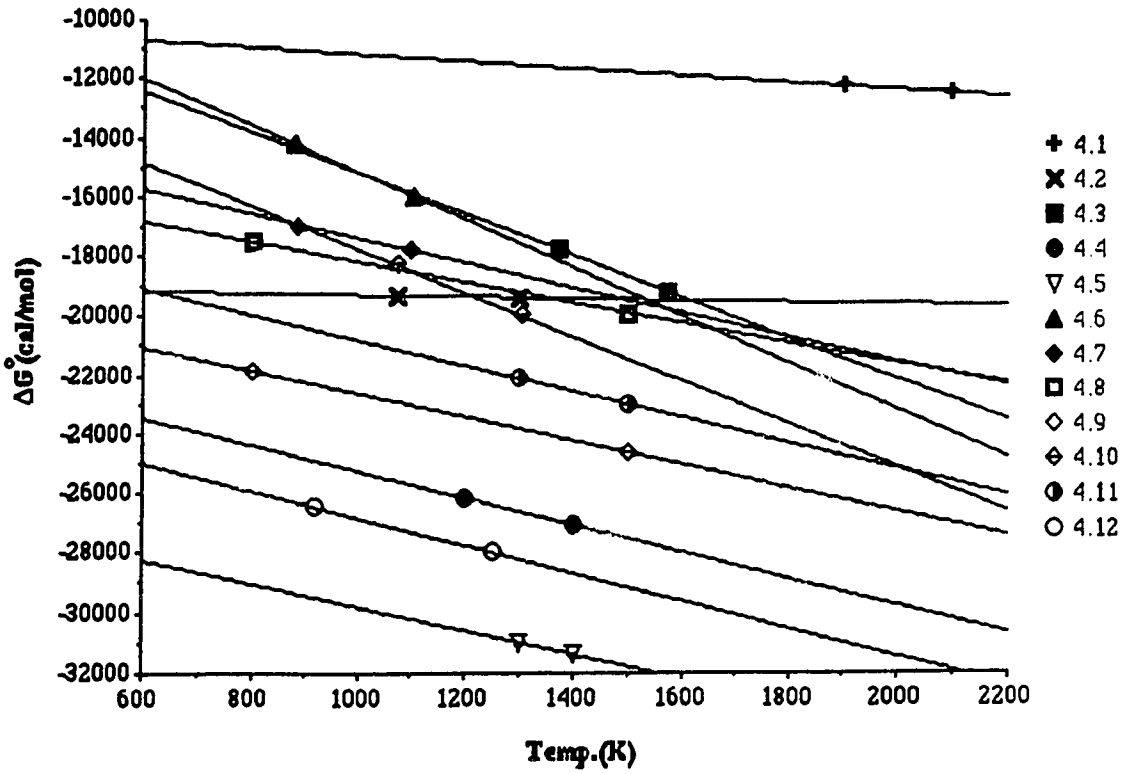

Fig. 4-1. Literature Free Energy Values (cal/mol) vs. Temperature (The numbers 4.1 to 4.12 refer to the equations as listed in the text).

4.2 Experimental Chromium Cell

The chromium cell consisted of the following elements :

(-) Cr, Cr_2O_3 / Electrolyte (ZrO_2-CaO or ThO_2-Y_2O_3) / Cr_2O_3, Cr_3C_2, C (+)

The cell reactions consist of :

$$\frac{4}{3}Cr + 2O^{-2} \Leftrightarrow \frac{2}{3}Cr_2O_3 + 4e^- \quad \text{Anode} \qquad (4.13)$$

$$\frac{2}{3}Cr_2O_3 + \frac{8}{9}C + 4e^- \Leftrightarrow \frac{4}{9}Cr_3C_2 + 2O^{-2} \quad \text{Cathode} \qquad (4.14)$$

$$\frac{4}{3}Cr + \frac{8}{9}C \Leftrightarrow \frac{4}{9}Cr_3C_2 \quad \text{Overall Reaction} \qquad (4.15)$$

The measured experimental voltage is equivalent to : $\Delta G = -4EF$ from equation (4.15).

By multiplying the overall reaction by 9/4 the reaction becomes :

$$3Cr + 2C \Leftrightarrow Cr_3C_2 \qquad (4.16)$$

To obtain the free energy for the formation of a single mole of Cr_3C_2 requires that the voltage obtained from the experiments is multiplied by a factor of 9/4 ; it follows that :

$$\Delta G^o_{Cr_3C_2} = -9EF \qquad (4.17)$$

Two types of electrolytes were utilized in the experiment, one consisting of zirconia stabilized with calcia and the other consisting of thoria stabilized with yttria. A total of four successful runs were completed with two from each electrolyte type from a total of 10 experimental runs.

The solid state electrochemical cell was constructed with either zirconia stabilized with 4w/o (8.4 m/o) calcia or thoria stabilized with 7w/o (8m/o) yttria. The tubes were purchased

from Zirconium Corporation of America (Zircoa). The zirconia tubes contain the following impurities : 0.60% SiO_2, 0.75% MgO, 0.10% Fe_2O_3, 0.20% Al_2O_3, and 0.10% TiO_2. For the thoria tubes, the impurities (given in ppm) consist of : 1000 Al, 3 Ca, 1 Cu, 4 Fe, 3 Mg, 1 Mn, 2 Ni, 1 K, 200 Si, 0.5 Ag, 10 Na, 1 Sr and 2000 Zr.

All materials used for the anode and cathode were of high purity. From Cerac Certified Chemicals the Graphite (C) was -200 mesh, typically 99.999% pure with impurities consisting of : 0.3 ppm Fe, 0.1 ppm Mg and 0.4 ppm Si . The Chromium Carbide (Cr_3C_2) also from Cerac was -325 mesh, typically 99% pure consisting of 86.10% Cr, 13.20% total C, 0.05% free C and 0.09 % Fe.

From Electronic Space Products the Chromium (Cr) was -200 mesh, typically 99.9% pure, with impurities of : 150 ppm Co, 10 ppm Cu and 100 ppm Fe. Finally, also from Electronic Space Products the Chromium Oxide (Cr_2O_3) was certified to be typically 99.999% pure, with impurities of: 1< ppm Cu, 1< ppm Mg, 5 ppm Fe and 3 ppm Si .

The potentiometer used for measuring the e.m.f. was a Keithley Model 616 digital electrometer, with an impedance in excess of 10^{14} Ω. All furnaces used were home made using various EuroTherm power / temperature controllers.

All Pt gauze used in the experiment consisted of 5% Rh - 5% Pd - 90% Pt , and thermocouples were Pt / Pt-13% Rh. The outer tube consisted of alumina from McDanel Refractory Company. After assembly the cells were evacuated and purged with ultra high purity helium and evacuated into the low millitorr range for several days so as to ensure a good quality of vacuum. The probes were then sealed under vacuum by melting the connection to the vacuum pump. In Fig. 4-2 the experimental chromium carbide cell is depicted.

Furnaces utilized for the chromium and carbon monoxide/dioxide experiments consisted of molybdenum elements for high temperatures protected with a 15% hydrogen-85% argon mixture and Kanthal elements and Chromel elements for lower temperatures.

Measurements of electromotive force were made with a Keithley electrometer with an impedance in excess of 10^{14} ohms, ensuring that virtually no current was allowed to flow. Each furnace was temperature profiled so as to determine the " hot zone " for the placement of the active portion of the electrolytic cells. It is important to locate the cells in a constant temperature zone so as to avoid errors due to the e.m.f. contribution from temperature variations.

The e.m.f. due to temperature variation is given by :

$$E = \frac{1}{4F}\left[\mu''_{O_2}\left(T_2, P''_{O_2}\right) - \mu'_{O_2}\left(T_1, P'_{O_2}\right)\right] + \alpha\left(T_2 - T_1\right) \qquad (4.18)$$

where μ''_{O_2} is the oxygen chemical potential at the cathode, μ'_{O_2} is the oxygen chemical potential at the cathode, T_2 and T_1 are the temperatures at the two electrode-electrolyte interfaces, P''_{O_2} & P'_{O_2} are the oxygen pressures , and α is a term for the partial entropy and heat of transfer at the electrolyte-electrode interface. For Pt electrodes the values for α are 0.095 +/- 0.005 mV/°C for zirconia-calcia and 0.05 +/- 0.005 mV/°C for thoria-calcia electrolytes[10].

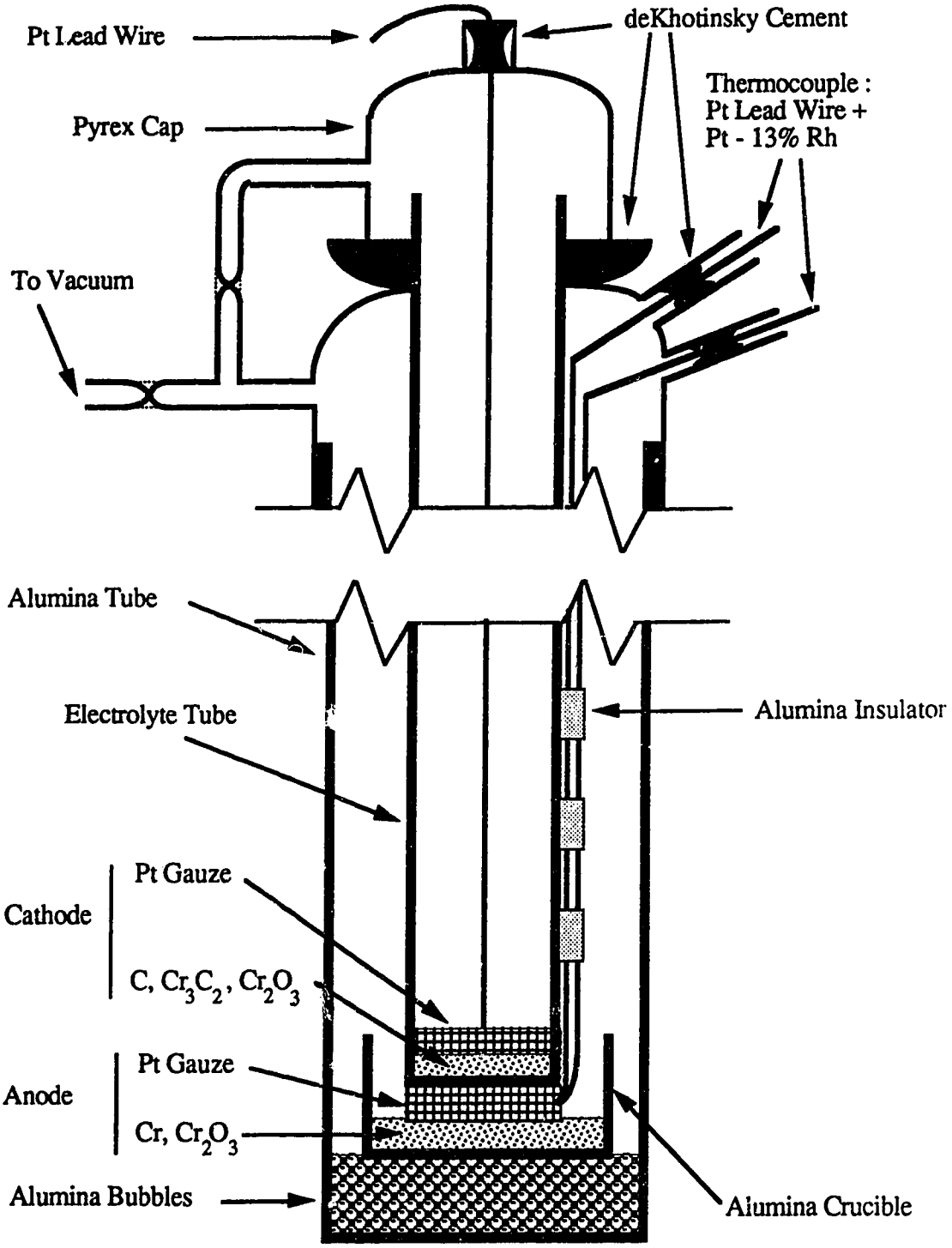

Fig. 4-2. Chromium Carbide Experimental Cell.

4.3 Furnace Temperature Profile

Figures 4.3 and 4.4 are the temperature profiles for the molybdenum wound furnace for 900 and 1000 °C. Both ends of the tube were sealed with fiberfrax so as to duplicate the conditions where the thermodynamic cell is placed in the tube furnace. From second order polynomial regression of the data, it was determined that a flat zone in temperature of about 100 mm in length and +/- 5 °C was centered at approximately 325 mm down the tube. The Kanthal and Chromel furnaces displayed similar temperature flat zone characteristics.

The probes were placed in the temperature flat zone so as to ensure minimal additional e.m.f.'s due to temperature variation.

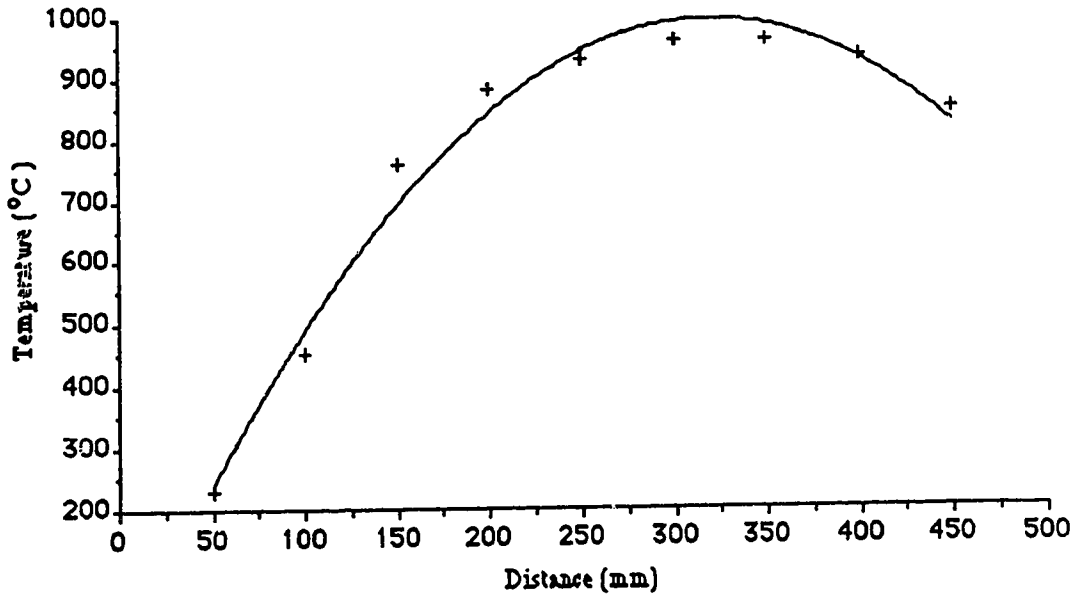

Fig. 4-3. Temperature Profile Moly Wound Furnace at 900 °C

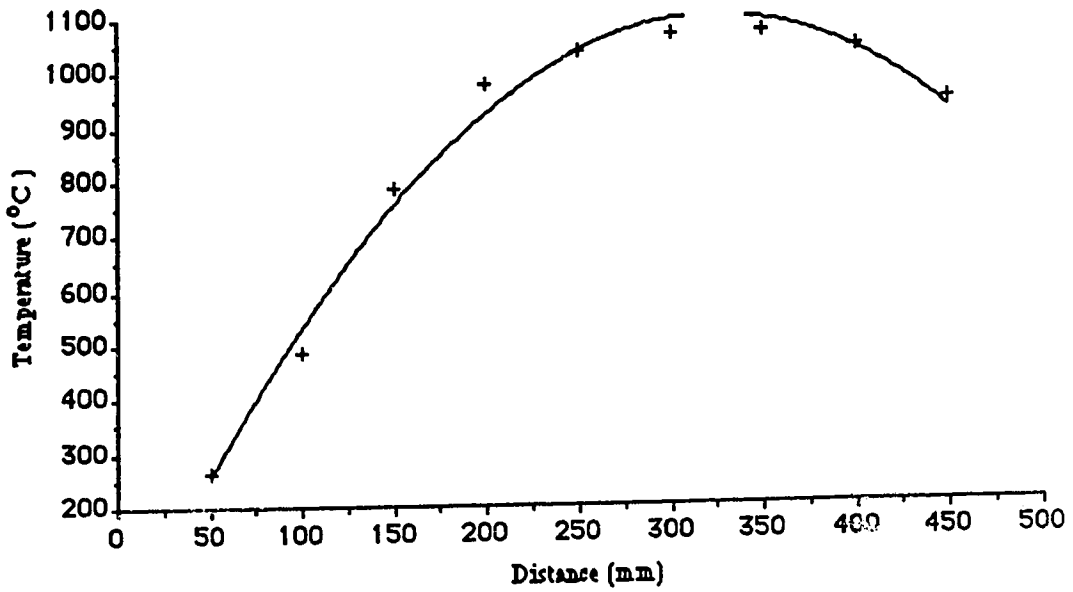

Fig. 4-4. Temperature Profile Moly Wound Furnace at 1000 °C.

4.4 Results and Discussion

Experimental results are presented in Appendix A in Tables A-1 to A-7, followed by plots of temperature versus free energy of formation of chromium carbide in Figs. A-1 to A-7. No results were obtained for run 1, 4 and 9 due to vacuum failure.

The data obtained from 10 experimental runs using both calcia stabilized zirconia and yttria doped thoria are summarized in Table 4-1.

Table 4-1 Summary of Chromium Carbide Experimental Data.

Run	Electrolyte	Number of Measurements	ΔG^o(cal/mol) vs. K
1	Thoria/Yttria	4 (premature failure)	vacuum failure
2	Zirconia/Calcia	25	-48336 + 32.70 T $R^2 = 0.17$
3	Zirconia/Calcia	5 (premature failure)	-3170 - 7.62 T $R^2 = 0.02$
4	Zirconia/Calcia	0	vacuum failure
5	Thoria/Yttria	55	-6248 - 11.39 T $R^2 = 0.76$
6	Zirconia/Calcia	39	-28611 + 16.47 T $R^2 = 0.36$
7	Thoria/Yttria	10	21116 - 20.87 T $R^2 = 0.85$
8	Zirconia/Calcia	36	-26766 + 21.95 T $R^2 = 0.38$
9	Thoria/Yttria	0	vacuum failure
10	Thoria/Yttria	25	-5427 - 10.77 T $R^2 = 0.83$

It has been determined that the best values obtained for the experimental reaction 3Cr + 2C = Cr_3C_2 whereby the electromotive forces measured provide values for the free energy of formation according to equation (4.17) are from Run 5 and 10 as follows :

Run 5 ΔG^o : (± 208 cal/mol) = -6248 - 11.39 T R^2=0.76 (1088 to 1208 K) (4.19)

Run 10 ΔG^o : (± 208 cal/mol) = -5427 - 10.77 T R^2=0.83 (1124 to 1353 K) (4.20)

In general the response of both the zirconia and thoria cells was found to be extremely sluggish upon small changes in temperature of 10 to 20 °C. Times in excess of 6-8 hr were required for the cells to reach equilibrium in the the upper temperature regions with even longer times in the lower temperature ranges. This would suggest either that the electrolytes are operating in a region of significant electronic conduction or that, due to the presence of the three phase mixture at the cathode (i.e. Cr_2O_3, Cr_3C_2, C), complete equilibrium is difficult if not impossible to obtain. When the cells were disconnected for brief periods of time, recovery to the previous e.m.f. did not occur suggesting polarization at the electrodes.

In order to determine the effect of the operating oxygen partial pressures on the electrolyte, the following analysis of operating conditions was performed. The equilibrium oxygen pressure for the chromium cell on the anode side is determined by the reaction of .

$$Cr_2O_3 \Leftrightarrow 2Cr + \frac{3}{2}O_2 \qquad \Delta G^o(\text{cal/mol}) = 277{,}190 - 53.25\,T \text{ [68]} \qquad (4.21)$$

Since ΔG^o is related to the equilibrium constant by :

$$\Delta G^o = -RT \ln K_p \quad \text{where } K_p = P_{O_2}^{3/2} \qquad (4.22)$$

therefore the oxygen pressure at the anode is given by the equation :

$$\ln P'_{O_2} = \frac{-93048}{T} + 17.88 \qquad (4.23)$$

The equilibrium oxygen pressure at the chromium cell at the cathode using available ΔG data[68,69] is determined by the reaction :

$$\frac{2}{3}Cr_2O_3 + \frac{8}{9}C \Leftrightarrow \frac{1}{9}Cr_3C_2 + O_2 \quad \Delta G^o(\text{cal/mol}) = 175{,}833 - 36.73\,T \qquad (4.24)$$

As in (4.23) from (4.21) & (4.22), the oxygen pressure at the cathode is determined from (4.22) and (4.24) resulting in :

$$\ln P''_{O_2} = \frac{-88536}{T} + 18.49 \qquad (4.25)$$

The value for t_{ion} has been calculated for confirmation of the effect of operating conditions. If the oxygen pressures P'_{O_2} and P''_{O_2} at either electrode are not too different then $\bar{t}_{ion}$ can be approximated to be equal to t_{ion} at $\bar{P}_{O_2}$ where :

$$\log \bar{P}_{O_2} = \frac{\log P'_{O_2} + \log P''_{O_2}}{2} \qquad (4.26)$$

From equations (4.23), (4.25), and (4.26) for the chromium cell :

$$\log \bar{P}_{O_2} = \frac{-39424}{T} + 7.90 \qquad (4.27)$$

For the calculation of t_{ion} the following data for commercial 3-4 w/o CaO stabilized ZrO_2 were utilized[70] :

$$\log P_{\oplus} = -29.4 + \frac{51000}{T} \tag{3.62}$$

$$\log P_{\ominus} = +31.5 - \frac{74000}{T} \tag{3.63}$$

Utilizing equation (3.56), (3.62), (3.63), and (4.27) t_{ion} was calculated, with the values displayed in Table 4-2.

Table 4-2. Temperature versus t_{ion} for Zirconia-Calcia .

Temperature (K)	$\log P_{\ominus}$ (atm.)	$\log P_{\oplus}$ (atm.)	$\log P_{O_2}$ (atm.)	t_{ion}
700	-74.21	43.46	-48.42	1.0000
800	-61.00	34.35	-41.38	1.0000
900	-50.72	27.27	-35.90	0.9998
1000	-42.50	21.60	-31.52	0.9982
1100	-35.77	16.96	-27.94	0.9891
1200	-30.17	13.10	-24.95	0.9526
1300	-25.42	9.83	-22.43	0.8488
1400	-21.36	7.03	-20.26	0.6528
1500	-17.[illegible]3	4.60	-18.38	0.4216
1600	-14.75	2.48	-16.74	0.2413
1700	-12.03	0.60	-15.29	0.1327
1800	-9.61	-1.07	-14.00	0.0739
1900	-7.45	-2.56	-12.85	0.0427
2000	-5.50	-3.90	-11.81	0.0257
2100	-3.74	-5.11	-10.87	0.0162
2200	-2.14	-6.22	-10.02	0.0106
2300	-0.67	-7.23	-9.24	0.0071

From the data in Table 4-2, t_{ion} versus temperature is plotted in Fig. 4-5. From this analysis and assuming that the data used for the calculations are accurate for the ZrO_2-CaO used in this experiment, it can be concluded that the cell would have been operated with significant electronic conduction at any temperature above 1200 K. This would partially explain the difficulty in obtaining equilibrium.

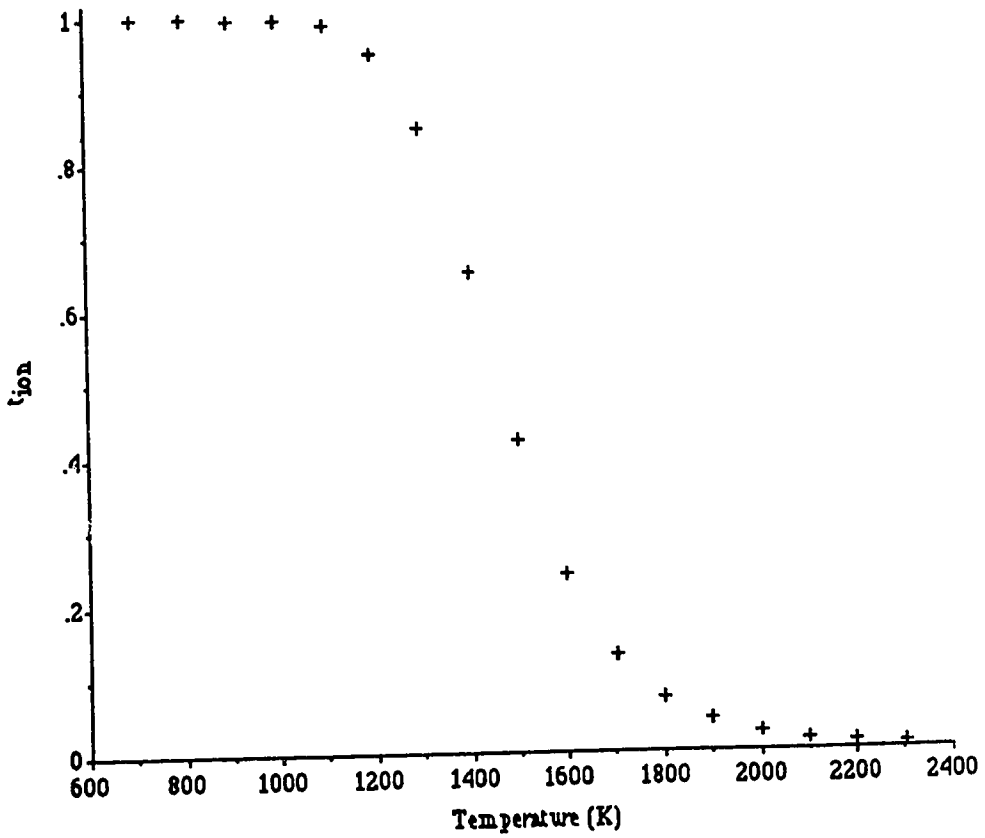

Fig. 4-5. t_{ion} versus Temperature for Zirconia-Calcia with $\overline{P}_{O_2}$ (atm) established by Cr-CrO_3 and Cr_3C_2-Cr_2O_3-C electrodes.

For the calculation of t_{ion} the following data for ThO_2-Y_2O_3 (10-20 mole % Y_2O_3) is utilized[26]:

$$\log P_{\oplus} = 1.8 \ (500 - 1600\ ^{\circ}C) \tag{3.66}$$

$$\log P_{\ominus} = \frac{-57900}{T} + 12.4 \ (500 - 1600\ ^{\circ}C) \tag{3.67}$$

Utilizing equation (3.56), (3.66), (3.67), and (4.27) t_{ion} was calculated, with the values displayed in Table 4-3, and the plot of t_{ion} versus temperature in Fig. 4-6.

Table 4-3. Temperature versus t_{ion} for Thoria-Ytria.

Temperature (K)	$\log P_{\ominus}$ (atm)	$\log P_{\oplus}$ (atm)	$\log \overline{P}_{O_2}$ (atm)	t_{ion}
700	-70.31	1.80	-48.42	1.0000
800	-59.98	1.80	-41.38	1.0000
900	-51.93	1.80	-35.90	0.9999
1000	-45.50	1.80	-31.52	0.9997
1100	-40.24	1.80	-27.94	0.9992
1200	-35.85	1.80	-24.95	0.9981
1300	-32.14	1.80	-22.43	0.9963
1400	-28.96	1.80	-20.26	0.9933
1500	-26.20	1.80	-18.38	0.9890
1600	-23.79	1.80	-16.74	0.9830
1700	-21.66	1.80	-15.29	0.9750
1800	-19.77	1.80	-14.00	0.9649
1900	-18.07	1.80	-12.85	0.9527
2000	-16.55	1.80	-11.81	0.9383
2100	-15.17	1.80	-10.87	0.9217
2200	-13.92	1.80	-10.02	0.9032
2300	-12.77	1.80	-9.24	0.8829

From Fig. 4-6 it can be observed that at temperatures above 1600 K (≈1400 °C) electronic conduction becomes significant (i.e. $t_{ion} < .98$). Since the experimental runs did not exceed 1400 K where t_{ion} exceeds 0.99, it can be assumed that the electrolyte was functioning as essentially a pure ionic conductor. If this is the case, then the most likely explanation for the lack of experimental reproducibility is the difficulty in establishing equilibrium with a three phase Cr_2O_3-Cr_3C_2-C mixture.

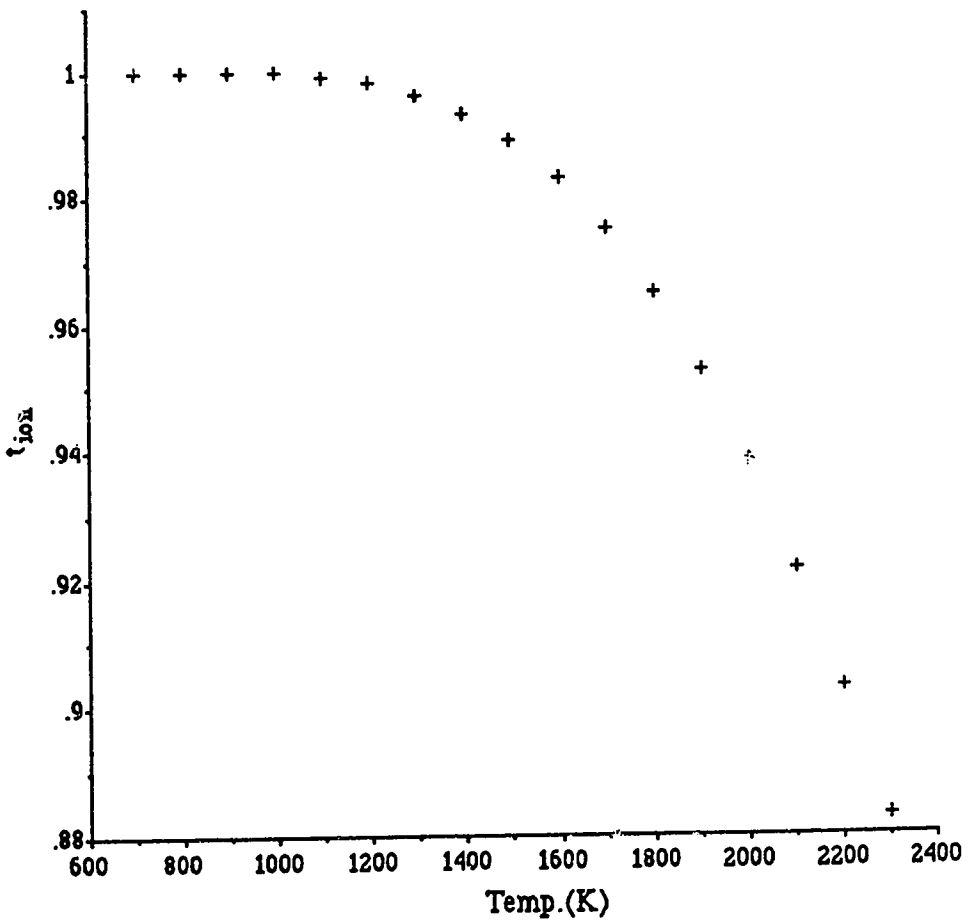

Fig. 4-6. t_{ion} versus Temperature for Thoria-Yttria with $\overline{P}_{O_2}$ (atm) established by Cr-CrO_3 and Cr_3C_2-Cr_2O_3-C Electrodes.

4.5 Recommendations

It appears that the three-phase mixture on the cathode side is not reaching equilibrium. The best solution to this problem is to redesign the cell so as to eliminate this mixture. It is proposed that the new cell would consist of :

$$3Cr + 2CO \Leftrightarrow Cr_3C_2 + O_2 \quad \text{Anode} \tag{4.28}$$

A mixture of CO and some inert carrier gas would flow through a mixture of Cr and Cr_3C_2 in the anode. For the anode reaction the equilibrium constant K_p consists of the oxygen pressure, P'_{O_2} and the carbon monoxide pressure, P_{CO} :

$$K_p = \frac{P'_{O_2}}{(P_{CO})^2} \tag{4.29}$$

The cathode would consist of oxygen. From equation (3.29) the e.m.f. from the cell would consist of :

$$E = \frac{RT}{4F} \ln \frac{P''_{O_2}}{P'_{O_2}} \tag{3.29}$$

Since the cathode consists of pure oxygen $P''_{O_2} \approx 1$ atm the e.m.f. from equation (3.29) becomes:

$$E = \frac{RT}{4F} \ln \frac{1}{P'_{O_2}} \tag{4.30}$$

Measuring the e.m.f. from this cell would allow us to calculate P_{O_2}' which is the oxygen pressure of the anodic reaction.

Since the free energy of formation for the anodic reaction is given by :

$$\Delta G^{\circ}_{anode} = -RT \ln \frac{P'_{O_2}}{(P_{CO})^2} \tag{4.31}$$

From determining P_{O_2}' and since P_{CO} is fixed, ΔG for the anode reaction can be determined. To calculate ΔG for the chromium carbide reaction the following needs to be performed :

$3Cr + 2CO \Leftrightarrow Cr_3C_2 + O_2$	ΔG^{o}_{anode}	From Cell
$2C + O_2 \Leftrightarrow 2CO$	$\Delta G^{o}_{literature}$	Literature
$3Cr + 2C \Leftrightarrow Cr_3C_2$	$\Delta G^{o}_{Cr_3C_2}$	

For the reaction $2C + O_2 \Leftrightarrow 2CO$, ΔG as a function of temperature has been determined by numerous authors with reasonably accurate values.

Instead of CO gas, CO_2 could also be utilized, keeping in mind that the resulting oxygen partial pressure from either the CO or CO_2 gas should be kept as close as possible to the oxygen pressure on the cathode side. In general keeping the P''_{O_2} and P'_{O_2} pressures close reduces the driving force for the polarization at the electrodes, resulting in improved accuracy. It may be that a metal-metal oxide reference is required in place of the oxygen so as to match the oxygen pressure on both sides of the electrolyte more closely.

In a similar fashion the free energy of formation for Cr_7C_3 and $Cr_{23}C_6$ could also be determined.

5.0 Carbon Monoxide / Dioxide Cell

5.1 Literature for Carbon Monoxide/Dioxide Reactions

The experimental portion of this section is concerned with the reaction consisting of :

$$CO + \tfrac{1}{2}O_2 \Leftrightarrow CO_2 \qquad (5.1)$$

However by recombination of the two reactions (5.2) and (5.3) :

$$CO \Leftrightarrow C + \tfrac{1}{2}O_2 \qquad (5.2)$$

$$C + O_2 \Leftrightarrow CO_2 \qquad (5.3)$$

$$CO + \tfrac{1}{2}O_2 \Leftrightarrow CO_2 \qquad (5.1)$$

the experimental reaction (5.1) is obtained. Therefore, in the literature section, reactions (5.2) and (5.3) have been included when appropriate.

The first determination of ΔG^o for reaction (5.1) used " Thüringer glass " a solid electrolyte. This was performed by Haber and Moser[71] with the following results :

$$\Delta G^o(\text{cal/mol}) = 67440 - 2.42T \ln T + 1.7\text{x}10^{-3}\, T^2 - 5.95\, T \qquad (5.4)$$

According to work carried out by Hahn[72] and Haber and Richardt [73] for the reaction :

$$CO_2 + H_2 \Leftrightarrow CO + H_2O_{(gas)} \qquad (5.5)$$

$$\Delta G^o(\text{cal/mol}) = 10100 - 1.81T \ln T + 4.45\text{x}10^{-3}\, T^2 - 6.8\text{x}10^{-7}\, T^3 - 0.54\, T \qquad (5.6)$$

By combining equation (5.5) with equation (5.7) given by[74] :

$$H_2 + \frac{1}{2}O_2 \Leftrightarrow H_2O_{(gas)} \qquad (5.7)$$

for which :

$$\Delta G^{\circ}(cal/mol) = -57410 + 0.94\,T\ln T + 1.65\times10^{-3}\,T^2 - 3.7\times10^{-7}\,T^3 + 3.92\,T \qquad (5.8)$$

resulting in equation (5.1), where :

$$\Delta G^{o}(cal/mol) = -67510 + 2.75T\ln T - 2.8\times10^{-3}\,T^2 + 3.1\times10^{-7}\,T^3 + 4.46\,T \qquad (5.9)$$

From direct measurements of the dissociation of carbon dioxide by Nernst and von Wartenberg[75], Langmuir[76] and Lowenstein[77], with linear regression of their data for reaction (5.1) :

$$\Delta G^{o}(cal/mole) = -58633 + 15.03\,T \quad R^2 = 0.954 \ (cal/mole) \qquad (5.10)$$

for the temperature range from 1122 to 1550 °C.

From Chipman et al.[78] for reaction (5.1)

$$\Delta G^{o}(cal/mol) = -66560 + 20.15\,T \quad \pm 1000\ cal \qquad (5.11)$$

According to Richardson and Jeffes[68] for reaction (5.2) :

$$\Delta G^{o}(cal/mol) = 26700 + 20.95\,T \quad \pm 1000\ cal \quad (298 - 2500\ K) \qquad (5.12)$$

and for reaction (5.3) :

$$\Delta G^{o}(cal/mol) = 94200 + 0.2\,T \quad \pm 1000\ cal \quad (298 - 2000\ K) \qquad (5.13)$$

finally for reaction (5.1) :

$$\Delta G^{o}(\text{ cal/mol}) = -67550 + 20.75\ T \quad \pm 1000\ \text{cal} \qquad (298 - 2500\ K) \qquad (5.14)$$

The above values from equations (5.12), (5.13), and (5.14) used by Richardson and Jeffes are originally from Thompson[79].

Peters and Mobius[80] used ThO_2-La_2O_3 and ZrO_2-Y_2O_3 electrolytes for the determination of ΔG for reaction (5.1) :

$$\Delta G^{o}\ (\text{cal/mol}) = -67560\ (\pm 200) - 21.02\ T\ (\pm 0.15) \qquad (1010 \text{ to } 1630\ K) \qquad (5.15)$$

also found for the reaction :

$$C + CO_2 \Leftrightarrow 2CO \qquad (5.16)$$

$$\Delta G^{o}\ (\text{cal/mol}) = -39430\ (\pm 120) - 40.83\ T\ (\pm 0.10) \quad (1000 \text{ to } 1500\ K) \qquad (5.17)$$

A carbon dioxide sensor consisting of ZrO_2-Y_2O_3 was used by Okamoto, Obayashi and Kudo[81] measured anomalously higher potentials in a cell with CO/CO_2 on one side and O_2 on the other side of the electrolyte at temperatures between 260-350 °C. The explanation given is that a mixed potential occurs at the CO/CO_2 electrode consisting of the reactions :

$$CO_{(adsorbed)} + O^{2-} \rightarrow CO_{2\,(gas)} + 2e^{-} \qquad (5.18)$$

$$O_{(adsorbed)} + 2e^{-} \rightarrow O^{2-} \qquad (5.19)$$

These two reactions result in a mixed electrode potential which produces an e.m.f. that is higher than expected, when equilibrium is not obtained.

In a study by Iwase and Mori[82] a cell utilizing ZrO_2-CaO measured the CO_2 in an oxygen gas stream which had combusted a metal sample. From the change in the e.m.f. over time, the weight percent of carbon in the metal samples was determined. From work by Iwase, et al.[83] a cell using ZrO_2 - CaO with a mixture of flowing CO/CO_2 gas was used to extract dissolved oxygen from liquid iron without using an external current. Using an electrochemical cell consisting of K_2CO_3, Cote and Gauthier[84] were able to determine partial pressures of CO_2 down to 9 ppm in air-CO_2 mixtures in the region of 575-1025 K at a total pressure of 1 atm. In an experiment by Colwell and Rapp[85] a ZrO_2-Y_2O_3 cell was used to monitor the CO/CO_2 ratio in a reaction zone with an air reference electrode. Maruyama, Ye and Saito[86] used an oxygen sensor consisting of ZrO_2-Y_2O_3 with CO-CO_2 mixtures on the anode side and air on the cathode side to act as a reference electrode. The

Table 5-1. Summary of Literature for the Reaction $CO + 1/2O_2 = CO_2$.

ΔG^o(cal/mol)	Reference
ΔG^o(cal/mol) = 67440 - 2.42T lnT + 1.7x10^{-3} T^2 - 5.95 T	71
-67510 + 2.75T lnT - 2.8x10^{-3}T^2 + 3.1x10^{-7} T^3+ 4.46 T	74
-58633 + 15.03 T	75, 76, 77
-66560 + 20.15 T	78
-67550 + 20.75 T	68
-67560 (± 200) - 21.02 T (± 0.15)	80

sensor was held at 1273 K resulting in an e.m.f. of -1.8 mV when air was used as a reference. In addition the system was run at 1093 and 1053 K with different CO - CO_2

mixtures measured by the ZrO_2-Y_2O_3 cell which were then also analyzed by a gas chromatograph. Both measurement techniques resulted in close agreement as to the exact composition of the CO - CO_2 mixtures.

Table 5-1 summarizes the values from the literature.The best values are the last three sets of data which fall in the region where ΔG^o(cal/mol) ≈ -67000 + 20.50 T.

5.2 Experimental Carbon Monoxide / Dioxide Cell

The cell is of the form :

(-) Pt | $CO-CO_2$ / P'_{O_2} | Electrolyte (ZrO_2-Y_2O_3) | O_2 / P''_{O_2} | Pt (+)

Oxygen pressure is established by pure oxygen at the cathode and at the anode due to equilibrium of the $CO-CO_2$ mixture.

The individual reactions at either electrode are given by :

$$CO + O^{-2} \Leftrightarrow CO_2 + 2e^- \quad \text{Anode} \qquad (5.20)$$

$$\tfrac{1}{2}O_2 + 2e^- \Leftrightarrow O^{-2} \quad \text{Cathode} \qquad (5.21)$$

$$CO + \tfrac{1}{2}O_2 \Leftrightarrow CO_2 \quad \text{Overall Reaction} \qquad (5.1)$$

The e.m.f. established by this system is given by :

$$E = \frac{RT}{4F}\bar{t}_i \ln \frac{P''_{O_2}\,(\text{cathode})}{P'_{O_2}\,(\text{anode})} \qquad (3.36)$$

The oxygen pressure P'_{O_2}, at the anode is established by :

$$\left(P'_{O_2}\right) = \left(\frac{P_{CO_2}}{K_P\, P_{CO}}\right)^2 \qquad (5.22)$$

where K_p is the equilibrium constant for the reaction $CO + 1/2O_2 = CO_2$, and each individual pressure term (i.e. P_{CO_2} and P_{CO}) is adjusted for barometric pressure at the time of calculation.

The oxygen pressure P''_{O_2}, at the cathode is established by oxygen :

$$P''_{O_2} = \text{Atm. Pressure} \tag{5.23}$$

Assuming that $\bar{t}_{ion} \approx 1$ it follows that :

$$E = \frac{RT}{4F} \ln P''_{O_2} - \frac{RT}{4F} \ln \left(\frac{P_{CO_2}}{K_p P_{CO}} \right)^2 \tag{5.24}$$

which is equivalent to :

$$E = \frac{RT}{4F} \ln P''_{O_2} + \frac{RT}{2F} \ln K_P + \frac{RT}{2F} \ln \left(\frac{P_{CO}}{P_{CO_2}} \right) \tag{5.25}$$

Since $\Delta G^o = - RT \ln K_p$ and $\Delta G^o = - z E^o F$ it follows that :

$$E^o = \frac{RT}{2F} \ln K_P \tag{5.26}$$

The e.m.f. for standard pressure becomes :

$$E^o = E - \frac{RT}{4F} \ln P''_{O_2} - \frac{RT}{2F} \ln \left(\frac{P_{CO}}{P_{CO_2}} \right) \tag{5.27}$$

and since :

$$\Delta G^o = -2E^oF \tag{5.28}$$

$$\Delta G^o = -2F \left[E + \frac{RT}{2F} \ln \frac{(P_{CO_2})}{(P_{CO})\,(P''_{O_2})^{\frac{1}{2}}} \right] \tag{5.29}$$

For all calculations involving equation (5.29) the following values[87] were used :

$$F = 23060.36 \quad +/- \ 0.065 \ \text{cal/V equiv} \tag{5.30}$$

$$R = 1.98719 \quad +/- \ 0.000062 \ \text{cal/mol K} \tag{5.31}$$

For corrections with the $CO\text{-}CO_2$ probes using air as the reference electrode, the value for the percentage oxygen in air used[87] was :

$$\text{Air} \ (\ \%\ O_2\ ) \ = \ 20.946 \ +/- \ 0.002 \ \%\ \text{Oxygen} \tag{5.32}$$

For both types of $CO\text{-}CO_2$ probes (air reference and the oxygen reference), barometric pressure was recorded so as to obtain a correction value for each of the pressure terms in equation (5.29).

The electrolyte utilized for the majority of this experiment consisted of zirconia with 8 weight w/o (4.5 m/o) yttria. This electrolyte was identical in purity to the calcia-stabilized zirconia as used in the chromium carbide experiment, except that yttria is the stabilizing agent. This was chosen due to superior thermal shock resistance and a slightly higher ionic transference number when compared to calcia stabilized zirconia. The gauze used in the cell is made of 90% Pt / 5% Rh / 5% Pd; the thermocouple was constructed with pure Pt and 87% Pt - 13% Rh. This thermocouple is the R-type commonly used for measurement at high temperatures. The outer tube used was mullite for its enhanced thermal shock resistance over alumina. In Fig. 5-1 the cell is depicted.

The Keithley Model 616 digital electrometer was used again for e.m.f. measurement. For control of gas flow a set of Matheson Series 8240 mass flow controllers were used.

Careful temperature profiling of the tube furnace was carried out so as to locate the active portion of the cell in the furnace area with the least amount of temperature variance so as to avoid additional electromotive forces.

A series of gases was chosen so as to ensure experimental consistency. The CO/CO_2 mixtures used are listed in Table 5-2.

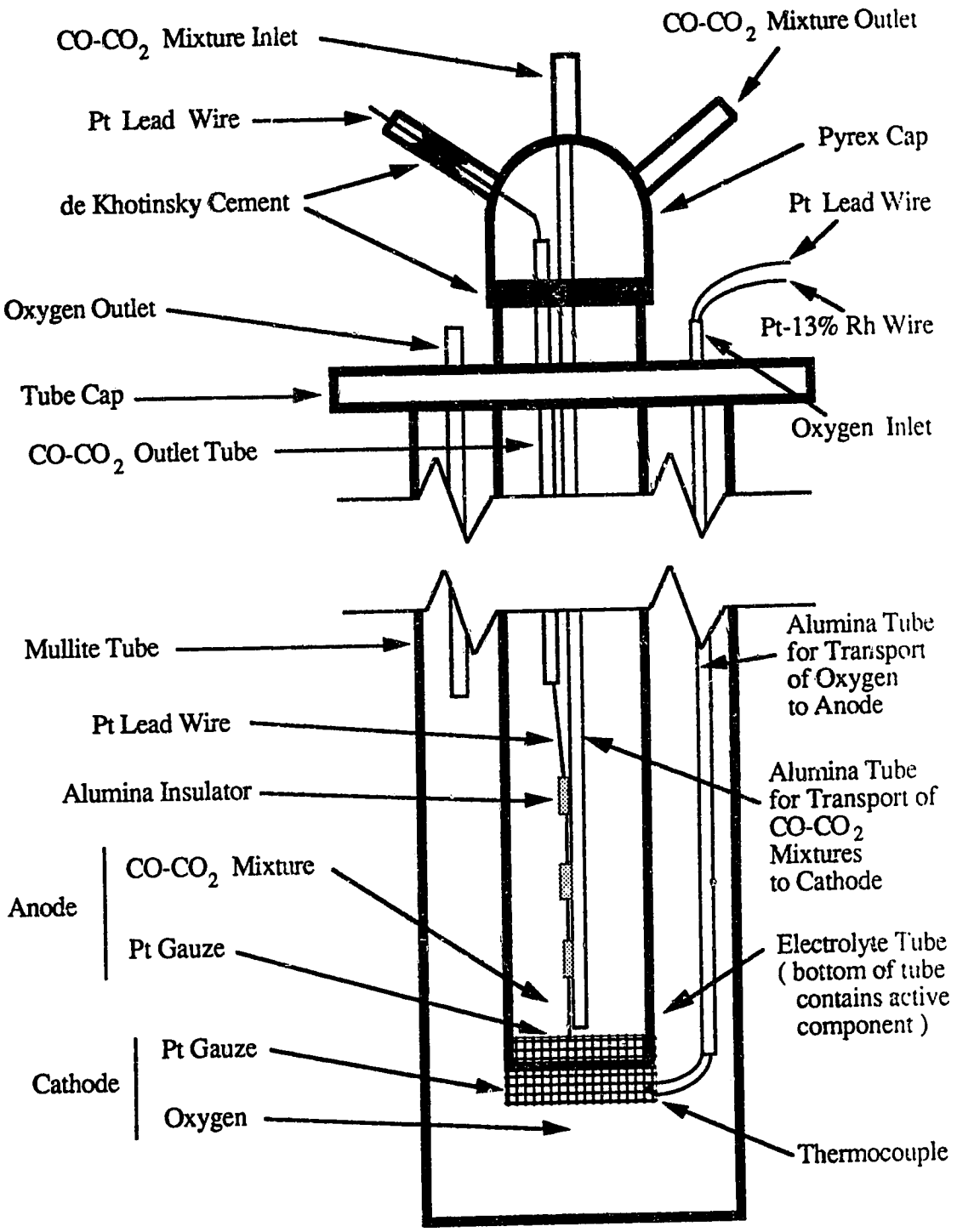

Fig. 5-1. Experimental CO/CO_2 Thermodynamic Cell.

Table 5-2. CO-CO_2 Experimental Gas Mixtures.

CO Content	Accuracy	CO_2 Content	Oxygen Level
5.00% CO	± 0.10% CO	95.00% CO_2	< 1 ppm O_2
0.1994% CO	± 0.004% CO	99.8006% CO_2	< 1 ppm O_2
52.50% CO	± 1.0% CO	47.50% CO_2	< 1 ppm O_2
97.94% CO	± 0.040% CO_2	2.03% CO_2	57 ppm O_2 *
0.097% CO	± 0.002% CO	99.903% CO_2	not analyzed
58.80% CO	± 1.2% CO	41.20% CO_2	not analyzed
89.0 ppm CO	± 1.8 ppm CO	99.9911% CO_2	not analyzed
99.9975% CO	± 0.0005% CO_2	0.0025% CO_2	< 5 ppm O_2

* also contains : 248 ppm of Nitrogen and 21 ppm of Hydrocarbons

5.3 Results

The data collected from the experimental runs are organized into four parts. In the first part cell one used air as a reference electrode for the cathode with the electrolyte consisting of calcia stabilized zirconia. Cell two used oxygen as a reference electrode and the electrolyte was yttria stabilized zirconia. All subsequent probes were constructed with yttria stabilized zirconia. Probes three and four were virtually identical to cell two, but cell four was primarily a test for polarization.

Part One - Air Reference

The data in Table 5-3 is a summary of the experimental data given in Tables B-1 to B-9 in Appendix B for the various gas compositions. For the individual plots of the experimental mixtures refer to Figs. B-1 to B-9 in the appendix.

Table 5-3. Summary of Experimental Data (Cell One - Air Reference).

Gas Composition	Measurements	Temp.(K)	ΔG^o(cal/mol) vs. Temp.(K)	R^2
58.8% CO / 41.2% CO_2	25	859-1478	-60531 + 16.36 T	0.94
52.5% CO / 47.5% CO_2	24	859-1482	-61822 + 17.24 T	0.97
5.0% CO / 95.0% CO_2	24	856-1476	-62041 + 17.11 T	0.95
0.1994% CO / 99.8006% CO_2	25	850-1478	-63465 + 18.39 T	0.96
0.097% CO / 99.903% CO_2	20	915-1475	-63215 + 18.65 T	0.88
89 ppm CO / 99.9911% CO_2	8	820-1171	-55566 + 11.83 T	0.62
97.98% CO / 2.02% CO_2	10	861-1220	-46157 + 6.25 T	0.20
99.884% CO / 0.116% CO_2	11	843-1207	-65856 + 25.40 T	0.91
99.9975% CO / 0.0025% CO_2	18	992-1488	-50507 + 21.43 T	0.69

From Table 5-3 the first 5 experimental runs are plotted in Fig. 5-2.

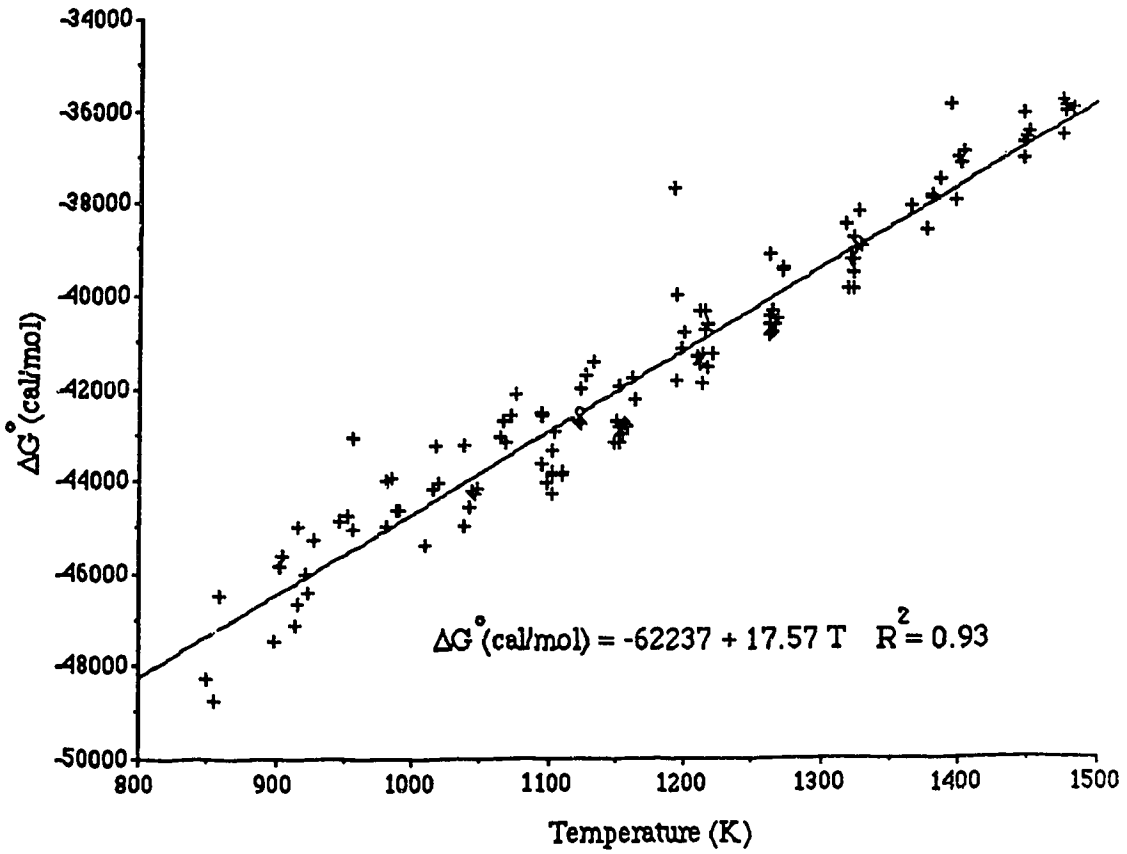

Fig. 5-2. Plot of 58.8% CO / 52.5% CO / 5.0% CO / 0.1994% CO / 0.097% CO.

It can be concluded for the CO-CO_2 cell in which air is used as a reference that the relationship between free energy and temperature for reaction (5.1) is given as :

$$\Delta G^o (\pm 75 \text{ cal/mol}) = -62237 + 17.57\,T \quad R^2 = 0.93 \quad (850\text{-}1482\text{ K}) \qquad (5.33)$$

The experimentally obtained data are somewhat in error since one of the accepted equations indicative of the reaction is given [68] where :

$$\Delta G^{o}(\text{cal/mol}) = -67550 + 20.75\,T \quad \pm 1000 \text{ cal.} \quad (298 - 2500\text{ K}) \qquad (5.13)$$

Conclusions and comments on the air reference system :

1. The air reference side was delivered from the building supply. This supply in itself could have been a problem due to impurities present in the supply system. However, it is assumed that this would have a small effect on the experiment.
2. In retrospect the cell should have been run in ambient atmosphere without any reliance on supply air with the possibility of contamination.
3. The next step was to replace the air reference supply with oxygen.
4. Failure of the system was attributed to fracture at the tip of the solid electrolyte tube;due to this it was decided at this point to change to yttria stabilized zirconia for better thermal shock resistance and possibly less interference due to electronic conduction.

Part Two - Oxygen Reference

In Table 5-4 the data from Tables A-10 to A-16 in Appendix B are summarized. The individual plots for each of the gas compositions are given in Figs. A-10 to A-16 in this appendix.

Table 5-4. Summary of Experimental Data (Cell Two - Oxygen Reference).

Gas Composition	Measurements	Temp. (K)	ΔG^o(cal/mol) vs. Temp. (K)	R^2
58.8% CO / 41.2% CO_2	16	924-1426	-73798 + 26.24 T	0.94
52.5% CO / 47.5% CO_2	16	922-1424	-73689 + 26.35 T	0.94
5.0% CO / 95.0% CO_2	16	922-1424	-69927 + 22.74 T	0.95
0.1994% CO / 99.8006% CO_2	16	922-1425	-80439 + 31.41 T	0.84
0.097% CO / 99.903% CO_2	16	923-1426	-84325 + 34.23 T	0.89
97.98% CO / 2.02% CO_2	16	922-1423	-75126 + 30.12 T	0.87
99.9975% CO / 0.0025% CO_2	15	922-1424	-77140 + 1.538 T	0.01

The results from this portion of the experiment were not satisfactory. Upon dismantling the cell, it was evident that failure of the electrolyte tube at the tip had again been the reason for the cell ceasing to function. It was determined also that the seal at the top of the electrolyte tube required some improvements, i.e. improved O-rings and the addition of deKhotinsky sealant; these were both added in cells three and four.

During operation of the cell it was noticed that periodically gas flow through the cell would become difficult and would require extensive purging with the CO-CO_2 mixtures. Since the gas mixture consists of CO and CO_2, it is very possible that carbon deposition was occurring in the gas distribution passages within the cell and / or the mass flow controller.

The deposition reaction would occur via the "Boudouard reaction" given as :

$$2CO \Leftrightarrow CO_2 + C \tag{5.34}$$

where :

$$\Delta G^o = -40800 + 41.70\,T \tag{5.35}$$ [88]

Using equations (5.34) and (5.35), the relationship between ΔG, temperature, P_{CO} and P_{CO_2} is given by equation (5.36) :

$$\Delta G^o(\text{cal/mol}) = -40800 + 41.70\,T + R\,T \ln \frac{P_{CO_2}}{(P_{CO})^2} \tag{5.36}$$

From analyzing equation (5.36) the following can be concluded :

1) As the temperature decreases the reaction is more favorable resulting in carbon deposition.
2) The gas mixtures high in CO will have a more negative value for the free energy of reaction which results in carbon deposition.

Upon dismantling the cell carbon-like deposits were observed; however, since the cell had been periodically purged (with gas low in CO) the effect of any carbon deposition in the cell was hard to determine. Considering that the cell is sensitive to the effects of pressure (see equation 5.29) any back pressures due to plugging of the gas passages would alter the results obtained for ΔG^o. With this in mind, probes 3 and 4 used alumina tubes with larger openings and extended purging between changes of gas mixtures.

Part Three - Oxygen Reference

The data in Table 5-5 are a summary of the experimental runs given in Tables B-17 to B-24 in Appendix B for the various gas compositions. In Figs. B-17 to B-24 in the appendix, individual plots of the experimental data are presented.

Table 5-5. Summary of Experimental Data (Cell Three - Oxygen Reference).

Gas Composition	Measurements	Temp. (K)	ΔG^o(cal/mol) vs. Temp. (K)	R^2
58.8% CO / 41.2% CO_2	30	946-1422	-65508 + 19.31 T	0.99
52.5% CO / 47.5% CO_2	30	781-1423	-66825 + 20.40 T	1.00
5.0% CO / 95.0% CO_2	29	781-1423	-66609 + 20.40 T	0.99
0.1994% CO / 99.8006% CO_2	13	946-1423	-75187 + 27.57 T	0.94
0.097% CO / 99.903% CO_2	13	946-1423	-72499 + 25.27 T	0.93
97.98% CO / 2.02% CO_2	27	842-1414	-62854 + 17.76 T	0.95
99.9911% CO_2 / 89ppm CO	14	945-1421	-823634 + 30.34 T	0.92
0.1994% CO / 99.8006% CO_2	50	782-1402	-74653 + 28.84 T	0.97

The data from this set of runs are good quality especially for the mixtures which are not dilute in one component. Plotting the mixtures consisting of 52.5% CO - 47.5% CO_2, 5.0% CO -95.0% CO_2, and 58.8% CO - 41.2% CO_2 in Fig. 5-3, the value obtained for the reaction :

$$CO + \frac{1}{2}O_2 \Leftrightarrow CO_2 \tag{5.1}$$

is given as :

$$\Delta G^o(\text{cal/mol}) = -65807 + 19.64\,T \quad R^2 = 0.99 \tag{5.37}$$

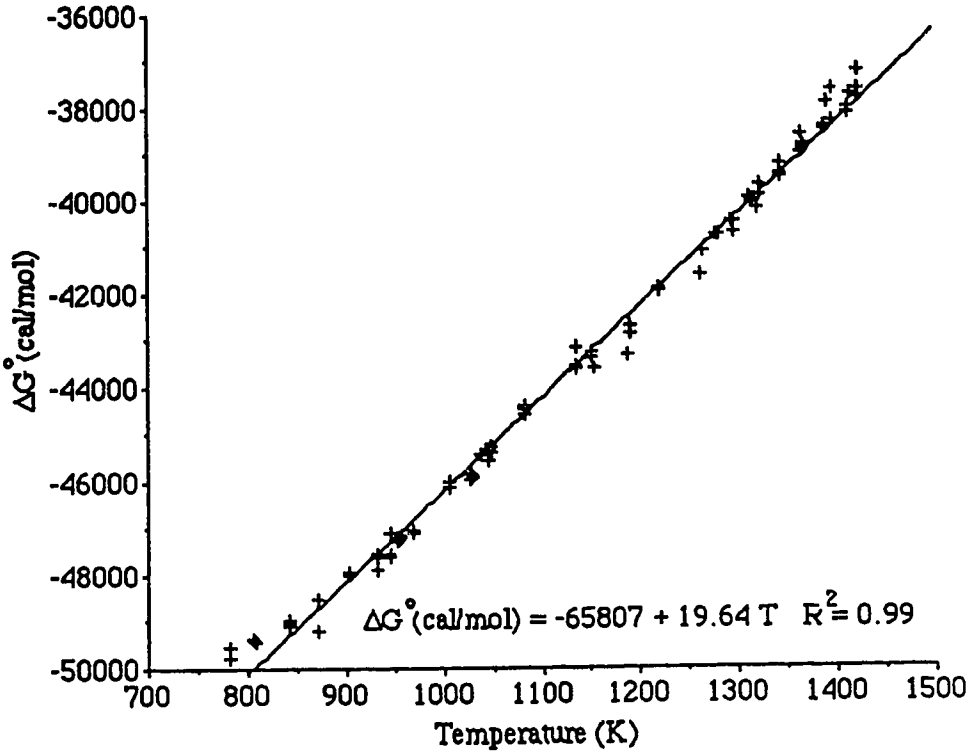

Fig. 5-3. Plot of 52.5% CO/47.5% CO_2, 5.0% CO/95.0% CO_2, and 58.8% CO/41.2%.

Part Four Polarization and Flow Rate

In this section the flow rates of several CO-CO_2 mixtures were varied so as to determine the effect on the e.m.f. of the CO-CO_2 cells. The flow rates have been reported as room-temperature volumetric flow rates. The effect of oxygen flow rate was found to have no effect except for extremely high flow rates in which the cell is being cooled from the excessive flow.

The dependence of the e.m.f. on the CO-CO_2 flow rate is listed in Tables B-25 to B-27 and plotted in Figs. B-25 to B-27. At low flow rates, increases in the flow rate produced a rise in the e.m.f. with an eventual plateau being reached. In addition, as the concentration of CO gas was increased, the amount of flow required to avoid polarization decreased (i.e. as the CO concentration decreases the cell becomes more sensitive to the flow rate).

The reason for the polarization phenomenon being related to the CO concentration is due to oxygen or oxygen ions migrating through the electrolyte to the CO-CO_2 electrode and then reacting with CO molecules producing CO_2 molecules. The actual migration could be due to either porosity or electronic conductivity in the electrolyte. This local decrease in the CO concentration will lower the e.m.f. of the cell as observed at low flow rates. Higher flow rates replace the CO molecules which have reacted at the electrode to CO_2, and restore the CO-CO_2 mixture to normal proportions. Gases which consist of low concentrations of either CO or CO_2 are affected to a greater extent than gases which consist of equal amounts of CO and CO_2.

In addition to the polarization study, two sets of thermodynamic data were also collected as summarized in Table 5-6. These runs were made with continuous use of the gas mixtures, i.e. the 5.0% CO mixture was used first and then the cell was switched to the 0.097% CO mixture. The data from these runs are listed in Tables B-28 and B-29 and plotted in Figs. B-28 and B-29 in Appendix B.

Of these two the 5.0% CO mixture was found to be more reliable. It was noticed that the cell began to give erratic results towards the end of use with the 0.097% CO mixture.

Table 5-6. Summary of Experimental Data (Cell Four - Oxygen Reference).

Gas Composition	Measurements	Temp. (K)	ΔG^{o}(cal/mol) vs. Temp. (K)	R^2
5.0% CO / 95.0% CO_2	28	789-1378	-67415 + 21.09 T	0.98
0.097% CO / 99.903% CO_2	35	781-1408	-69659 + 25.73 T	0.96

5.4 Discussion

The values obtained from the air reference cell are lower than the accepted values. This has been attributed to either electronic conductivity, cracking of the electrolyte due to thermal stresses, cross contamination of the electrode compartments, contamination of the air supply, or a combination of these factors. In response the the second cell was built so as to use pure oxygen. The results from this portion of the experiment were incomplete and upon dismantling the system it was observed that the tip of the solid electrolyte tube had failed. This failure is probably the reason for the poor results at this stage.

For cell three some minor improvements were made to the seals resulting in accurate and reproducible readings especially with the gas mixtures which were not dilute in either component of the CO-CO_2 gas mixture. Cell three was used until the cell tip failed in the identical manner to that previously.

Cell four was assembled so as to verify the results from cell three and examine the phenomena of gas flow rate and polarization of the electrode interface. This cell provided valuable information on polarization and verification of the results from cell three.

To verify that the system was operating under ionic conditions (i.e. $t_{ion} \approx 1$) the value for t_{ion} was calculated for the experimental operating conditions. For $P_{\oplus}$ and $P_{\ominus}$:

$$P_{\oplus} = 4.55 \times 10^{3} \exp \frac{3.04\ (eV)}{kT} \quad (500 - 1600 \text{ Celsius}) \tag{3.65}$$

$$P_{\ominus} = 5.23 \times 10^{14} \exp - \frac{11.8\ (eV)}{kT} \quad (500 - 1600 \text{ Celsius}) \tag{3.66}$$

For the calculation of $\overline{P}_{O_2}$ equation 4.26 was used :

$$\log \overline{P}_{O_2} = \frac{\log P'_{O_2} + \log P''_{O_2}}{2} \tag{4.26}$$

For the reaction $CO + \frac{1}{2}O_2 \Leftrightarrow CO_2$:

$$\Delta G^o(\text{cal/mol}) = -67550 + 20.75\,T \quad (298 - 2500\ K)\ ^{68} \tag{5.14}$$

and since $\Delta G^o = -RT \ln K_p$, therefore :

$$\ln K_p = \frac{33968}{T} - 10.44 \tag{5.37}$$

The oxygen pressure at the anode side is calculated by :

$$P'_{O_2} = \left[\frac{P_{CO_2}}{P_{CO}\,K_p}\right]^2 \tag{5.21}$$

and at the cathode $P''_{O_2} = 1$ atm.

Equation (3.56) was utilized for t_{ion}, i.e.:

$$t_{ion} = \left[1 + \left(\frac{P_{O_2}}{P_{\oplus}}\right)^{\frac{1}{4}} + \left(\frac{P_{O_2}}{P_{\ominus}}\right)^{\frac{-1}{4}}\right]^{-1} \tag{3.56}$$

The ionic transference number was calculated for the widest range of gas composition used in the experiment (i.e. 0.0025% CO_2 and 89 ppm CO for the range of 500 - 1600 °C) and is summarized in Tables 5-7 and 5-8. Within this range of temperatures and experimental oxygen pressures the ionic transference number of the electrolyte is observed in Fig. 5-4 to be greater than $t_{ion} = 0.995$. With this evidence it is suggested that a combination of porosity and/or small amounts of electronic conduction allowed the transference of oxygen to the anode side of the cell. The poor results obtained from the gas mixtures low in either

component occur since they can be easily altered in composition at the anode due to this oxygen transference. In this case the best measurements are obtained with mixtures carrying a significant amount of both components (say ≥ 2%).

Table 5-7. Temperature versus t_{ion} for 0.0025% CO_2 / 99.9975% CO.

Temp.(K)	Log $P_{\ominus}$	Log $P_{\oplus}$	log $\overline{P}_{O_2}$	t_{ion}
373	-144.58	44.70	-39.62	1.0000
473	-110.90	36.02	-31.26	1.0000
573	-88.98	30.37	-25.81	1.0000
673	-73.57	26.40	-21.99	1.0000
773	-62.15	23.46	-19.15	1.0000
873	-53.34	21.19	-16.97	1.0000
973	-46.35	19.39	-15.23	1.0000
1073	-40.66	17.92	-13.82	1.0000
1173	-35.93	16.71	-12.64	1.0000
1273	-31.96	15.68	-11.66	1.0000
1373	-28.56	14.81	-10.81	1.0000
1473	-25.62	14.05	-10.08	0.9999
1573	-23.05	13.39	-9.45	0.9996
1673	-20.80	12.81	-8.89	0.9989
1773	-18.79	12.29	-8.39	0.9975
1873	-17.00	11.83	-7.94	0.9946
1973	-15.40	11.42	-7.54	0.9892
2073	-13.94	11.04	-7.18	0.9800
2173	-12.62	10.70	-6.86	0.9651
2273	-11.42	10.39	-6.56	0.9426
2373	-10.32	10.11	-6.28	0.9107
2473	-9.31	9.85	-6.03	0.8681
2573	-8.37	9.61	-5.80	0.8146
2673	-7.51	9.38	-5.59	0.7515

Table 5-8. Temperature versus t_{ion} for 89 ppm CO.

Temp.(K)	Log $P_{\ominus}$	Log $P_{\oplus}$	log $\overline{P}_{O_2}$	t_{ion}
373	-144.58	44.70	-30.96	1.0000
473	-110.90	36.02	-22.60	1.0000
573	-88.98	30.37	-17.16	1.0000
673	-73.57	26.40	-13.34	1.0000
773	-62.15	23.46	-10.50	1.0000
873	-53.34	21.19	-8.31	1.0000
973	-46.35	19.39	-6.58	1.0000
1073	-40.66	17.92	-5.16	1.0000
1173	-35.93	16.71	-3.99	1.0000
1273	-31.96	15.68	-3.00	1.0000
1373	-28.56	14.81	-2.16	0.9999
1473	-25.62	14.05	-1.43	0.9999
1573	-23.05	13.39	-0.79	0.9997
1673	-20.80	12.81	-0.23	0.9994
1773	-18.79	12.29	0.26	0.9990
1873	-17.00	11.83	0.71	0.9983
1973	-15.40	11.42	1.11	0.9973
2073	-13.94	11.04	1.47	0.9958
2173	-12.62	10.70	1.80	0.9939
2273	-11.42	10.39	2.09	0.9912
2373	-10.32	10.11	2.37	0.9879
2473	-9.31	9.85	2.62	0.9836
2573	-8.37	9.61	2.85	0.9784
2673	-7.51	9.38	3.07	0.9722

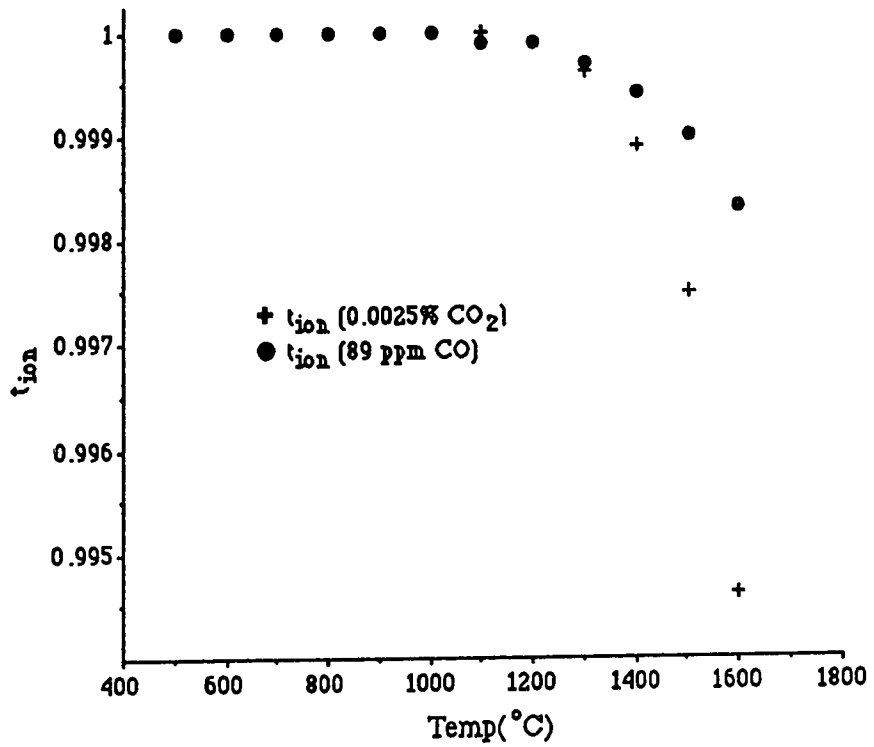

Fig. 5-4. t_{ion} versus Temperature for 0.0025% CO_2 and 89 ppm CO.

5.5 Recommendations

Some suggestions for improvements in the CO-CO_2 cell are in order at this point :

1. It is recommended that copper turnings are placed in the gas flow so as to remove oxygen from the CO-CO_2 mixture. It has been suggested by Colwell and Rapp[89] that a reaction of CO with the steel in the gas cylinder forms iron carbonyl which decomposes in the inlet and exit lines to Fe and CO. The decomposed Fe then catalyzes the Boudouard reaction at low temperatures resulting in the formation of carbon soot which can cause problems with back-pressure and proper control of flow. The copper acts as a hot surface where iron carbonyl can decompose. This treatment is especially important for CO-CO_2 gas flows low in either component.
2. Water should be removed from both gas streams with either $Mg(ClO_4)_2$ or P_2O_5.
3. A pre-heat for both gas flows would eliminate any doubt about cooling in the cell.
4. Improved accuracy is obtained in using mixtures not too dilute in either component, due to the fact that any reactions which reduce the concentration of either component will have a minimal effect.
5. Using solid metal-metal oxide reference electrodes with equilibrium oxygen pressures close to that imposed by the CO-CO_2 mixtures would greatly reduce the driving force for polarization at the electrodes.
6. If multiple CO-CO_2 mixtures are run in series through a cell, a purging gas should be used when changing from one gas to the next. Purging first with argon and then with oxygen would scavenge carbon deposits which could plug gas passages or possibly alter electrode activities. Gas passages should be as large as possible and operation below $\approx 700\ ^{o}C$ with gas mixtures higher than 50% CO should be avoided due to carbon deposition.

Appendix A Experimental Data for the Chromium Carbide Cell

Table A-1. Run 2 Chromium / Zirconia-Calcia.

E (mv)	Temp. (°C)	Temp. (K)	ΔG^o cal/mol
25.00	1015.0	1288	-5189
24.16	1004.0	1277	-5014
17.03	986.5	1259	-3535
13.54	1004.0	1277	-2810
13.02	1026.0	1299	-2702
12.20	1004.0	1277	-2532
13.70	981.0	1254	-2843
18.84	958.0	1231	-3910
24.05	937.0	1210	-4991
31.67	914.0	1187	-6573
41.82	890.0	1163	-8680
96.56	866.0	1233	-20040
91.15	891.0	1256	-18918
74.96	915.0	1280	-15557
54.40	937.0	1304	-11290
33.98	960.0	1328	-7052
20.40	983.0	1339	-4234
9.46	1007.0	1349	-1963
7.81	1031.0	1366	-1621
9.64	1055.0	1376	-2001
12.15	1066.0	1389	-2522
14.22	1076.0	1349	-2951
17.13	1093.0	1366	-3555
17.24	1103.0	1376	-3578
19.34	1116.0	1389	-4014

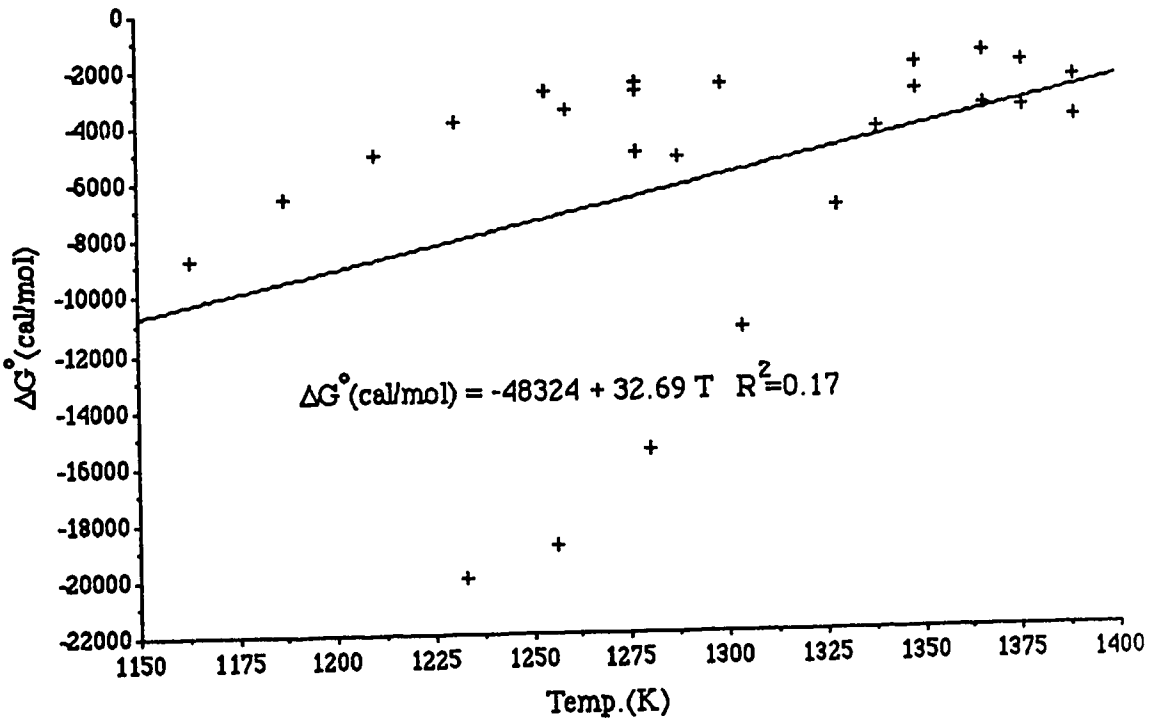

Fig. A-1. Run 2 Chromium / Zirconia-Calcia - ΔG^o versus Temperature.

Table A-2. Run 3 Chromium / Zirconia-Calcia.

E (mv)	Temp.(°C)	Temp.(K)	ΔG^o cal/mol
74.1	833	1106	-15379
54.0	826	1099	-11207
70.9	929	1202	-14715
54.5	948	1221	-11311
34.1	854	1127	-7077

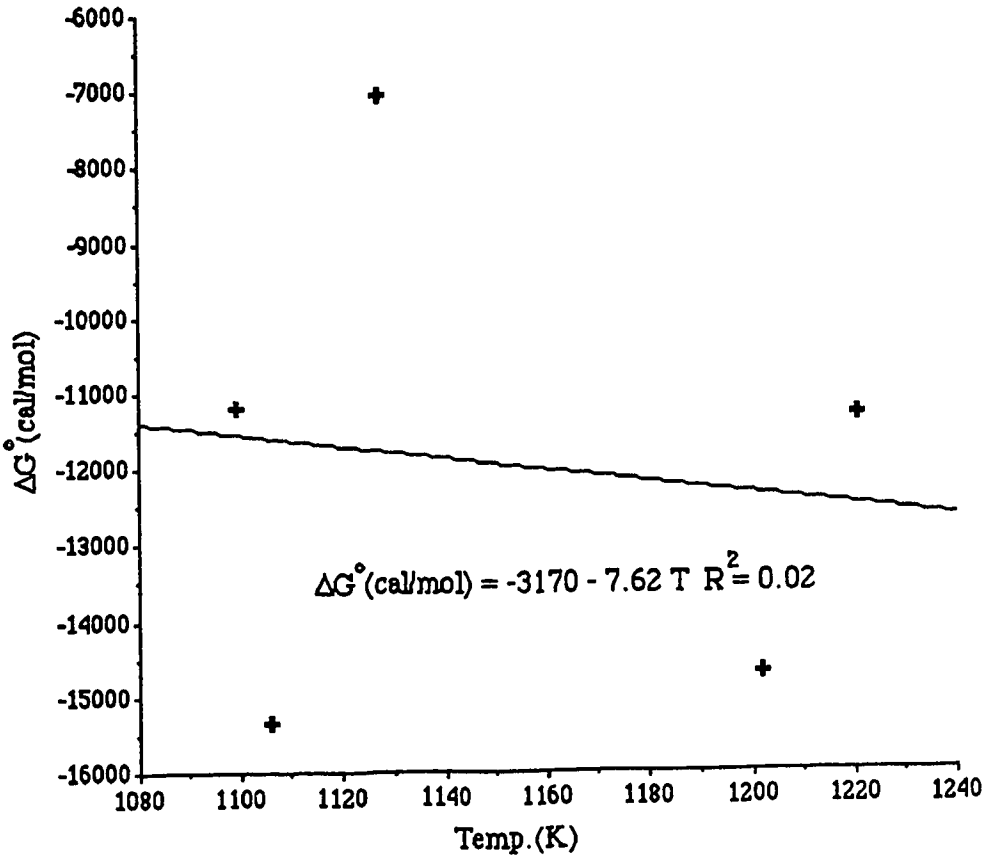

Fig. A-2. Run 3 Chromium / Zirconia-Calcia - ΔG^o versus Temperature.

Table A-3. Run 5 Chromium / Thoria-Yttria.

E (mv)	Temp.(°C)	Temp.(K)	ΔG^o (cal/mol)
94.4	890	1163	-19592
92.3	901	1174	-19156
91.0	912	1185	-18886
92.1	899	1172	-19115
91.9	886	1159	-19073
93.9	875	1148	-19488
91.2	891	1164	-18928
90.4	906	1179	-18762
94.0	937	1210	-19509
95.3	915	1188	-19779
96.1	903	1176	-19945
96.0	894	1167	-19924
96.0	877	1150	-19924
93.3	880	1153	-19364
95.0	851	1124	-19717
90.5	875	1148	-18783
92.2	898	1171	-19136
96.3	922	1195	-19986
96.8	946	1219	-20090
98.6	965	1238	-20464
98.3	946	1219	-20402
99.0	965	1238	-20547
98.7	967	1240	-20485
98.9	940	1213	-20526
96.7	920	1193	-20069
97.6	895	1168	-20256
96.9	886	1159	-20111
96.8	905	1178	-20090

Table A-3. Run 5 Chromium / Thoria-Yttria Continued :

E (mv)	Temp.(°C)	Temp.(K)	ΔG° (cal/mol)
95.8	935	1208	-19883
94.4	913	1186	-19592
94.0	911	1184	-19509
93.1	888	1161	-19322
92.8	865	1138	-19260
92.8	864	1137	-19260
90.4	840	1113	-18762
94.4	815	1088	-19592
88.5	838	1111	-18368
88.6	903	1176	-18388
99.1	963	1236	-20568
100.2	979	1252	-20796
102.2	1000	1273	-21211
102.0	1021	1294	-21169
101.3	1033	1306	-21024
102.3	1042	1315	-21232
102.7	1066	1339	-21315
103.7	1060	1333	-21522
103.0	1082	1355	-21377
102.5	1079	1352	-21273
102.5	1064	1337	-21273
105.6	1038	1311	-21917
102.4	1038	1311	-21252
100.3	1040	1313	-20817
102.9	1019	1292	-21356
101.3	993	1266	-21024
98.0	960	1233	-20339

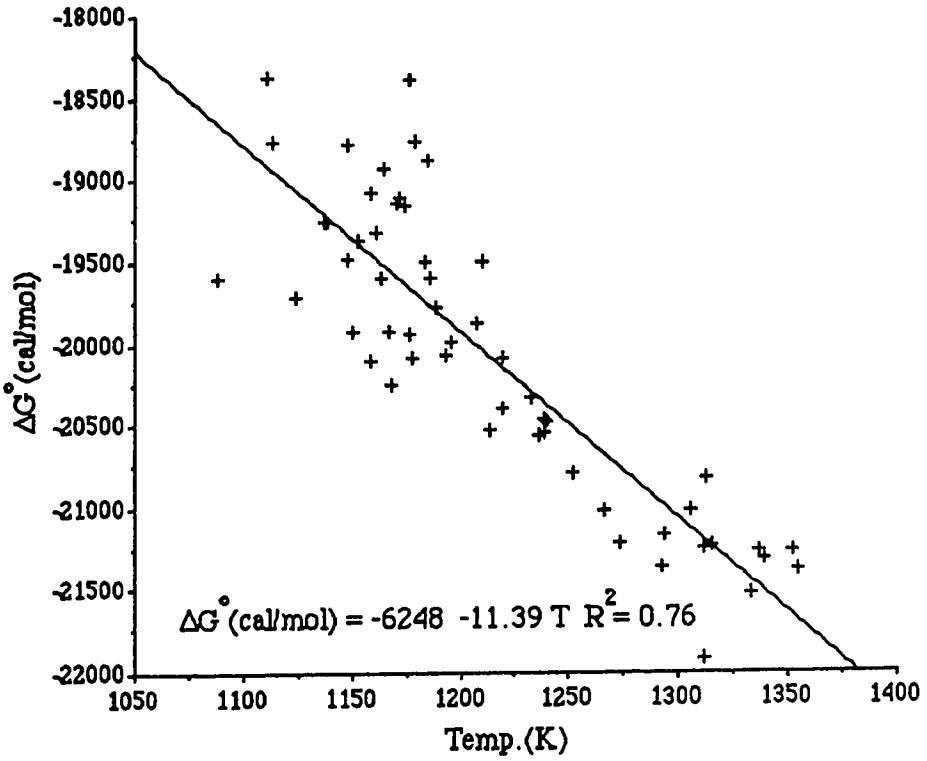

Fig. A-3. Run 5 Chromium / Thoria-Yttria - ΔG^o versus Temperature.

Table A-4. Run 6 Chromium / Zirconia-Calcia.

E (mv)	Temp.(°C)	Temp.(K)	ΔG^o (cal/mol)
36.0	704	977	-7472
59.4	726	999	-12334
67.7	748	1021	-14042
68.8	748	1021	-14277
65.3	771	1044	-13559
69.0	794	1067	-14321
59.2	819	1092	-12289
55.5	842	1115	-11519
56.5	867	1140	-11720
47.5	990	1263	-9860
49.4	1013	1286	-10249
43.2	1041	1314	-8970
45.1	1066	1339	-9360
45.4	1065	1338	-9423
40.1	1045	1318	-8312
39.2	1022	1295	-8136
31.2	997	1270	-6475
25.2	976	1249	-5230
21.2	952	1225	-4400
23.4	976	1249	-4859
28.0	1021	1294	-5811
34.7	941	1214	-7202
34.6	965	1238	-7181
37.2	989	1262	-7721
40.7	1014	1287	-8447
43.5	1040	1313	-9028
45.5	1064	1337	-9443
42.4	1051	1324	-8800

Table A-4. Run 6 Chromium / Zirconia-Calcia Continued :

E (mv)	Temp.(°C)	Temp.(K)	ΔG^o (cal/mol)
39.4	1038	1311	-8171
31.2	1045	1318	-6480
33.7	1067	1340	-7000
30.9	1044	1317	-6413
28.6	1020	1293	-5936
27.5	995	1268	-5707
25.0	996	1269	-5189
24.6	974	1247	-5106
22.9	952	1225	-4753
22.7	986	1259	-4711
24.0	1005	1278	-4981

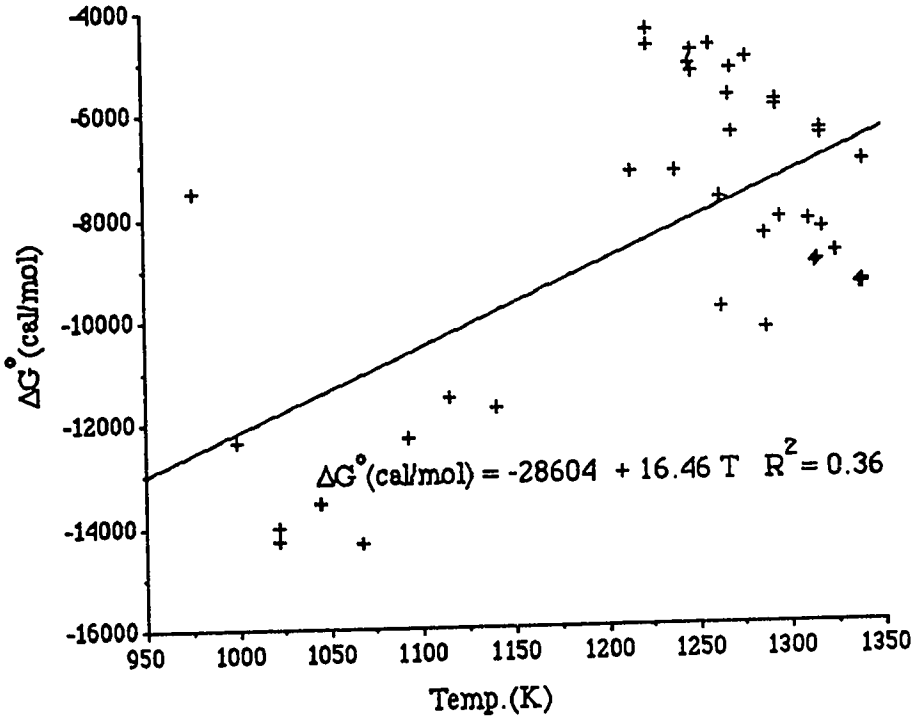

Fig. A-4. Run 6 Chromium / Zirconia-Calcia - ΔG^o versus Temperature.

Table A-5. Run 7 Chromium / Thoria-Yttria.

E (mv)	Temp.(°C)	Temp.(K)	ΔG^o (cal/mol)
31.2	1045	1318	-6480
33.7	1067	1340	-7000
30.9	1044	1317	-6413
28.6	1020	1293	-5936
27.5	995	1268	-5707
25.0	996	1269	-5189
24.6	974	1247	-5106
22.9	952	1225	-4753
22.7	986	1259	-4711
24.0	1005	1278	-4981

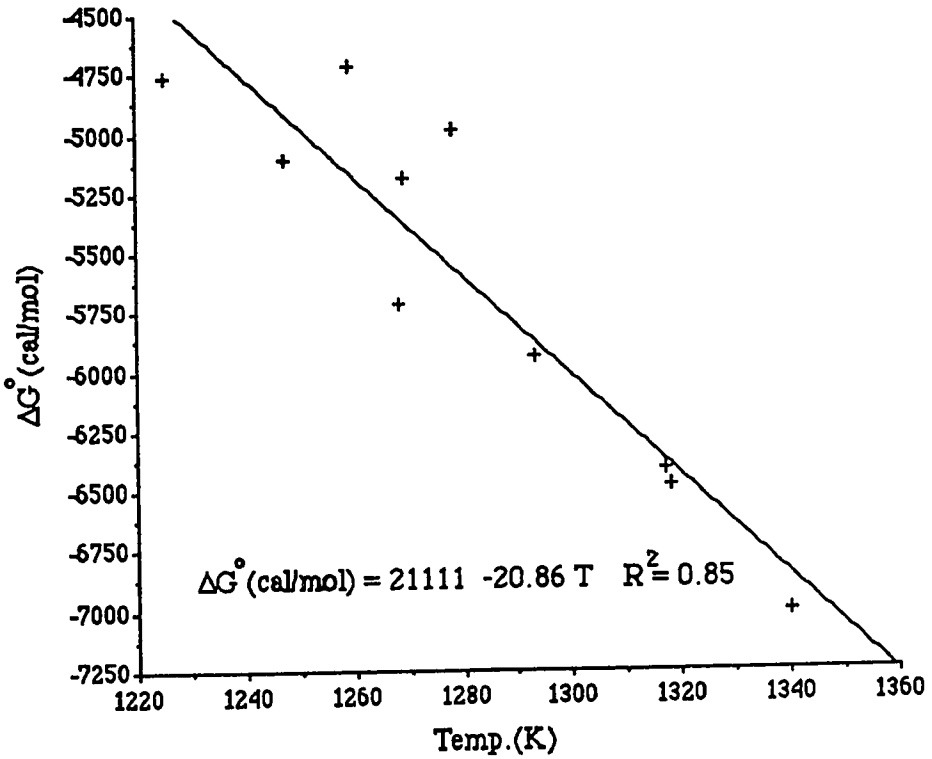

Fig. A-5. Run 7 Chromium / Thoria-Yttria - ΔG^o versus Temperature.

Table A-6. Run 8 Chromium / Zirconia-Calcia.

E (mv)	Temp.(°C)	Temp(K)	ΔG° (cal/mol)
-7.60	1132	1405	1577
-7.50	1142	1415	1557
-10.20	1130	1403	2117
-8.75	1142	1415	1816
-10.9	1120	1393	2275
-15.6	1094	1367	3240
-21.4	1071	1344	4439
-25.1	1047	1320	5207
-3.3	1119	1392	691
-3.8	1108	1381	795
-7.8	1097	1370	1615
-12.1	1083	1356	2509
-15.1	1073	1346	3140
-16.5	1061	1334	3433
-15.6	1050	1323	3229
-15.5	1037	1310	3217
-16.8	1026	1299	3478
-18.5	1014	1287	3844
-20.9	992	1265	4338
-24.5	981	1254	5077
-13.6	959	1232	2827
-1.7	936	1209	353
1.4	914	1187	-280
25.0	892	1165	-5193
35.2	867	1140	-7314
43.4	822	1095	-9003
12.6	845	1118	-2615
16.1	868	1141	-3346
8.1	891	1164	-1683
-2.9	913	1186	600

Table A-6. Run 8 Chromium / Zirconia-Calcia Continued :

E (mv)	Temp.(°C)	Temp(K)	ΔG^o (cal/mol)
-15.4	936	1209	3198
-13.7	959	1232	2839
-16.8	981	1254	3487
-20.2	1006	1279	4188
-17.2	1027	1300	3568
-9.5	1067	1340	1970

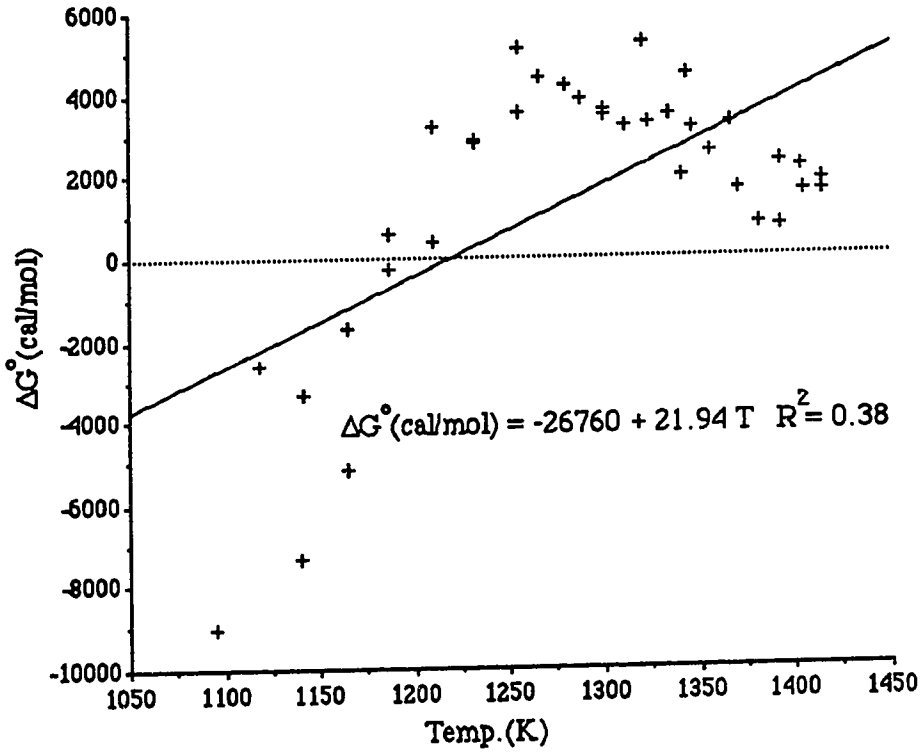

Fig. A-6. Run 8 Chromium / Zirconia-Calcia - ΔG^o versus Temperature.

Table A-7. Run 10 Chromium / Thoria-Yttria.

E (mv)	Temp.(°C)	Temp.(K)	ΔG^o (cal/mol)
86.1	948	1221	-17868
87.8	959	1232	-18225
89.0	972	1245	-18434
90.0	984	1257	-18679
91.4	996	1269	-18972
92.2	1008	1281	-19138
93.8	1020	1293	-19464
93.9	1032	1305	-19487
94.3	1044	1317	-19570
95.2	1056	1329	-19759
95.7	1068	1341	-19867
95.9	1080	1353	-19906
96.5	1103	1376	-20033
96.2	1090	1363	-19960
95.7	1079	1352	-19871
95.6	1066	1339	-19836
95.7	1041	1314	-19865
95.7	1016	1289	-19856
94.7	992	1265	-19665
92.9	968	1241	-19283
92.2	944	1217	-19142
90.0	921	1194	-18675
86.9	898	1171	-18032
84.1	874	1147	-17448
84.4	851	1124	-17521

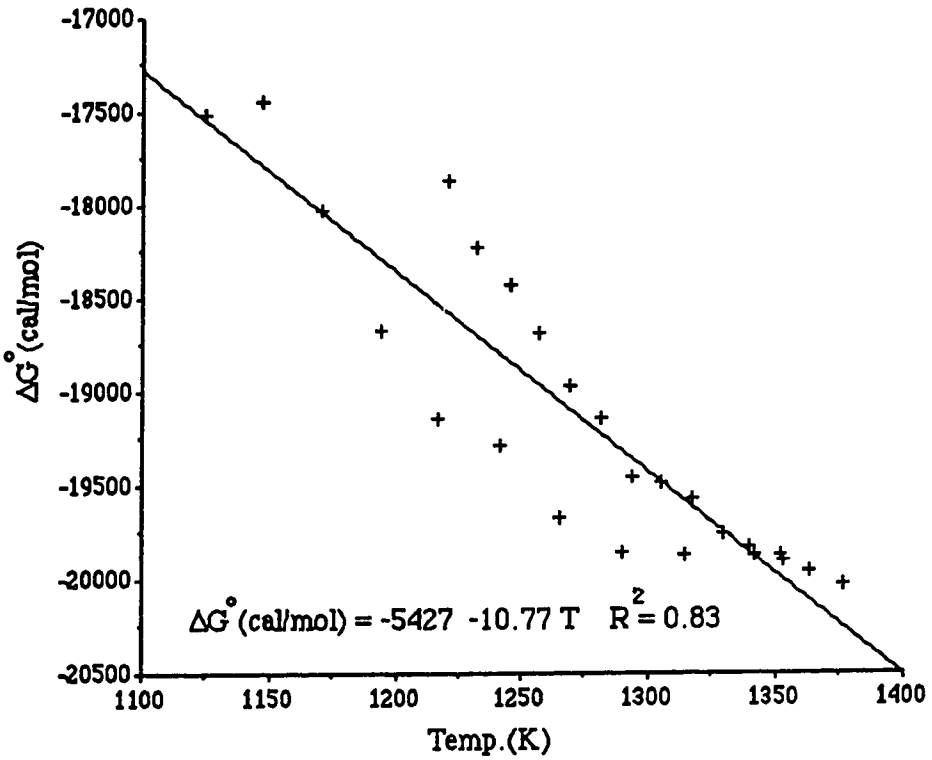

Fig. A-7. Run 10 Chromium / Thoria-Yttria - ΔG versus Temperature.

Appendix B Experimental Data for Carbon Monoxide / Dioxide Cell

Part I Air Reference

Table B-1. Run 1-Air Reference 58.8% CO / 41.2% CO_2.

Pressure (millibar)	Temp.(°C)	Temp.(K)	E (volts)	ΔG^o (cal/mol)
966	837	1110	0.930	-43884
969	883	1156	0.905	-42769
972	947	1220	0.872	-41300
974	994	1267	0.854	-40509
975	1051	1324	0.816	-38806
976	1091	1364	0.800	-38102
977	1178	1451	0.764	-36516
978	1205	1478	0.752	-35986
978	1129	1402	0.779	-37164
964	1054	1327	0.803	-38224
965	999	1272	0.830	-39419
971	925	1198	0.869	-41144
953	859	1132	0.877	-41475
952	802	1075	0.892	-42116
952	743	1016	0.918	-43262
955	683	956	0.915	-43066
969	643	916	0.958	-45000
975	586	859	0.991	-46465
972	655	928	0.964	-45285
965	717	990	0.949	-44655
976	775	1048	0.937	-44141
976	772	1045	0.940	-44277
977	832	1105	0.910	-42946
974	888	1161	0.884	-41799
971	942	1215	0.851	-40328

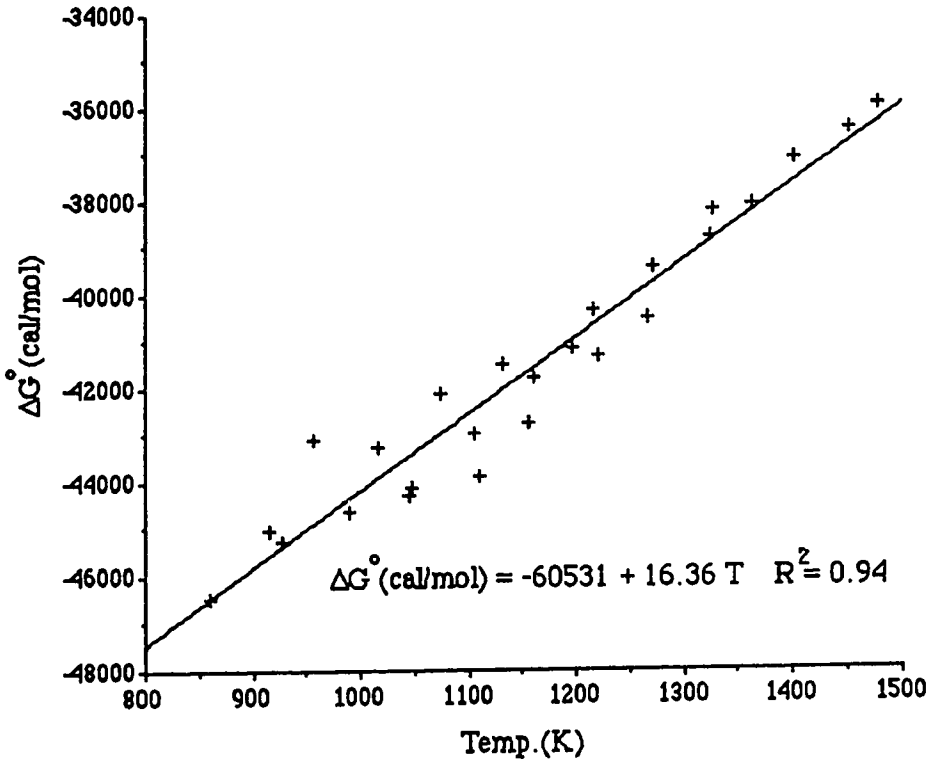

Fig. B-1. Run 1-Air Reference 58.8% CO / 41.2% CO_2.

Table B-2. Run 2-Air Reference 52.5% CO / 47.5% CO_2.

Pressure (millibar)	Temp.(°C)	Temp.(K)	E (volts)	ΔG^o(cal/mol)
966	837	1110	0.917	-43848
969	881	1154	0.897	-42984
972	943	1216	0.864	-41545
974	993	1266	0.843	-40644
975	1052	1325	0.806	-39019
976	1108	1381	0.780	-37896
977	1175	1448	0.751	-36650
978	1209	1482	0.737	-36050
978	1130	1403	0.759	-36955
964	1055	1328	0.804	-38946
965	998	1271	0.818	-39510
971	927	1200	0.849	-40833
953	854	1127	0.870	-41720
952	799	1072	0.891	-42612
952	742	1015	0.926	-44146
955	683	956	0.947	-45028
969	631	904	0.961	-45586
975	586	859	0.982	-46487
972	650	923	0.978	-46395
965	715	988	0.937	-44601
976	771	1044	0.927	-44207
977	830	1103	0.907	-43365
974	890	1163	0.881	-42253
971	943	1216	0.844	-40624

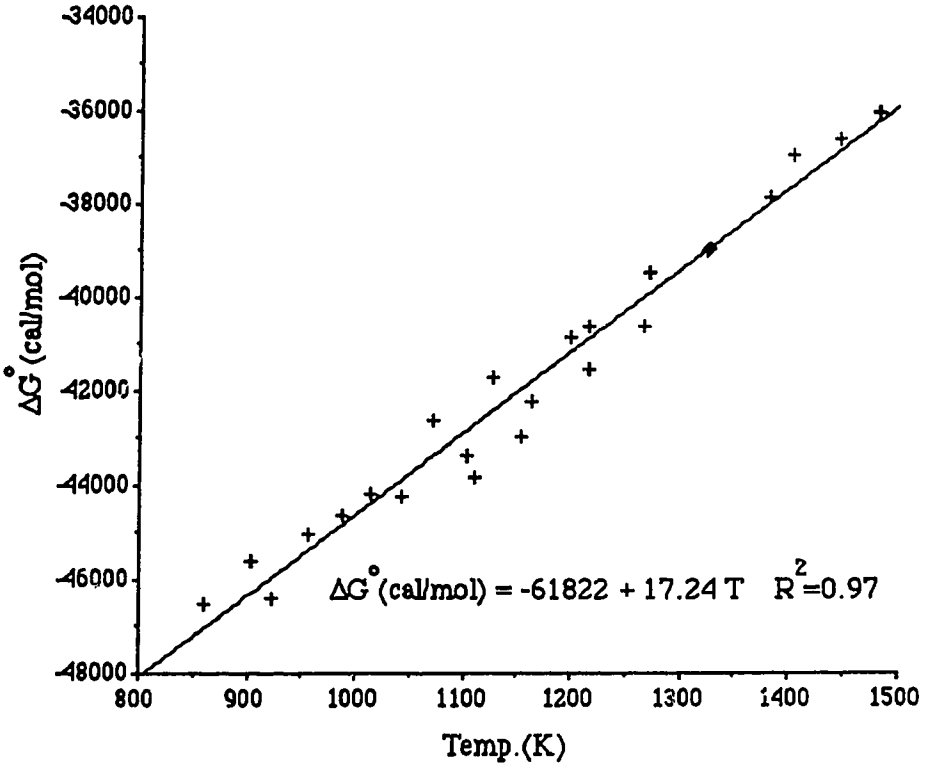

Fig. B-2. Run 2-Air Reference 52.5% CO / 47.5% CO_2.

Table B-3. Run 3-Air Reference 5.0% CO / 95.0% CO_2.

Pressure (millibar)	Temp.(°C)	Temp.(K)	E (volts)	ΔG^o(cal/mol)
966	830	1103	0.782	-44286
969	876	1149	0.751	-43196
972	940	1213	0.713	-41917
974	991	1264	0.681	-40818
975	1047	1320	0.652	-39896
976	1107	1380	0.600	-37943
977	1173	1446	0.572	-37141
978	1203	1476	0.555	-36579
978	1126	1399	0.578	-37067
964	1051	1324	0.643	-39526
965	991	1264	0.671	-40369
971	921	1194	0.715	-41869
953	850	1123	0.729	-42007
952	795	1068	0.763	-43165
952	745	1018	0.790	-44037
955	679	952	0.816	-44741
969	629	902	0.848	-45830
975	583	856	0.919	-48757
972	648	921	0.849	-46015
965	712	985	0.794	-43962
976	769	1042	0.798	-44559
977	825	1098	0.778	-44052
974	884	1157	0.742	-42834
971	938	1211	0.705	-41534

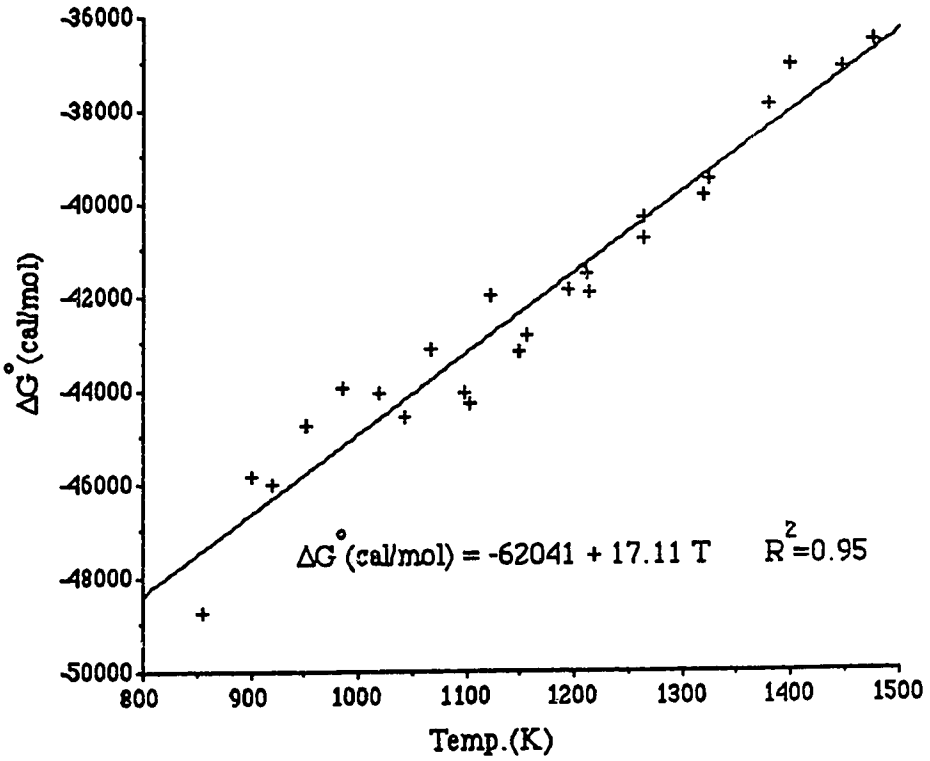

Fig. B-3. Run 3-Air Reference 5.0% CO / 95.0% CO_2.

Table B-4. Run 4-Air Reference 0.1994% CO / 99.8006% CO_2.

Pressure(millibar)	Temp.(°C)	Temp.(K)	E (volts)	ΔG^o(cal/mol)
966	830	1103	0.618	-43894
969	877	1150	0.579	-42747
972	940	1213	0.528	-41270
974	990	1263	0.504	-40858
975	1049	1322	0.452	-39281
976	1104	1377	0.421	-38617
977	1174	1447	0.360	-36777
978	1205	1478	0.336	-36102
978	1125	1398	0.401	-37985
964	1051	1324	0.450	-39232
965	990	1263	0.467	-39164
971	920	1193	0.507	-40025
953	849	1122	0.587	-42745
952	791	1064	0.612	-43088
952	736	1009	0.678	-45364
955	674	947	0.686	-44864
969	625	898	0.757	-47442
975	577	850	0.790	-48289
972	643	916	0.735	-46676
965	708	981	0.678	-44960
976	765	1038	0.661	-44960
977	821	1094	0.593	-42603
977	821	1094	0.616	-43664
974	878	1151	0.588	-43170
971	936	1209	0.531	-41354

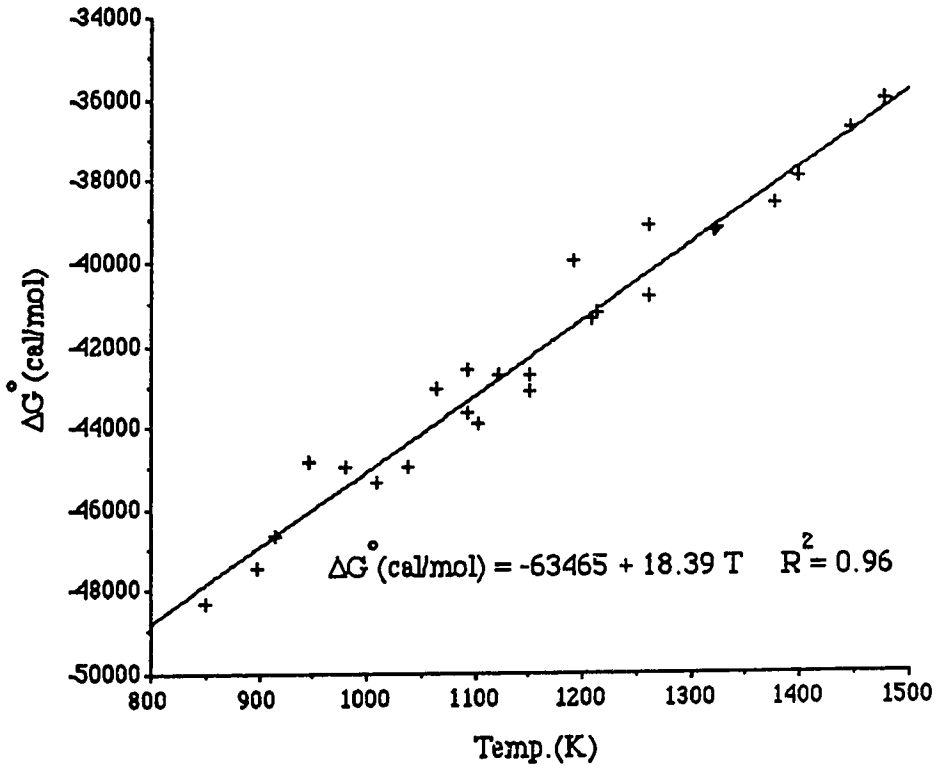

Fig. B-4. Run 4-Air Reference 0.1994% CO / 99.8006% CO_2.

Table B-5. Run 5-Air Reference 0.097% CO / 99.903% CO_2.

Pressure (millibar)	Temp.(C)	Temp.(K)	E (volts)	ΔG^o(cal/mol)
966	830	1103	0.582	-43815
969	878	1151	0.526	-41968
972	941	1214	0.479	-40765
974	990	1263	0.460	-40640
975	1044	1317	0.396	-38518
976	1113	1386	0.351	-37502
977	1174	1447	0.301	-36132
978	1202	1475	0.285	-35823
978	1121	1394	0.314	-35916
964	1050	1323	0.423	-39870
965	990	1263	0.456	-40468
971	918	1191	0.420	-37692
953	850	1123	0.552	-42755
952	794	1067	0.570	-42723
972	642	915	0.716	-47098
965	708	981	0.626	-43969
976	765	1038	0.591	-43220
977	822	1095	0.558	-42573
974	878	1151	0.545	-42838
971	937	1210	0.472	-40382

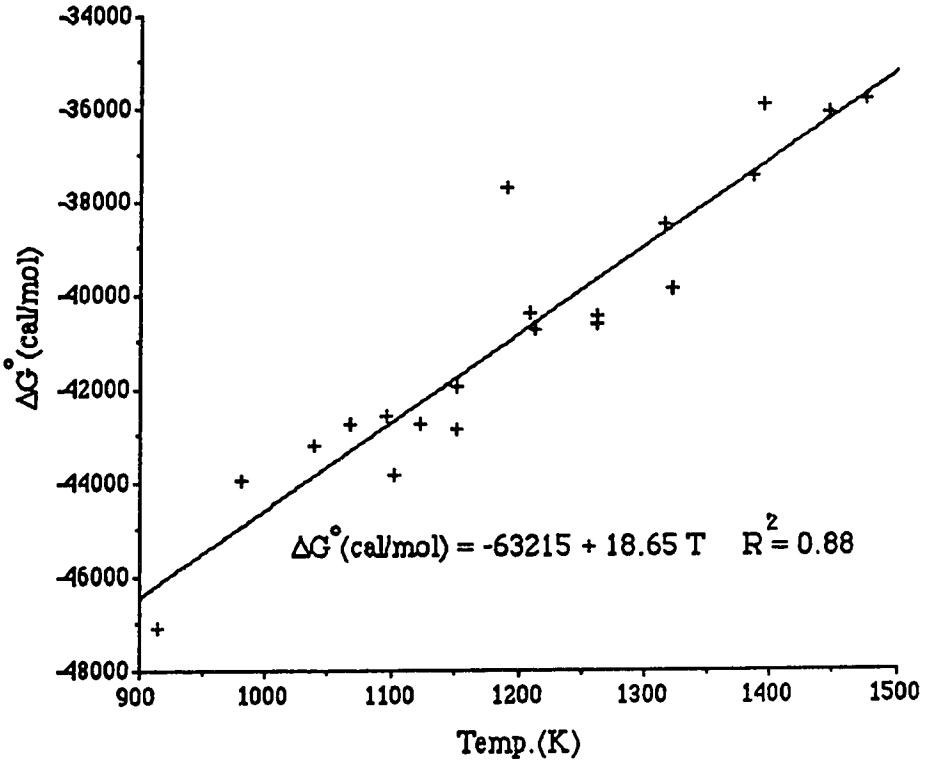

Fig. B-5. Run 5-Air Reference 0.097% CO / 99.903% CO_2.

Table B-6. Run 6-Air Reference 89ppm CO / 99.9911% CO_2.

Pressure (millibar)	Temp.(°C)	Temp.(K)	E (volts)	ΔG^o(cal/mol)
966	828	1101	0.469	-43802
969	878	1151	0.376	-40516
972	942	1215	0.346	-40417
974	989	1262	0.352	-41637
975	1074	1347	0.282	-40118
976	1100	1373	0.260	-39625
977	1171	1444	0.222	-39299
978	1120	1393	0.204	-37442

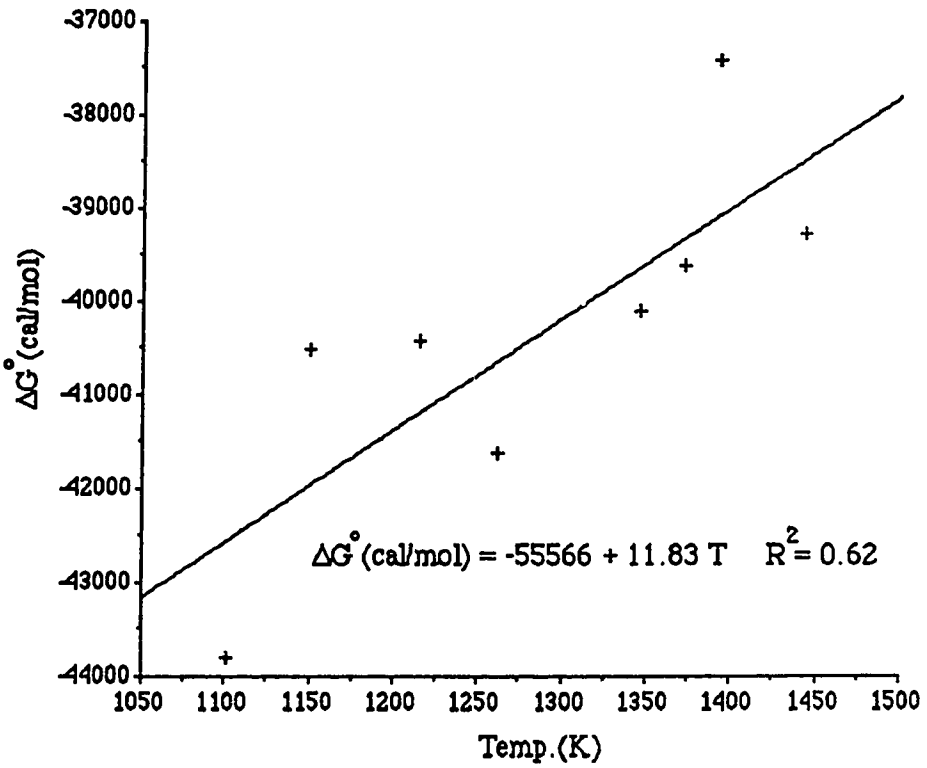

Fig. B-6. Run 6-Air Reference 89ppm CO / 99.9911% CO_2.

Table B-7. Run 7-Air Reference 97.98% CO / 2.02% CO_2.

Pressure (millibar)	Temp.(°C)	Temp.(K)	E (volts)	ΔG^o(cal/mol)
952	856	1129	1.036	-40908
952	802	1075	1.017	-40361
969	648	921	0.931	-37315
975	588	861	1.029	-42196
972	652	925	1.005	-40702
965	723	996	0.991	-39629
976	774	1047	1.007	-40044
977	833	1106	0.997	-39221
974	889	1162	1.003	-39159
971	947	1220	0.959	-36779

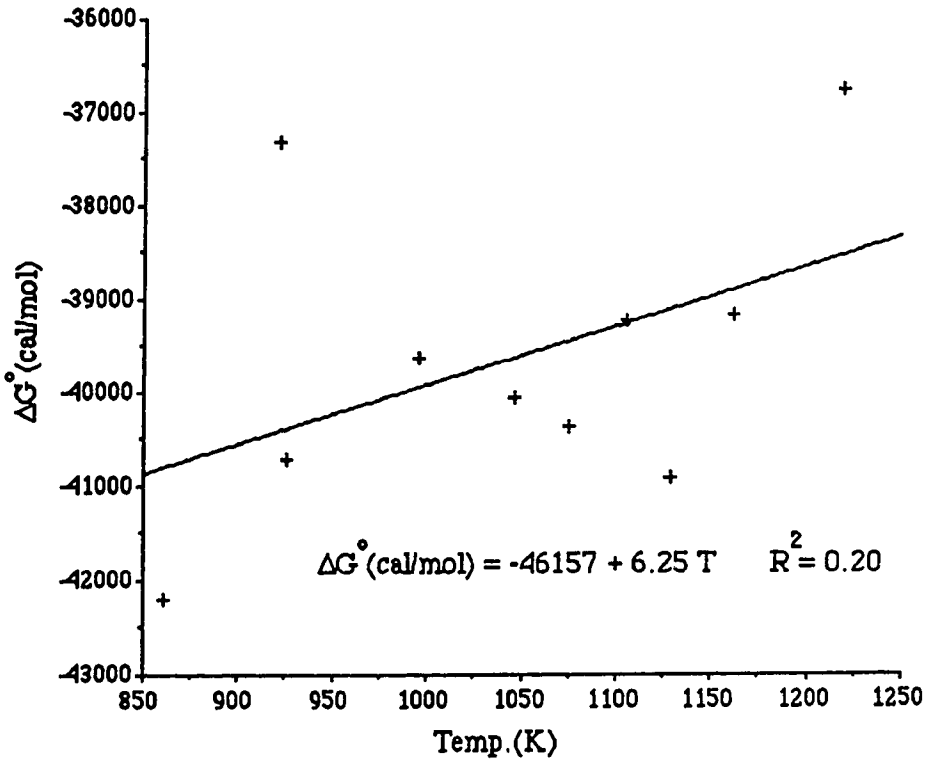

Fig. B-7. Run 7-Air Reference 97.98% CO / 2.02% CO_2.

Table B-8. Run 8-Air Reference 99.884%CO / 0.116% CO_2.

Pressure (millibar)	Temp.(°C)	Temp.(K)	E (volts)	ΔG^o(cal/mol)
966	843	1116	1.100	-37529
969	884	1157	1.103	-37179
972	945	1218	1.088	-35762
974	1000	1273	1.070	-34278
975	1049	1322	1.045	-32544
976	1136	1409	1.026	-30636
977	1181	1454	0.993	-28579
990	1207	1480	0.977	-27515
964	1056	1329	1.014	-31047
965	1010	1283	1.075	-34403
953	858	1131	1.048	-34970

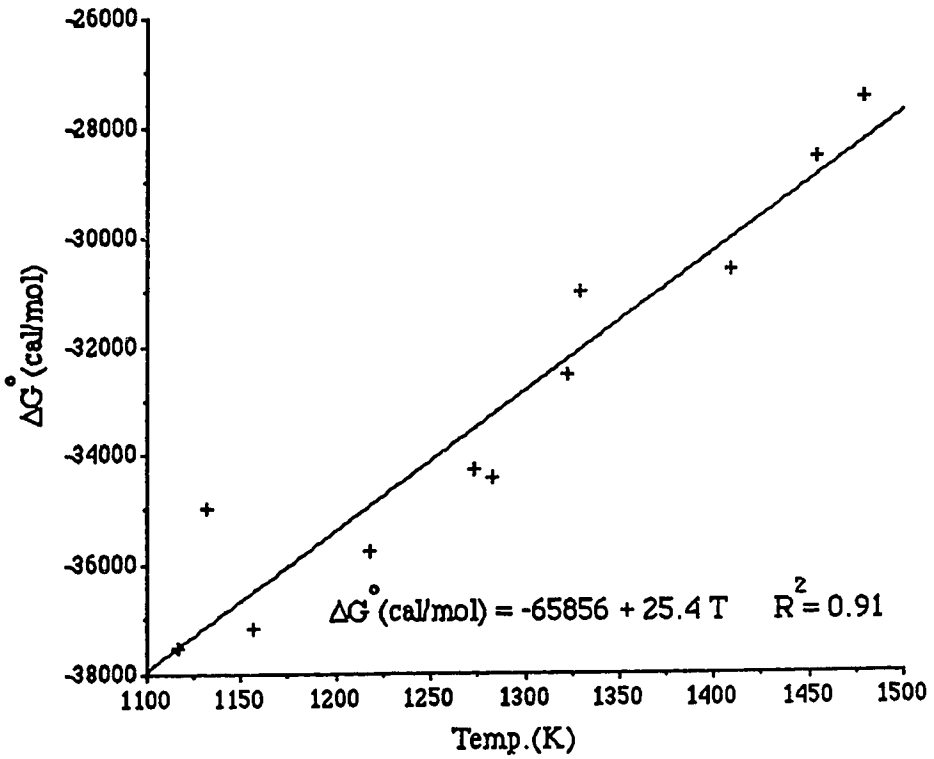

Fig. B-8. Run 8-Air Reference 99.884% CO / 0.116% CO_2.

Table B-9. Run 9-Air Reference 99.9975%CO / 0.0025% CO_2.

Pressure (millibar)	Temp.(°C)	Temp.(K)	E (volts)	ΔG°(cal/mol)
966	843	1116	1.105	-29992
969	884	1157	1.095	-28758
972	948	1221	1.078	-26767
974	999	1272	1.079	-25852
975	1056	1329	1.062	-23996
976	1115	1388	1.041	-21916
977	1183	1456	1.012	-19299
978	1215	1488	0.969	-16713
964	1059	1332	0.992	-20726
971	1017	1290	1.023	-22936
953	862	1135	1.049	-27069
965	719	992	1.007	-27804
976	779	1052	1.003	-26480
976	776	1049	1.022	-27413
977	833	1106	1.006	-25602
974	889	1162	0.993	-23953
971	948	1221	0.970	-21787
970	1004	1277	0.949	-19767

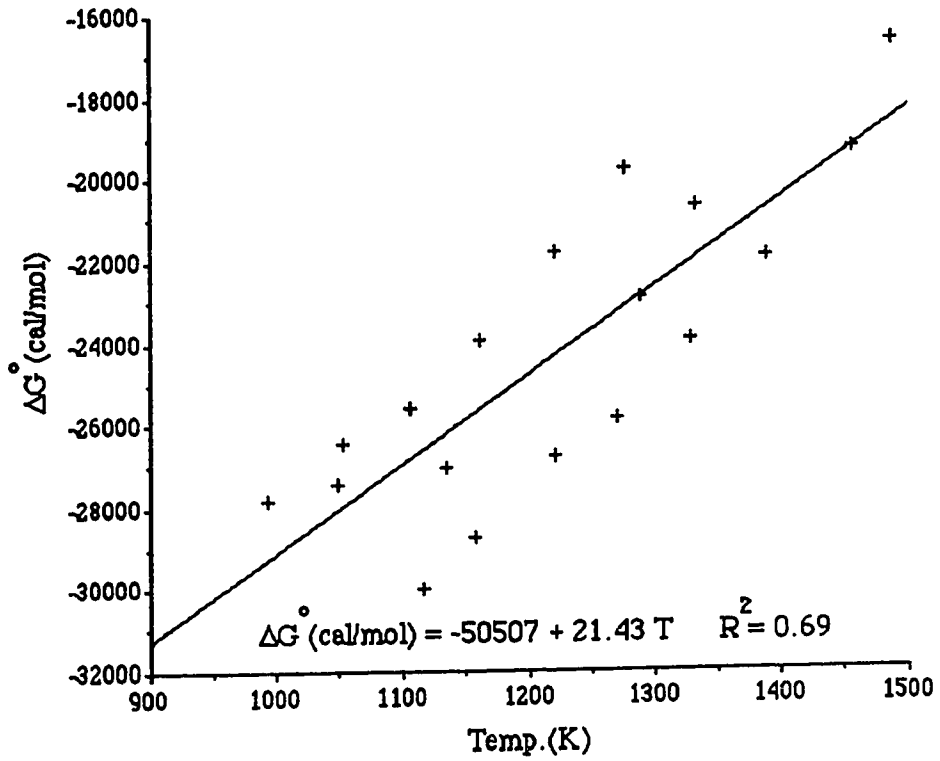

Fig. B-9. Run 9-Air Reference 99.9975% CO / 0.0025% CO_2.

Part II Oxygen Reference versus CO/CO_2

Table B-10. Run 10-Oxygen Reference 0.097% CO / 99.9903% CO_2.

Pressure (millibar)	Temp.(°C)	Temp.(K)	E (volts)	ΔG^o(cal/mol)
982	650	923	0.838	-51344
981	770	1043	0.773	-49997
968	781	1054	0.709	-47182
975	889	1162	0.725	-49412
981	932	1205	0.609	-44661
982	988	1261	0.551	-42757
984	1066	1339	0.386	-36222
982	1131	1404	0.382	-36930
981	1153	1426	0.335	-35063
987	1141	1414	0.364	-36244
989	1092	1365	0.375	-36080
989	1050	1323	0.448	-38869
979	1001	1274	0.508	-40948
979	942	1215	0.549	-42029
980	889	1162	0.607	-43975
980	836	1109	0.622	-43939

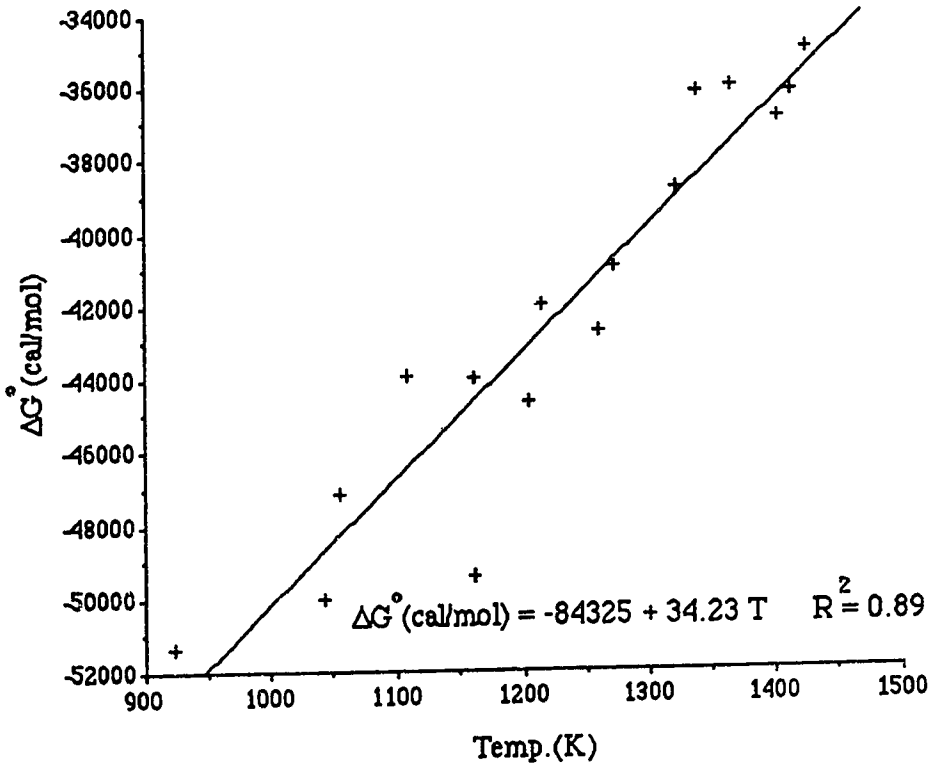

Fig. B-10. Run 10-Oxygen Reference 0.097% CO / 99.9903% CO_2.

Table B-11. Run 11-Oxygen Reference 97.947% CO / 2.02% CO_2.

Pressure (millibar)	Temp.(°C)	Temp.(K)	E (volts)	ΔG^o(cal/mol)
982	649	922	1.135	-45234
981	767	1040	1.137	-44414
968	781	1054	1.109	-42999
975	880	1153	1.034	-38781
981	925	1198	1.019	-37749
982	1006	1279	0.991	-35832
984	1067	1340	1.002	-35870
982	1130	1403	0.96	-33443
981	1150	1423	0.925	-31673
987	1141	1414	0.896	-30413
989	1092	1365	0.93	-32363
989	1050	1323	0.967	-34394
979	1001	1274	1.07	-39511
979	943	1216	1.12	-42266
980	890	1163	1.109	-42169
980	834	1107	1.104	-42372

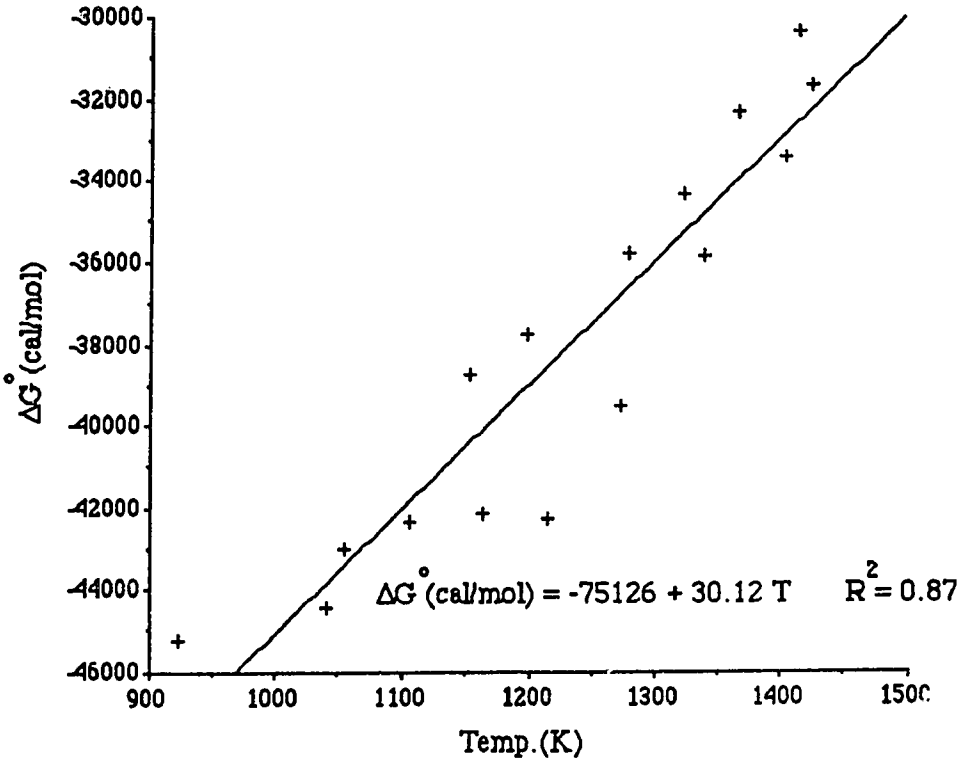

Fig. B-11. Run 11-Oxygen Reference 97.947% CO / 2.02% CO_2.

Table B-12. Run 12-Oxygen Reference 52.5% CO / 47.50% CO_2.

Pressure (millibar)	Temp.(°C)	Temp.(K)	E (volts)	ΔG^o(cal/mol)
982	649	922	1.038	-47673
981	768	1041	1.006	-46169
968	783	1056	1.001	-45920
975	885	1158	0.928	-42536
981	925	1198	0.929	-42580
982	1000	1273	0.905	-41457
984	1066	1339	0.845	-38676
982	1130	1403	0.801	-36629
981	1151	1424	0.786	-35932
987	1140	1413	0.768	-35111
989	1092	1365	0.784	-35863
989	1050	1323	0.861	-39425
979	1001	1274	0.892	-40853
979	944	1217	0.925	-42389
980	889	1162	0.959	-43971
980	835	1108	0.990	-45414

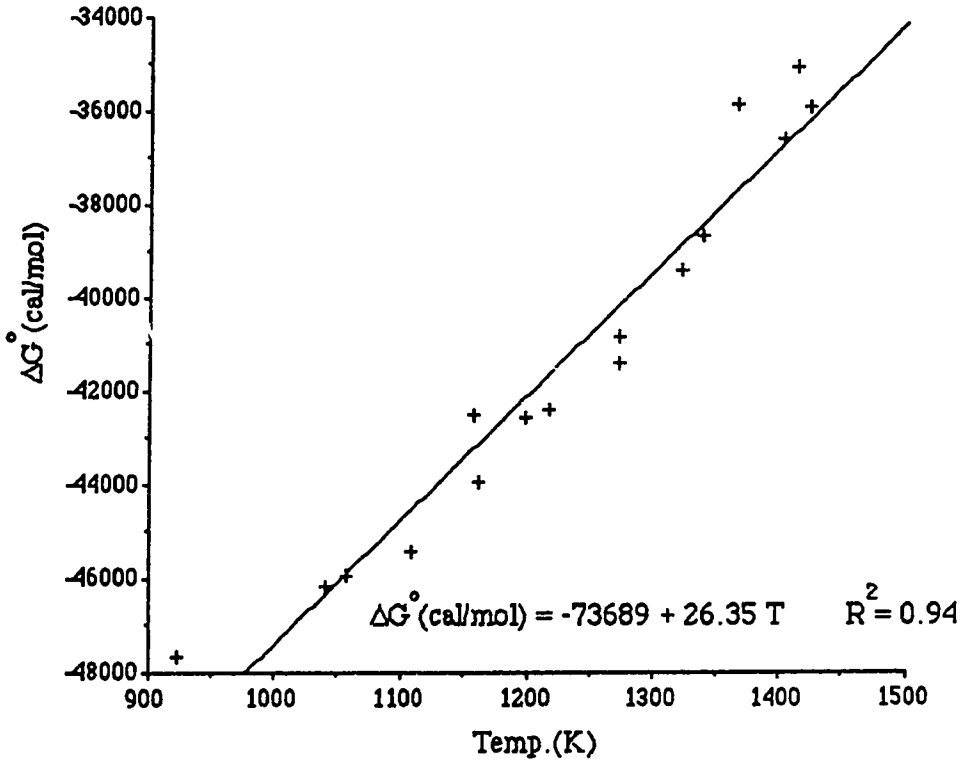

Fig. B-12. Run 12-Oxygen Reference 52.5% CO / 47.50% CO_2.

Table B-13. Run 13-Oxygen Reference 58.8% CO / 41.2% CO_2.

Pressure (millibar)	Temp.(C)	Temp.(K)	E (volts)	ΔG^o(cal/mol)
982	651	924	1.041	-47386
981	766	1039	1.015	-46107
968	782	1055	1.039	-47188
975	884	1157	0.963	-43619
981	925	1198	0.955	-43229
982	991	1264	0.918	-41477
984	1066	1339	0.868	-39121
982	1130	1403	0.817	-36722
981	1153	1426	0.785	-35229
987	1140	1413	0.783	-35153
989	1092	1365	0.832	-37450
989	1050	1323	0.879	-39647
979	1001	1274	0.909	-41051
979	940	1213	0.944	-42708
980	891	1164	0.974	-44127
980	837	1110	0.981	-44488

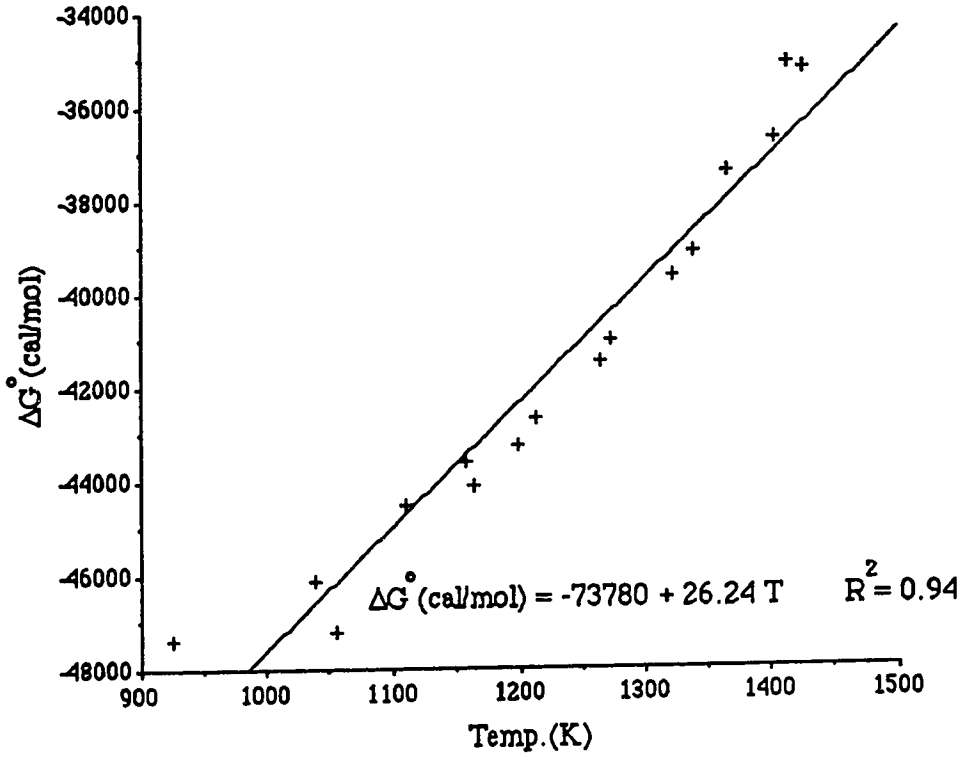

Fig. B-13. Run 13-Oxygen Reference 58.8% CO / 41.2% CO_2.

Table B-14. Run 14-Oxygen Reference 5.0% CO / 95.0% CO_2.

Pressure (millibar)	Temp.(°C)	Temp.(K)	E (Volts)	ΔG^o(cal/mol)
982	649	922	0.909	-47297
981	767	1040	0.882	-46737
968	783	1056	0.875	-46493
975	882	1155	0.806	-43893
981	924	1197	0.791	-43452
982	1004	1277	0.732	-41196
984	1067	1340	0.694	-39812
982	1130	1403	0.659	-38562
981	1151	1424	0.621	-36930
987	1141	1414	0.616	-36649
989	1092	1365	0.653	-38073
989	1050	1323	0.687	-39398
979	1003	1276	0.747	-41878
979	943	1216	0.767	-42453
980	886	1159	0.814	-44290
980	835	1108	0.820	-44271

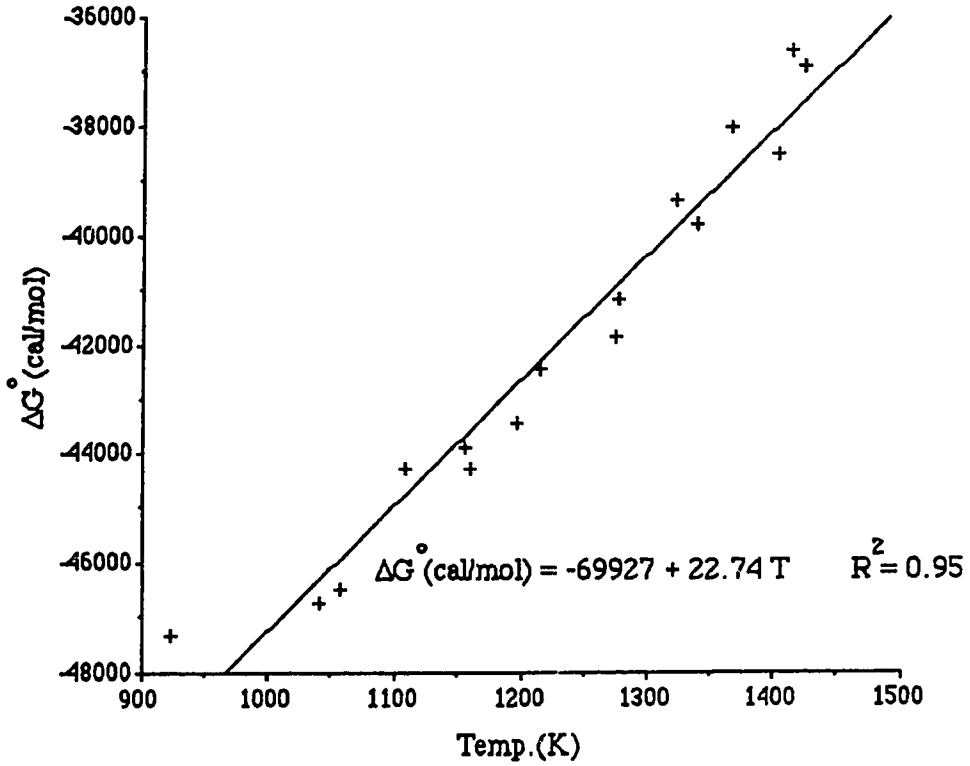

Fig. B-14. Run 14-Oxygen Reference 5.0% CO / 95.0% CO_2.

Table B-15. Run 15-Oxygen Reference 0.0025% CO / 99.9975% CO_2.

Pressure (millibar)	Temp.(°C)	Temp.(K)	E (volts)	ΔG^o (cal/mol)
982	649	922	1.124	-70611
981	767	1040	1.187	-75917
968	782	1055	1.201	-76854
975	878	1151	1.228	-80060
981	924	1197	1.078	-74083
982	1002	1275	1.039	-73871
984	1066	1339	1.103	-78129
982	1130	1403	1.004	-74861
981	1151	1424	0.985	-74411
987	1140	1413	1.009	-75302
989	1092	1365	0.975	-72760
989	1050	1323	0.98	-72136
979	943	1216	1.03	-72253
980	889	1162	1.216	-79735
980	835	1108	1.201	-77945

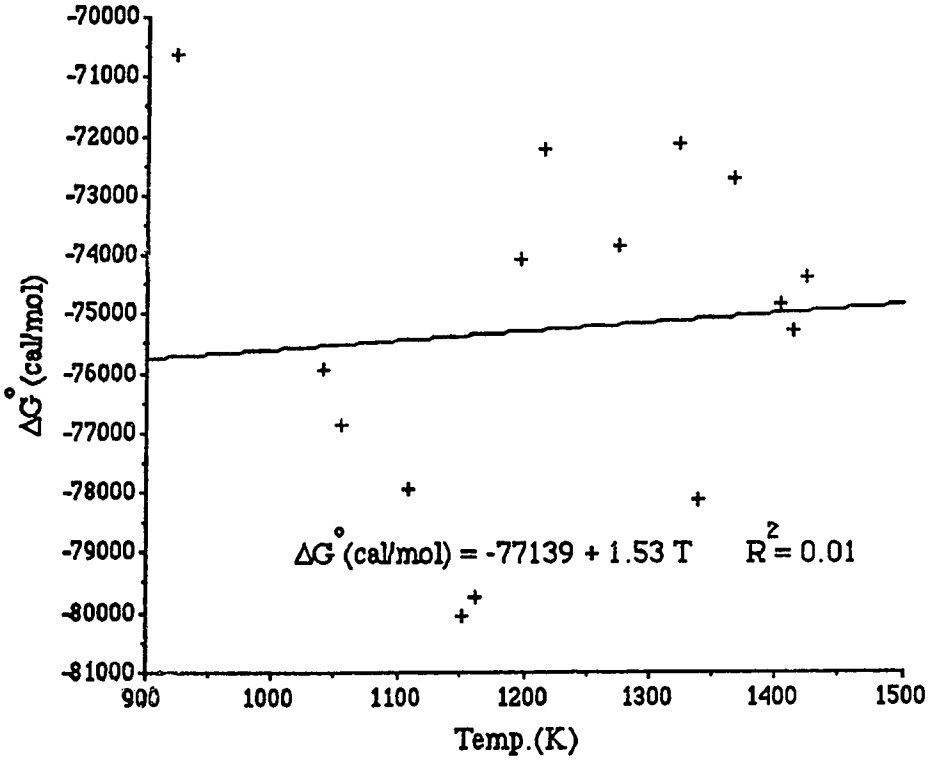

Fig. B-15. Run 15-Oxygen Reference 0.0025% CO / 99.9975% CO_2.

Table B-16. Run 16-Oxygen Reference 0.1994% CO / 99.8006% CO_2.

Pressure (millibar)	Temp.(°C)	Temp.(K)	E (volts)	ΔG^o(cal/mol)
982	652	925	0.770	-46908
981	768	1041	0.789	-49212
968	783	1056	0.780	-48967
975	874	1147	0.642	-43728
981	935	1208	0.693	-46839
982	1000	1273	0.556	-41319
984	1066	1339	0.507	-39874
982	1130	1403	0.388	-35170
981	1152	1425	0.374	-34794
987	1140	1413	0.366	-34285
989	1092	1365	0.398	-35173
989	1050	1323	0.495	-39131
979	1001	1274	0.545	-40820
979	943	1216	0.620	-43567
980	889	1162	0.645	-44056
980	828	1101	0.690	-45382

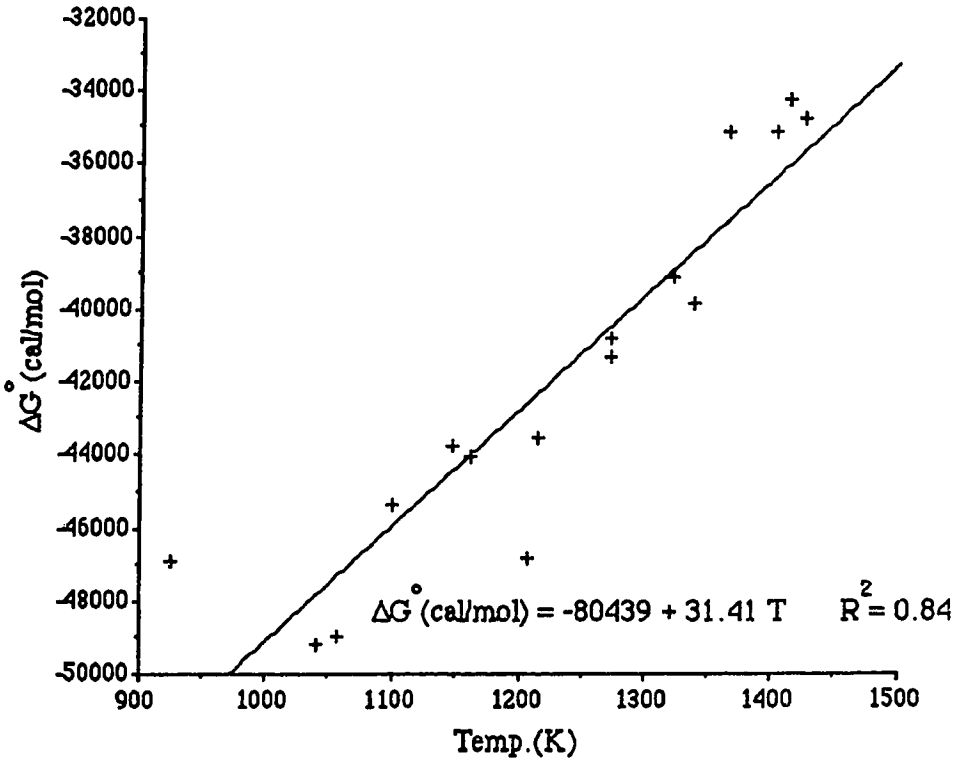

Fig. B-16. Run 16-Oxygen Reference 0.1994% CO / 99.8006% CO_2.

Part III Oxygen Reference versus CO/CO_2 mixtures Probe Three

Table B-17. Run 17-Oxygen Reference 0.097% CO / 99.903% CO_2.

Pressure (millibar)	Temp.(°C)	Temp.(K)	E (volts)	ΔG^o(cal/mol)
933	673	946	0.739	-47204
933	775	1048	0.702	-46912
934	878	1151	0.610	-44097
934	992.5	1265	0.532	-42087
932	1022	1295	0.480	-40100
936	1049	1322	0.457	-39409
939	1071	1344	0.406	-37357
940	1092	1365	0.393	-37047
935	1115	1388	0.364	-36036
929	1141	1414	0.398	-37974
930	1150	1423	0.352	-35974
930	1123	1396	0.401	-37860
933	1096	1369	0.409	-37851

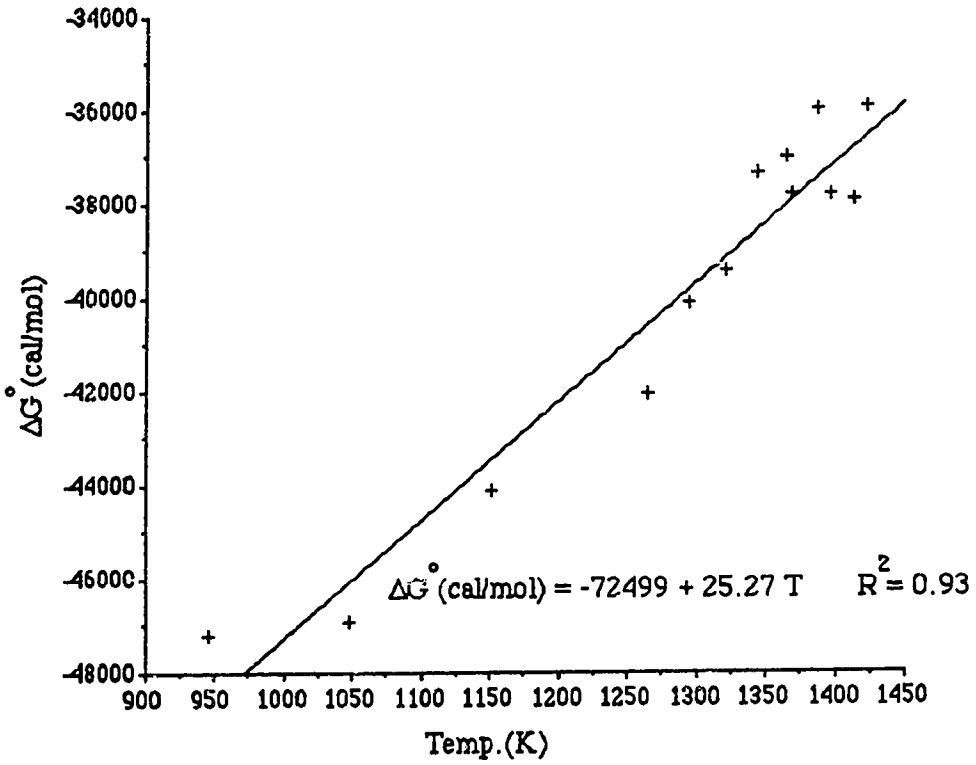

Fig. B-17. Run 17-Oxygen Reference 0.097% CO / 99.903% CO_2.

Table B-18. Run 18-Oxygen Reference 52.5% CO / 47.5% CO_2.

Pressure(millibar)	Temp.(°C)	Temp.(K)	E (volts)	ΔG°(cal/mol)
933	673	946	1.034	-47590
933	775	1048	0.984	-45271
934	879	1152	0.943	-43367
934	991	1264	0.894	-41093
932	1022	1295	0.880	-40446
936	1049	1322	0.868	-39885
939	1070	1343	0.859	-39463
940	1092	1365	0.848	-38951
935	1117	1390	0.836	-38402
929	1141	1414	0.827	-37993
930	1150	1423	0.822	-37758
930	1125	1398	0.833	-38269
933	1095	1368	0.847	-38915
933	1041	1314	0.872	-40074
943	1006	1279	0.887	-40756
943	946	1219	0.912	-41917
942	918	1191	0.932	-42844
942	863	1136	0.947	-43543
940	809	1082	0.967	-44475
940	770	1043	0.985	-45310
938	755	1028	0.998	-45914
938	733	1006	1.000	-46009
931	697	970	1.022	-47036
931	682	955	1.025	-47176
931	659	932	1.033	-47548
932	629	902	1.042	-47965
932	599	872	1.054	-48522
932	569	842	1.064	-48987
936	534	807	1.073	-49403
936	508	781	1.076	-49544

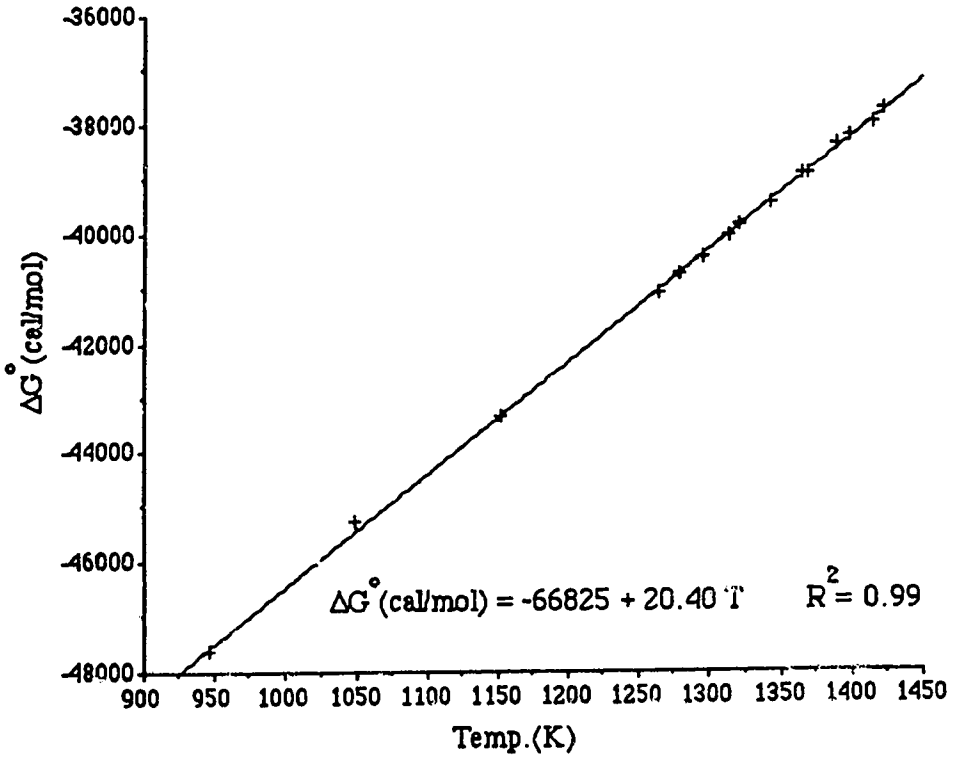

Fig. B-18. Run 18-Oxygen Reference 52.5% CO / 47.5% CO_2.

Table B-19. Run 19-Oxygen Reference 0.1994% CO / 99.8006% CO_2.

Pressure (millibar)	Temp.(°C)	Temp.(K)	E (volts)	ΔG^o(cal/mol)
933	673	946	0.774	-47458
933	774	1048	0.745	-47382
938	879	1152	0.644	-44022
938	992	1265	0.560	-41553
932	1023	1296	0.521	-40136
936	1049	1322	0.511	-39999
939	1070	1343	0.452	-37534
940	1092	1365	0.440	-37253
935	1117	1390	0.402	-35818
929	1145	1418	0.428	-37374
930	1150	1423	0.386	-35497
930	1124	1397	0.406	-36096
933	1096	1369	0.412	-36021

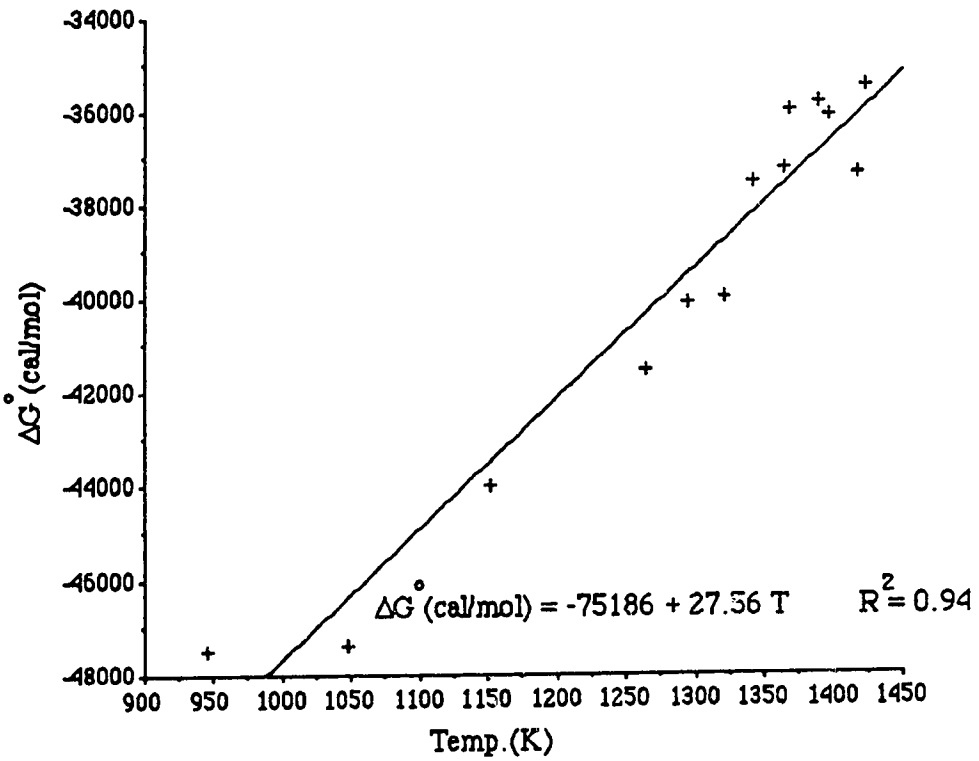

Fig. B-19. Run 19-Oxygen Reference 0.1994% CO / 99.8006% CO_2.

Table B-20. Run 20-Oxygen Reference 95.0% CO_2 / 5.0% CO.

Pressure (millibar)	Temp.(°C)	Temp.(K)	E (volts)	ΔG°(cal/mol)
933	673	946	0.909	-47537
933	775	1048	0.849	-45375
934	879	1152	0.790	-43270
934	992	1265	0.728	-41081
932	1023	1296	0.710	-40438
936	1049	1322	0.690	-39664
936	1070	1343	0.677	-39189
935	1092	1365	0.661	-38583
935	1118	1391	0.643	-37907
929	1142	1415	0.635	-37690
930	1150	1423	0.623	-37181
930	1125	1398	0.635	-37586
933	1096	1369	0.665	-38794
933	1040	1313	0.697	-39938
943	1007	1280	0.719	-40742
943	946	1219	0.751	-41857
942	918	1191	0.772	-42661
942	863	1136	0.790	-43165
940	810	1083	0.824	-44422
940	764	1037	0.852	-45440
938	756	1029	0.862	-45857
938	733	1006	0.868	-45997
931	697	970	0.896	-47082
931	679	952	0.902	-47252
931	660	933	0.918	-47877
932	629	902	0.925	-48015
932	599	872	0.954	-49175
932	569	842	0.956	-49089
936	508	781	0.978	-49738

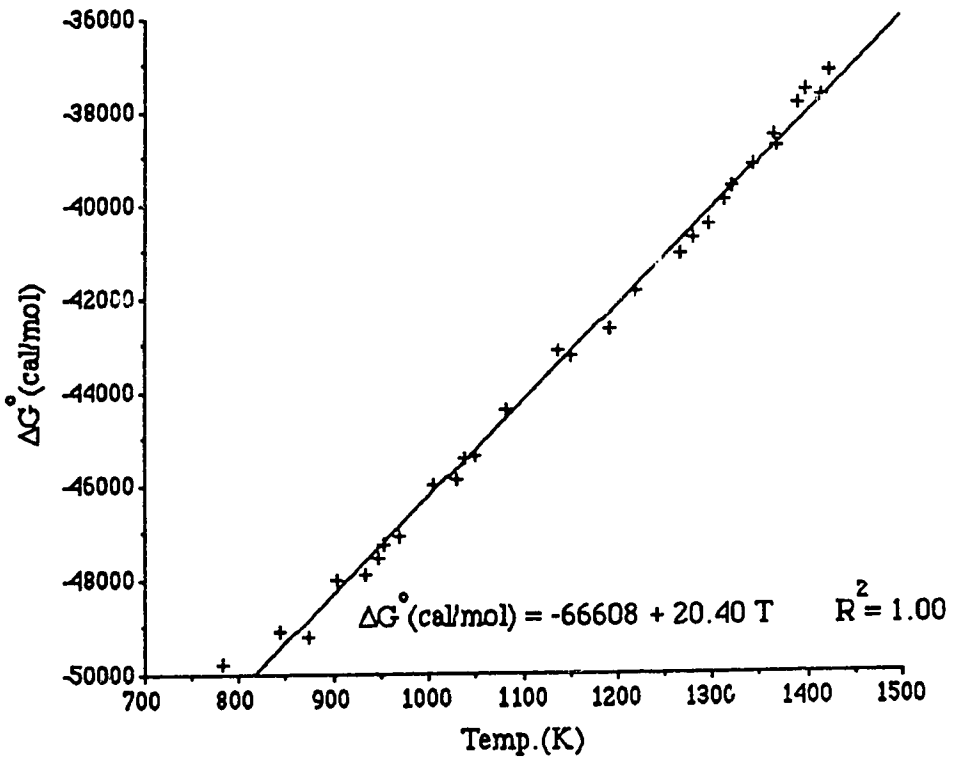

Fig. B-20. Run 20-Oxygen Reference 95.0% CO_2 / 5.0% CO.

Table B-21. Run 21-Oxygen Reference 58.8% CO / 42.2% CO_2.

Pressure (millibar)	Temp.(°C)	Temp.(K)	E (volts)	ΔG^o (cal/mol)
933	673	946	1.033	-47097
933	773	1046	1.000	-45517
934	880	1153	0.959	-43563
934	988	1261	0.918	-41610
932	1023	1296	0.898	-40670
936	1048	1321	0.887	-40143
936	1071	1344	0.872	-39438
935	1092	1365	0.862	-38966
935	1117	1390	0.851	-38444
935	1141	1414	0.844	-38107
930	1149	1422	0.833	-37602
930	1125	1398	0.847	-38261
933	1096	1369	0.859	-38828
933	1041	1314	0.884	-40013
943	1007	1280	0.899	-40710
943	948	1221	0.925	-41944
942	916	1189	0.954	-43301
942	863	1136	0.959	-43563
940	810	1083	0.980	-44565
940	774	1047	0.996	-45324
938	755	1028	1.007	-45845
938	733	1006	1.012	-46088
931	697	970	1.031	-46993
931	682	955	1.034	-47140
931	659	932	1.043	-47568
932	629	902	1.051	-47953
932	598	871	1.063	-48524
932	569	842	1.073	-49002
936	533	806	1.080	-49343
936	508	781	1.083	-49496

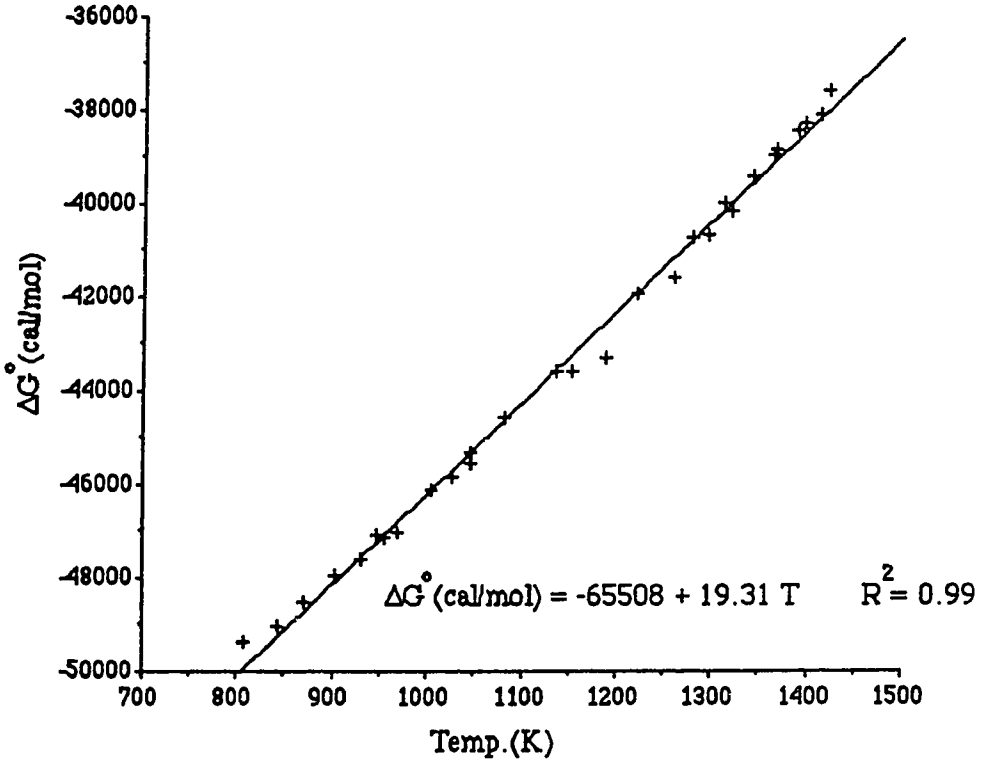

Fig. B-21. Run 21-Oxygen Reference 58.8% CO / 42.2% CO_2.

Table B-22. Run 22-Oxygen Reference 98.0% CO / 2.0% CO_2.

Pressure (millibar)	Temp.(°C)	Temp.(K)	E (volts)	ΔG^o(cal/mol)
933	673	946	1.101	-43818
933	774	1047	1.125	-44177
934	880	1153	1.116	-42981
934	989	1262	1.087	-40841
932	1023	1296	1.080	-40270
936	1049	1322	1.072	-39705
936	1071	1344	1.061	-39036
935	1093	1366	1.053	-38506
935	1117	1390	1.019	-36761
929	1141	1414	1.023	-36778
933	1095	1368	1.045	-38125
943	1007	1280	1.087	-40696
943	948	1221	1.106	-42007
942	914	1187	1.119	-42858
942	864	1137	1.123	-43411
940	810	1083	1.095	-42520
940	775	1048	1.096	-42824
938	754	1027	1.151	-45518
938	734	1007	1.157	-45943
931	697	970	1.150	-45899
931	682	955	1.150	-46010
931	659	932	1.160	-46640
933	629	902	1.143	-46075
932	598	871	1.172	-47641
932	569	842	1.166	-47578
936	526	799	1.174	-48261
936	477	750	1.208	-50189

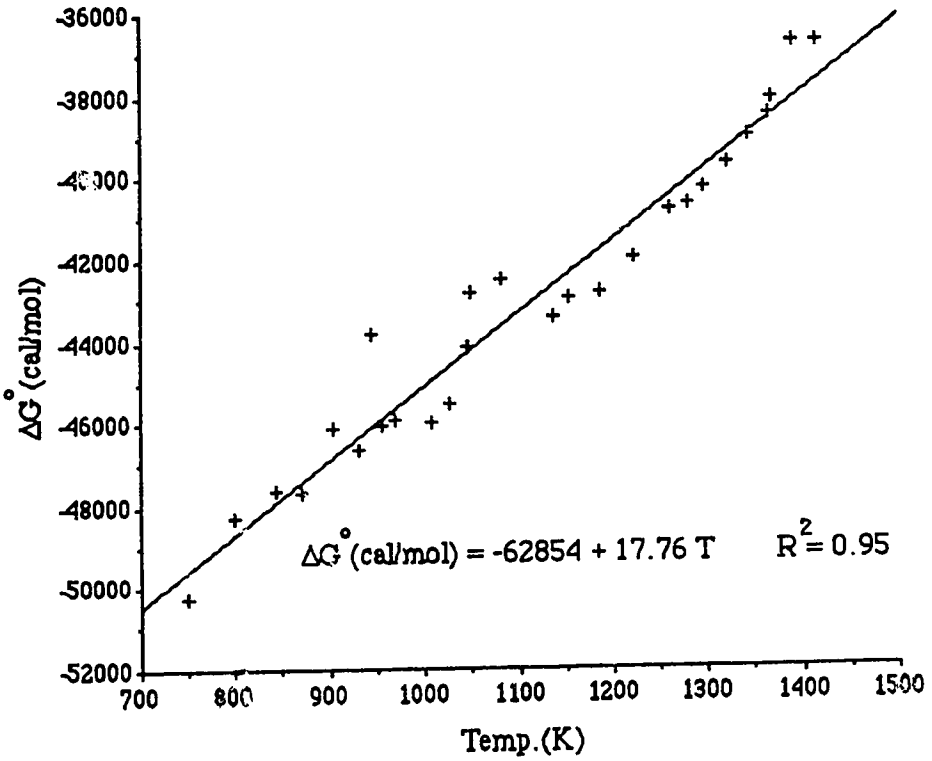

Fig. B-22. Run 22-Oxygen Reference 98.0% CO / 2.0% CO_2.

Table B-23. Run 23-Oxygen Reference 89ppm CO / 99.9911% CO_2.

Pressure (millibar)	Temp.(°C)	Temp.(K)	E (volts)	ΔG^o(cal/mol)
933	672	945	0.792	-54123
933	774	1047	0.680	-50856
934	882	1155	0.559	-47285
934	986	1259	0.454	-44378
932	1023	1296	0.397	-42441
936	1049	1322	0.328	-39737
936	1071	1344	0.321	-39824
935	1092	1365	0.308	-39617
935	1114	1387	0.304	-39842
929	1142	1415	0.303	-40326
930	1148	1421	0.298	-40204
930	1123	1396	0.319	-40707
933	1096	1369	0.392	-43568
933	1038	1311	0.409	-43272

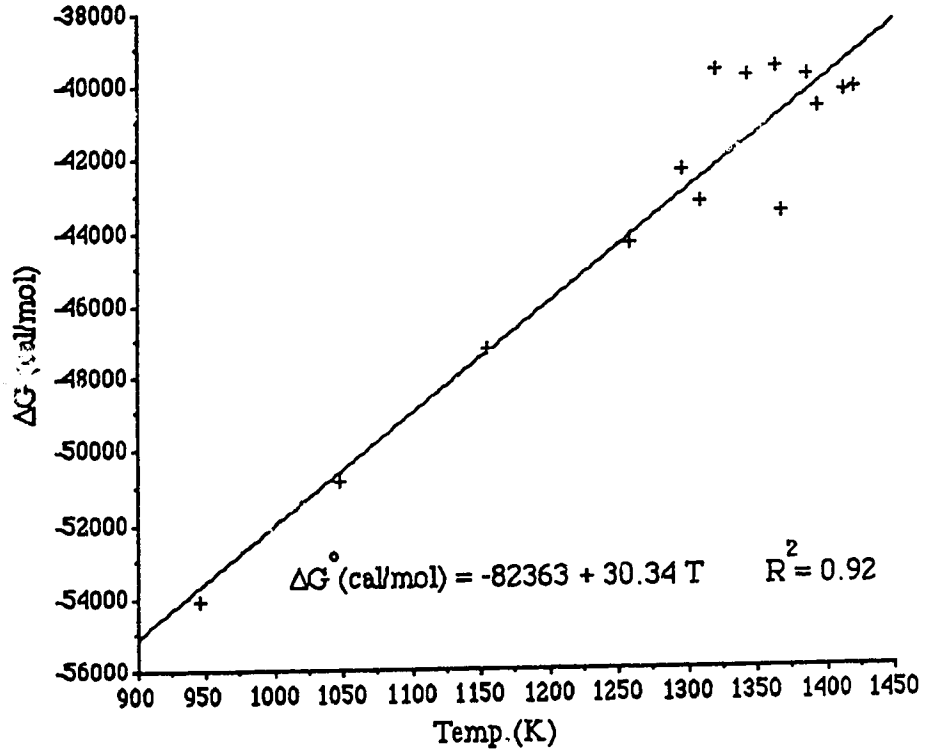

Fig. B-23. Run 23-Oxygen Reference 89ppm CO / 99.9911% CO_2.

Table B-24. Run 24-Oxygen Reference 0.1994% CO / 99.8006% CO_2.

Pressure (millibar)	Temp.(°C)	Temp.(K)	E (volts)	ΔG^o(cal/mol)
923	526	799	0.903	-51444
918	558	831	0.874	-50494
917	587	860	0.840	-49280
939	619	892	0.799	-47803
940	649	922	0.784	-47479
940	679	952	0.771	-47248
940	711	984	0.799	-48933
940	744	1017	0.736	-46432
937	775	1048	0.686	-44504
937	808	1081	0.663	-43848
937	845	1118	0.647	-43565
937	874	1147	0.607	-42076
935	907	1180	0.564	-40494
935	940	1213	0.542	-39885
935	968	1241	0.517	-39075
936	972	1245	0.464	-36681
936	1005	1278	0.448	-36348
936	1039	1312	0.414	-35197
940	1072	1345	0.390	-34501
946	1107	1380	0.402	-35494
946	1129	1402	0.389	-35164
946	1112	1385	0.397	-35325
946	1114	1387	0.397	-35349
946	1116	1389	0.397	-35371
944	1093	1366	0.412	-35780
944	1073	1346	0.425	-36134
926	1048	1321	0.440	-36493
926	1025	1298	0.451	-36719
921	991	1264	0.473	-37309
919	970	1243	0.485	-37603

Table B-24. Run 24-Oxygen Reference 0.1994% CO / 99.8006% CO_2 Continued :

Pressure (millibar)	Temp.(°C)	Temp.(K)	E (volts)	ΔG^o(cal/mol)
932	948	1221	0.494	-37765
932	927	1200	0.513	-38384
932	894	1167	0.540	-39224
930	861	1134	0.567	-40063
927	829	1102	0.592	-40819
927	796	1069	0.636	-42443
927	773	1046	0.659	-43222
927	753	1026	0.678	-43854
927	733	1006	0.695	44393
927	707	980	0.708	-44673
928	686	959	0.722	45063
940	670	943	0.748	-46077
942	651	924	0.758	-46307
942	630	903	0.768	-46511
944	609	882	0.778	-46716
941	589	862	0.789	-46974
940	570	843	0.795	-47018
939	549	822	0.801	-47036
938	530	803	0.806	-47032
936	509	782	0.786	-45850

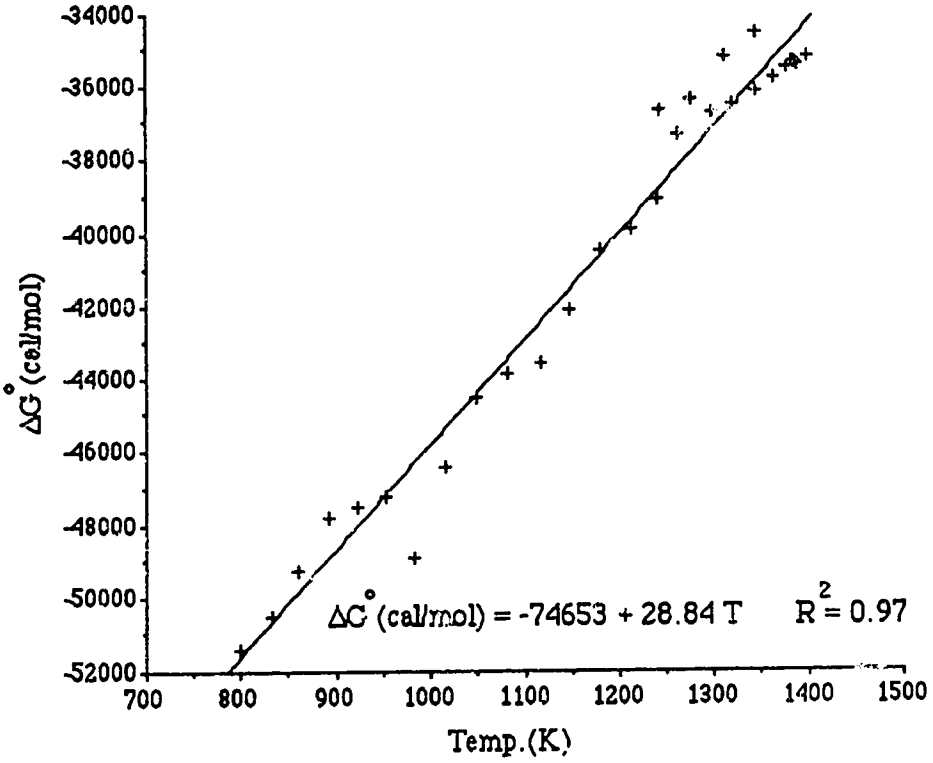

Fig. B-24. Run 24-Oxygen Reference 0.1994% CO / 99.8006% CO_2.

Part IV : Probe Four Oxygen Reference versus CO/CO_2 Mixtures

Table B-25. Run 25-Oxygen Reference 0.1994% CO / 99.8006% CO_2 Polarization. Test.

Temp.(K)	CO/CO_2 Flow (sccm)	O_2 Flow (sccm)	E (volts)
1070	18	174	0.363
1072	26	174	0.379
1072	34	174	0.384
1072	43	174	0.388
1072	51	174	0.390
1072	60	174	0.391
1072	68	174	0.392
1072	77	174	0.393
1072	85	174	0.394
1071	102	174	0.394
1071	119	174	0.395
1070	136	174	0.396
1071	153	174	0.396
1070	170	174	0.396
1070	213	174	0.397
1068	255	174	0.397
1067	298	174	0.397
1068	340	174	0.397
1067	383	174	0.397
1062	597	174	0.397

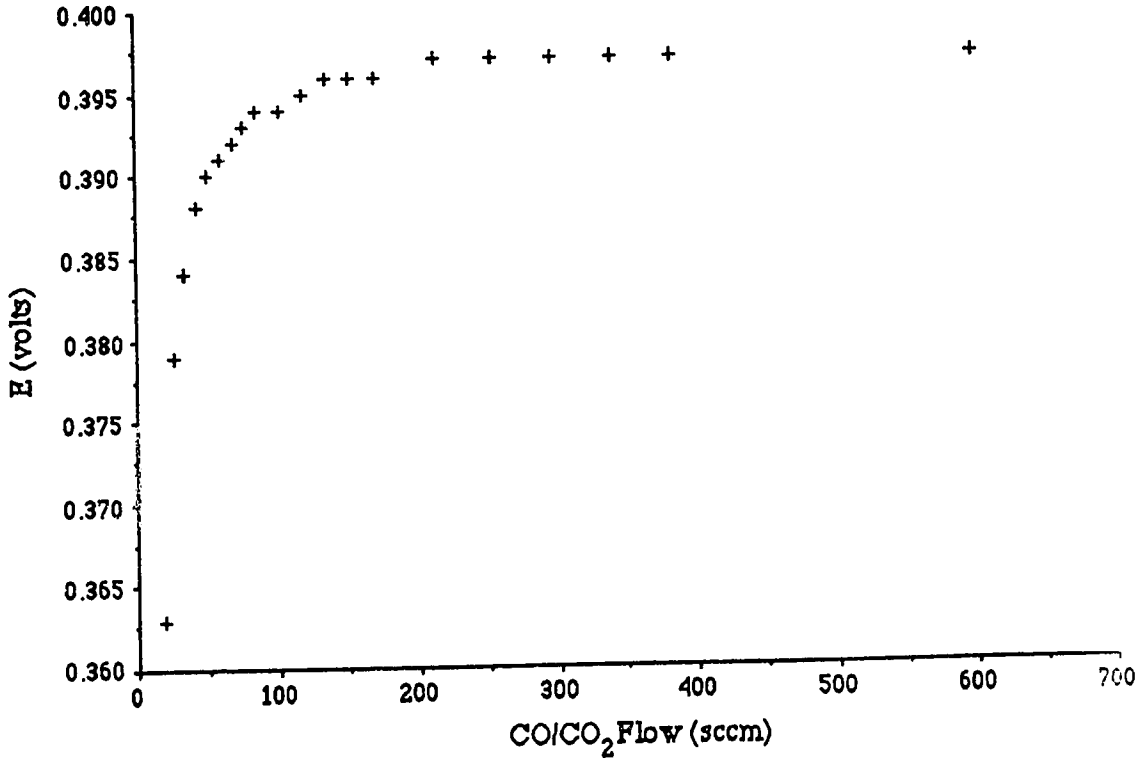

Fig. B-25. Run 25-Oxygen Reference 0.1994% CO / 99.8006% CO_2 Polarization Test.

Table B-26. Run 26-Oxygen Reference 0.1994% CO / 99.8006% CO_2 Polarization Test.

Temp.(K)	CO/CO_2 Flow (sccm)	O_2 Flow (sccm)	E (volts)
1073	14	174	0.338
1073	17	174	0.347
1073	20	174	0.360
1073	24	174	0.370
1073	30	174	0.377
1074	35	174	0.379
1073	40	174	0.382
1073	45	174	0.384
1073	55	174	0.387
1073	64	174	0.389
1074	72	174	0.391
1073	81	174	0.392
1073	101	174	0.393
1072	119	174	0.394
1072	136	174	0.394
1073	153	174	0.395
1072	170	174	0.395
1071	213	174	0.396
1070	255	174	0.396
1070	298	174	0.397
1069	340	174	0.397
1068	383	174	0.397

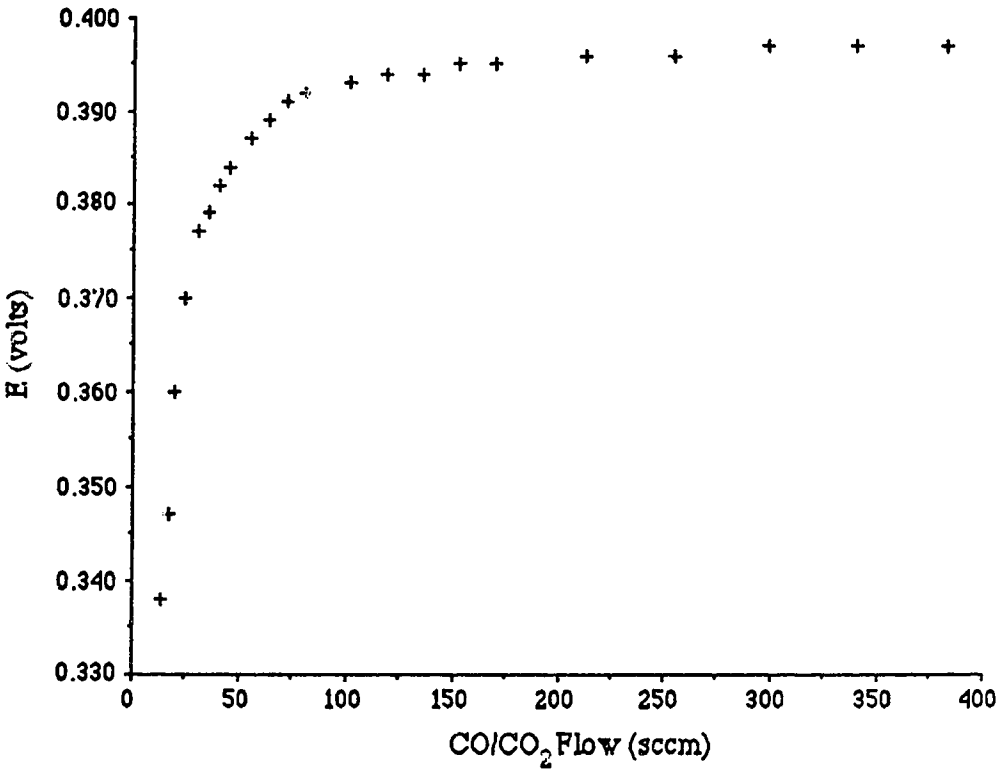

Fig. B-26. Run 26-Oxygen Reference 0.1994% CO / 99.8006% CO_2 Polarization Test.

Table B-27. Run 27-Oxygen Reference 5.0% CO / 95.0% CO_2 Polarization Test.

Temp.(K)	CO/CO_2 Flow (sccm)	O_2 Flow (sccm)	E (volts)
1003	43	174	0.712
1003	31	174	0.710
1002	28	174	0.716
1002	84	174	0.719
1002	128	174	0.719
1003	148	174	0.720
1002	170	174	0.720
1002	213	174	0.720
1002	255	174	0.720
[illegible]	298	174	0.719
[illegible]	340	174	0.720
[illegible]003	383	174	0.719
1003	9	174	0.337
1003	14	174	0.712
1003	15	174	0.714
1003	14	174	0.714
1003	14	174	0.714
1003	13	174	0.712
1003	12	174	0.711
1003	11	174	0.707
1002	10	174	0.706

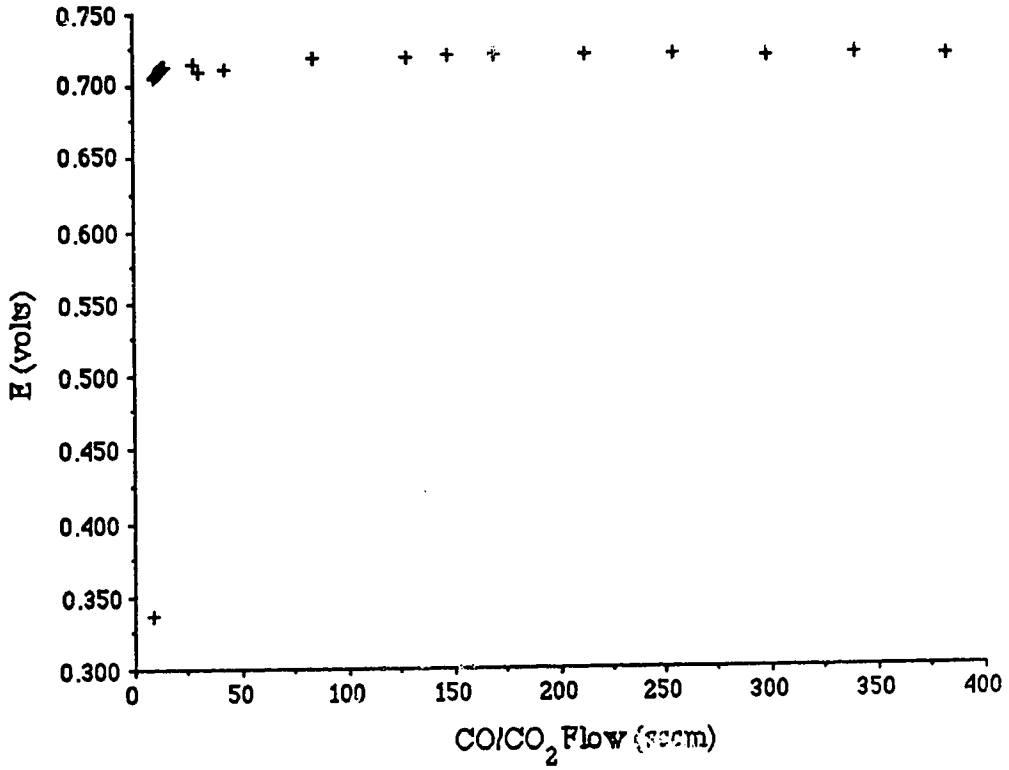

Fig. B-27. Run 27-Oxygen Reference 5.0% CO / 95.0% CO_2 Polarization Test.

Table B-28. Run 28-Oxygen Reference 5.0% CO / 95.0% CO_2.

Pressure (millibar)	Temp.(°C)	Temp.(K)	E (volts)	ΔG^o(cal/mol)
946	1003	1276	0.718	-40668
946	1003	1276	0.719	-40715
946	1035	1308	0.698	-39936
945	1101	1374	0.652	-38206
945	1072	1345	0.667	-38726
945	1105	1378	0.650	-38138
940	924	1197	0.755	-41915
931	892	1165	0.785	-43120
930	858	1131	0.810	-44073
929	826	1099	0.824	-44529
913	665	938	0.903	-47233
915	634	907	0.922	-47923
932	516	789	0.991	-50389
932	555	828	0.972	-49744
932	582	855	0.959	-49304
934	605	878	0.941	-48609
934	639	912	0.948	-49134
934	679	952	0.937	-48864
940	718	991	0.914	-48028
939	803	1076	0.827	-44521
939	922	1195	0.754	-41859
928	903	1176	0.776	-42774
933	798	1071	0.835	-44867
934	745	1018	0.852	-45334
945	724	997	0.865	-45799
945	699	972	0.876	-46158
945	682	955	0.896	-46980
932	650	923	0.915	-47679

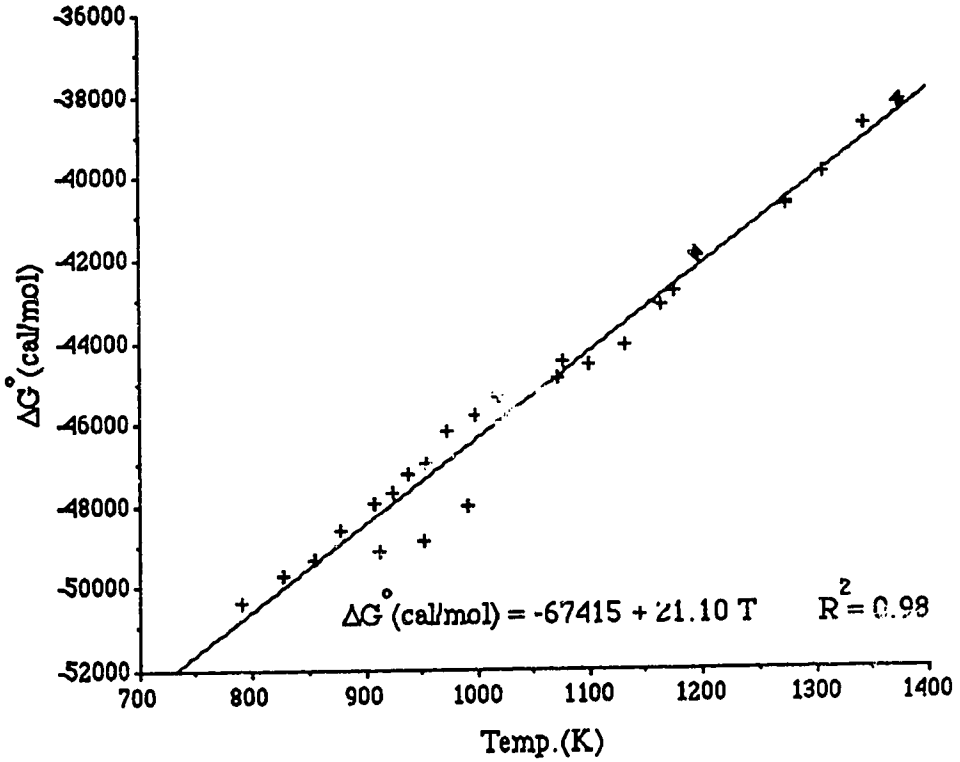

Fig. B-28. Run 28-Oxygen Reference 5.0% CO / 95.0% CO_2.

Table B-29. Run 29-Oxygen Reference 0.097% CO / 99.9903% CO_2.

Pressure (millibar)	Temp.(°C)	Temp.(K)	E (volts)	ΔG°(cal/mol)
936	508	781	0.832	-49202
936	538	811	0.816	-48880
928	568	841	0.793	-48243
928	598	871	0.775	-47829
926	629	902	0.756	-47385
917	657	930	0.730	-46583
914	689	962	0.709	-46063
913	720	993	0.688	-45525
911	751	1024	0.659	-44621
910	784	1057	0.611	-42866
915	816	1089	0.554	-40676
918	850	1123	0.523	-39715
919	882	1155	0.501	-39143
923	914	1187	0.477	-38475
923	948	1221	0.435	-37010
920	981	1254	0.411	-36365
920	1012	1285	0.390	-35827
920	1042	1315	0.372	-354[illegible]
923	1081	1354	0.359	-35351
930	1102	1375	0.352	-35309
927	1127	1400	0.347	-35429
923	1135	1408	0.343	-35362
916	1104	1377	0.357	-35588
917	1069	1342	0.369	-35654
918	1037	1310	0.386	-35992
921	1004	1277	0.400	-36176
923	967	1240	0.419	-36536
927	937	1210	0.448	-37451
926	905	1178	0.479	-38438
926	871	1144	0.507	-39259

Table B-29. Run 29-Oxygen Reference 0.097% CO / 99.9903% CO_2 Continued :

Pressure (millibar)	Temp.(°C)	Temp.(K)	E (volts)	ΔG^o(cal/mol)
919	839	1112	0.529	-39837
929	806	1079	0.558	-40705
929	774	1047	0.610	-42659
933	742	1015	0.643	-43733
933	711	984	0.671	-44594

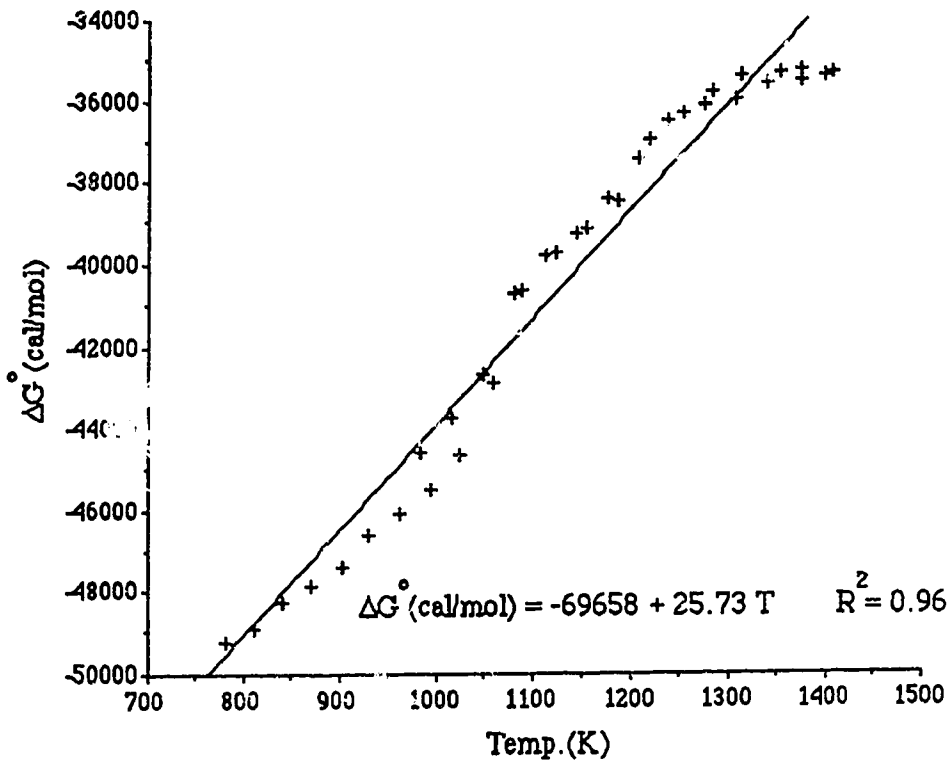

Fig. 5-34. Run 29-Oxygen Reference 0.097% CO / 99.9903% CO_2.

References

1 Kiukkola, K., and Wagner, C., J. Electrochem. Soc. **1957**, vol.104, p. 379.

2 Ure, R.W., J. Chem. Phys. **1957**, vol.26, p. 1363.

3 Rankin, G.A., Merwin, H.E., J. Am. Chem. Soc. **1916**, vol. 38, p. 563.

4 Tuband, C., and Lorenz, E. Z., J. Phys. Chem. **1968**, vol. 72, p. 2106.

5 Agarwal, Y.K., Short, D.W., Gruenke, R., and Rapp, R.A., J. Electrochem. Soc. **1974**, vol. 121, p. 354.

6 Sandler, Y.L., J.Electrochem.Soc. **1974**, vol. 121, p. 764.

7 Spacil, H.S., and Tedmon, [illegible] Electrochem.Soc. **1969**, vol. 116, p. 1618.

8 Etsell, T.H., and Flengas, S.[illegible], Chem. Rev. **1970**, vol. 70, p. 339.

9 Steele, B.C.H., "High Temperature Thermodynamic Measurements involving Solid Electrolyte Systems", in: Alcock, C.B., (Ed.), Electromotive Force Measurements in High Temperature Systems. Portsmouth: Grosvenor Press, **1968**, p. 3.

10 Goto, K., and Plusckell, W. , "Oxygen Concentration Cells", in: Hladik, J., (Ed.), Physics of Electrolytes. New York: Academic Press, **1972**, vol. 2, p. 539.

11 Rapp, R.A. and Shores, D.A., "Electrochemical Measurements", in: Bunshah, R.F. (Ed.), Techniques in Metals Research. New York: Wiley and Sons, **1970**, vol. 4, Part 2, p. 123.

12 Tretyakov, Y.D., and Kaul, A.R., "Electrochemical Cells with Non-Oxygen Conductivity", in: Hladik, J., (Ed.), Physics of Electrolytes. New York: Academic Press, **1972**, vol. 2, p. 623.

13 Schmalzried, H., and Pelton, A.D., Am. Rev. Mater. Sci., **1972**, vol. 2, p. 143.

14 Worrell, W.L., Bull. Am. Ceram. Soc. **1974**, vol. 53, p. 425.

15 Voinov, M., "Various Utilizations of Solid Electrolytes", in: Kleitz, M. and Dupuy, J. (Eds.), Electrode Processes in Solid State Ionics. Dordrecht: Reidel, **1976**, p. 431.

16 Steele, B.C.H. and Shaw, R.W. "Thermodynamic Measurements with Solid Electrolytes", in: Hagenmuller, P. and Gool, W.V. (Eds.), Solid Electrolytes-General Principles, Characterizations, Materials, Applications. New York: Academic Press, **1978**, p. 483.

17 Chandrasekharaiah, M.S., Sreedharan, O.M., and Chattopadhyay, G. "Thermodynamic Studies of Alloys and Intermetallic Compounds" in: Subbarao, E.C. (Ed.), Solid Electrolytes and Their Applications. New York: Academic Press, **1980**, p. 99.

18 Barr, L.W., and Le Claire, A.D., Proc. Brit. Ceram. Soc. **1964**, vol. 1 , p. 109.

19 Simpson, L.A. and Carter, R.E., J. Am. Ceram. Soc. **1966**, vol. 49, p. 139.

20 Choudhary, H.S., Maiti, H.S., and Subbarao, E.C. "Defect Structure and Transport Properties" in: Subbarao, E.C. (Ed.), Solid Electrolytes and Their Applications. New York: Academic Press, 1980. p. 40.

21 Ibid., p. 6.

22 Barker, W.W., Mater. Sci. Eng., **1967**, vol. 2, p. 208.

23 Guggenheim, E.A., in: Thermodynamics 4th. Edition, Amsterdam: North Holland Press, **1959**, p. 456.

24 Wagner, C., "The Electromotive Force of Galvanic Cells Involving Phases of Locally Variable Composition" in: Delahay, P. (Ed.), Advances in Electrochemistry and Electrochemical Engineering. New York: John Wiley and Sons, **1966**, p. 1.

25 Tretyakov, Y.D. .and Muan, A., J. Electrochem. Soc. **1970**, vol. 117, p. 1267.

26 Etsell, T.H., Z. Naturforsch. **1972**, vol. 27a, p. 1138.

27 Janke, D. and Fischer, W.A., Arch. Eisenhüttenw.. **1975**, vol. 8, p. 477.

28 Swinkels, D.A.J., J. Electrochem Soc. **1970**, vol. 117, p. 1267.

29 Richards, S.R., Swinkels, D.A.J. and Henderson J., Trans. Iron Steel Inst. Japan **1971**, vol. 11, p. 371.

30 Etsell, T.H. and Flengas, S.N., J. Electrochem. Soc. **1972**, vol. 119, p. 1.

31 Rao, A.V.R. and Tare, V.B., Scripta Metallurg. **1972**, vol. 6, p. 141.

32 Patterson, J.W., J.Electrochem. Soc. **1971**, vol. 118, p. 1033.

33 Friedman, L.W., Oberg, K.E., Boorstein, W.M. and Rapp, R.A., Met. Trans. **1973**, vol. 4, p. 69.

34 Strickler, D.W. and Carson, W.G., J. Am. Ceram. Soc. **1964**, vol. 47, p. 122.

35 Kofstad, P., in: Nonstoichiometry, Diffusion and Electrical Conductivity in Binary Metal Oxides. 3rd. ed. New York: Wiley-Interscience, **1972**, p. 1.

36 Worrell, W.L., "Solid Electrolytes", in: Geller, S. (Ed.), vol. 21 of Topics of Applied Physics. Berlin: Springer-Verlag, **1977**, p. 143.

37 Steele, B.C.H., and Dudley, G.J., "Mass Transport in Ionic Solids", in: Solid State Chemistry; Roberts, L.E.J. (Ed.), London: Butterworths, **1975**, Chap. 6, p. 181.

38 Worrell, W.L., and Liu, Q.G., Proceedings of the Int. Meeting on Chem. Sensors, in: vol. 17 Anal. Chem. Symp. Series, New York: Elsevier, **1983**, p. 332.

39 Ramanarayanan, T.A., and Worrell, W.L., Can. Met.Quart. **1974**, vol. 13, p. 325.

40 Subbarao, E.C., Maiti, H.S., and Srivastava, K.K., Phys. Status Solidi A **1974**, vol. 21, p. 9.

41 Tien, T.Y. and Subarrao, E.C., J. Chem. Phys. **1963**, vol. 39, p. 1041.

42 Schmalzried, H., Z. Elektrochem. **1962**, vol. 66, p. 572.

43 Kingery, W. D., Papis, J., Doty, M.E., and Hill, D.C., J. Am. Ceram. Soc. **1959**, vol. 42, p. 393.

44 Kontopoulos, A. and P.S. Nicholson, J. Am. Ceram. Soc. **1971**, vol. 54, p. 317.

45 Smith, A. W., Meszaros, F.W., and Amata, C.D., J. Am. Ceram. Soc. **1966**, vol. 49, p. 240.

46 Nernst, W., Z. Elektrochem. **1899**, vol. 6, p. 41.

47 Bauer, E., and Preis, H., Z. Elektrochem. **1937**, vol. 43, p. 727.

48 Markin, T.L., Bones, R.J., and Dell, R.M., in: Superionic Conductors; Mahan, G.D. and Roth, W.L. (Eds.) New York: Plenum Press, **1976**, p. 15.

49 Baukal, W., Electrochim. Acta. **1969**, vol. 14, p. 1071.

50 Subbarao, E.C., Sutter, P.H., and Hrizo, J., J. Am. Ceram. Soc. **1965**, vol. 48, p. 443.

51 Wimmer, J.M., Bidwell, L.R., and Tallan, N.M., J. Am. Ceram. Soc. **1967**, vol. 50, p. 198.

52 Steele, B.C. H. and Alcock, C.B., Trans. Metall. Soc. AIME **1965**, vol. 233, p. 1359.

53 Lasker, M.F. and Rapp, R.A., Z. Phys. Chem. N.F. **1966**, vol. 49, p. 198.

54 Fujishiro, S., and Gokcen, N.A., Trans. Met. Soc. AIME **1961**, vol. 221, p. 275

55 Speiser, R., Johnston, H.L., and Blackburn, P., J. Am. Chem. Soc. **1950**, vol. 72, p. 4142.

56 Vintaykin, Y. Z., Dokl. Akad. Nauk SSSR, **1959**, vol. 129, p. 2.

57 Alekseyev, V.I., and Shvartsman, L.A., in: Fiz.-mekh. osnovy proizvodstva stali (Physical and mechanical principles of steel making). Izd. Akad. Nauk SSSR, **1962**, p. 8.

58 Vintaykin, Y. Z., Fiz. Metal. i Metalloved. **1963**, vol. 16, p. 144.

59 Kelley, K.K., Boericke, F.S., Moore, G.E., Huffman, E.H. and Bangert, W.M., U.S. Bureau of Mines, Tech. Paper 662. **1944**.

60 Gleiser, M., J. Phys. Chem. **1965**, vol. 69, p. 1771.

61 Storms, E.K., in: The Refractory Carbides, New York: Academic Press, **1967**, p. 105.

62 Kleykamp, H., Ber. Bunsenges. Physik. Chem. **1969**, vol. 73, p. 354.

63 Tanaka, H., Kishida, Y., Kawaguchi, A., and Moriyama, J., Department of Metallurgy, Kyoto University, Japan, unpublished research, **1970**.

64 Wicks, C.E., and Block, F.E., U.S. Bureau of Mines, Bull. 605. **1963**.

65 Mabuchi, H., Sano, N., and Matsushita, Y., Met. Trans. **1971**, vol. 2, p. 1503.

66 Kulkarni, A.D., and Worrell, W.L., Met. Trans. **1972**, vol. 3, p. 2363.

67 Coltters, R.G., and Belton, G.R., Met. Trans. B. **1984**, vol. 15B, p. 517.

68 Richardson, F.D., and Jeffes, J.H.E., ΔG (formation) of Metal Oxides : Assessment, J. Iron Steel Institute. **1948**, vol. 160, p. 261; **1949**, vol. 163, p. 397.

69 Richardson, F.D., ΔG (formation) of Metal Carbides : Critical Review, J. Iron Steel Institute. **1953**, vol. 175, p. 53.

70 Friedman, L.W., Oberg, K.E., Boorstein, W.M., and Rapp, R.A., Met. Trans. **1973**, vol. 4, p. 69.

71 Haber. F. and Moser, A., Z. Physik. Chem. **1905**, vol. 36, p. 593.

72 Hahn, Z. Physik. Chem. **1903**, vol. 44, 513; **1904**, vol. 48, p. 735.

73 Haber, F., and Richardt, Z. Anorg. Chem. **1904**, vol. 38, p. 5.

74 Lewis, G.N., Randall, M., "Oxygen and Its Compounds with Hydrogen and with some Metals", in: Thermodynamics and the Free Energy of Chemical Substances. 1st. ed. New York: McGraw Hill, **1923**, p. 485.

75 Nernst, W., and Wartenberg, H. v., Z. Physik. Chem. **1906**, vol. 56, p. 548.

76 Langmuir, I., J. Am. Chem. Soc. **1906**, vol. 28, p. 1357.

77 Lowenstein, F., Z. Physik. Chem. **1905**, vol. 54, p. 707.

78 Chipman, J., Thomson, R.M., Guernsey, D.L., and Fulton, J.C., Trans. Am. Soc. Metals. 1952, vol. 44, p. 1215.

79 M. De Kay Thompson : The Total and Free Energies of Formation of the Oxides of Thirty-Two Metals" New York: Electrochem. Soc. 1942

80 Peters, H., and Mobius, H.H., Z. Physik.Chem. **1958**, vol. 209, p. 298.

81 Okamoto, H., Obayashi, H. and Kudo, T., Solid State Ionics **1980**, vol. 1 ,p. 319.

82 Iwase, M., and Mori, T., Can. Met. Quart. **1980**, vol. 19, p. 285.

83 Iwase, M., Tanida, M., Mclean, A. and Mori, T., Met. Trans. B. **1980**, vol. 12B, p. 517.

84 Cote, R., and Gauthier, M., J. Electrochem. Soc. **1984**, vol. 31, p. 63.

85 Colwell, J. A., and Rapp, R. A., Met. Trans. A. **1986**, vol. 17A, p. 1065.

86 Maruyama, T., Ye, X.Y. and Saito, Y., Solid State Ionics **1987**, vol. 24, p. 281.

87 Weast, R.C. and Astle, M.J. (Eds.), in: CRC Handbook of Chemistry and Physics, 59th ed., West Palm Beach: CRC Press, 1978, F-210, 249-250.

88 Rosenqvist, T., in: Principles of Extractive Metallurgy. New York: McGraw Hill, **1974**; p 227.

89 Colwell, J. A. and Rapp, R. A., Met. Trans. **1986**, vol. 17A, p. 1065.